

Volume I Suppl 1, 2008

Meeting abstracts

1st Congress of the International Foot & Ankle Biomechanics (i-FAB) community

Bologna, Italy

4–6 September 2008

Published: 26 September 2008

These abstracts are available online at [<http://www.jfootankleres.com/supplements/1/S1>]

KEYNOTE PRESENTATIONS

K1

Advances in biomechanics of posterior tibial tendon dysfunction and flatfoot deformity

Harold B Kitaoka

Department of Orthopedic Surgery, Mayo Clinic, Rochester, Minnesota, USA

E-mail: kitaoka.harold@mayo.edu

Journal of Foot and Ankle Research 2008, **1**(Suppl 1):K1

Introduction: The objective of this presentation is to highlight the clinical and laboratory-based research related to posterior tibial tendon dysfunction (PTTD).

Methods and results:

- Defining the flatfoot: clinical, foot pressure, radiologic
- Critical evaluation of flatfoot deformity: in vitro
- How often does the flatfoot occur?
- Normal arch development
- Why is the flatfoot a problem?
- Why does the flatfoot occur?
 - Effects of weightbearing [1]
 - Lost of static support [2]
 - Loss of dynamic support [3]
 - Anatomic predisposition
 - Joint subluxation
- Causes of flatfoot in adults
 - Posterior tibial tendon dysfunction (PTTD)
 - Arthritis: Midfoot, hindfoot, ankle
 - Hypermobil flatfoot
 - Neuropathic arthropathy
 - Fracture malunion
 - Inflammatory arthropathy
 - Peroneal spastic flatfoot
 - Neuromuscular disorder
 - Other
- PTTD etiology
- PT muscle, tendon anatomy
- PT function
- PT muscle activity during gait
- Factors predisposing to PTTD
 - PT gliding resistance
 - PT pathoanatomy

- Natural history of PTTD
- PTTD evaluation: symptoms, signs
- Investigative studies
- Gait analysis in PTTD patients
- Simulated walking: Normal, PTTD [4]
- PTTD treatment
- PTTD treatment results
- Failures, complications

Conclusion:

- Current recommendations

Acknowledgements

Kai-Nan An, PhD; Kenton R Kaufman, PhD

References

1. Kitaoka HB: *Foot Ankle Int* 1995, **16**:492–9.
2. An KN: *J Biomech* 1988, **21**:613–20.
3. Kim KJ: *J Musculoskeletal Res* 2001, **5**(2):113–21.

K2

Sailing charted seas: biomechanics and the orthopedic surgeon

George A Arangio

Department Orthopaedic Surgery, Penn State, Milton S.

Hershey Medical College

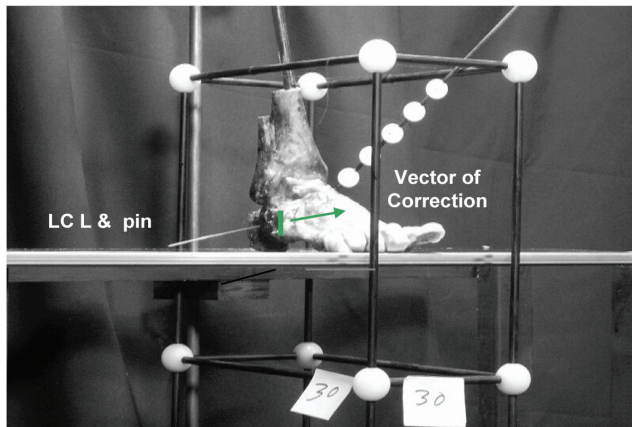
E-mail: casarangio@aol.com

Journal of Foot and Ankle Research 2008, **1**(Suppl 1):K2

Introduction: Biomechanical models have been used to study the distribution of foot forces, metatarsal stresses, heel pad, arch height, plantar aponeurosis, subtalar joint, extrinsic muscles, medial displacement calcaneal osteotomy, subtalar arthroereisis and lateral column lengthening calcaneal osteotomy in the normal and flatfoot. We review past research data and discuss results as they relate to relevant clinical topics [1–6].

Table 1 (abstract K2) Moments in Newton-meters (N-m)

Joint	Normal Nm	Flatfoot Nm	Flatfoot + LCL Nm
1 st Metatarsal medial cuneiform	0.20	8.76	0.51
Medial – cuneiform navicular	0.33	14.48	0.84
Talo-navicular	5.61	21.63	8.05(–63%)
Calcaneal-cuboid	5.69	0.00	7.72

Figure 1 (abstract K2)

Cadaver Foot with calibrated cage and pointer for Direct Linear Transformation Photography illustrating LCL.

Methods: A three dimensional multi-segment biomechanical model [7] was used with anatomical data from normal feet, feet made flat and corrected feet. The model includes a series of equations that describe how the foot deforms under a theoretical applied load of 683 Newtons (70 Kg.) on one foot in static stance phase

Results: Lateral Column Lengthening Calcaneal Osteotomy (LCL) decreases the forces needed by ligaments to resist moments at the medial arch joints by -79% and the talonavicular joint -63% in the flattened foot.

Conclusion: The model has accurately predicted the deformation of the foot under a theoretical load of 683 Newtons. We have analyzed the effect of various surgical procedures on the flatfoot. We discussed the clinical relevance of the model data to the ankle sprain, 5th metatarsal stress fracture, posterior tibial tendon insufficiency, the flatfoot and the cavus foot.

Acknowledgement

Eric P Salathe Sr. PhD.

References

1. Arangio GA, et al: *Clin Biomech* 2007, **22**:472-477.
2. Arangio GA, et al: *Clin Biomech* 2004, **19**:847-852.
3. Arangio GA, et al: *Clin Biomech* 2001, **16**:539-539.
4. Arangio GA, et al: *Foot Ankle Int* 2000, **21**:216-220.
5. Arangio GA, et al: *Foot and Ankle Surgery* 1998, **4**:123-128.
6. Arangio GA, et al: *Clin Orthop* 1997, **339**:227-231.
7. Salathe EP, et al: *J Biomech Eng* 2002, **124**:241-281.

K3

The role of research in the development of athletic footwear

Mario Lafortune

Nike Sport Research Laboratory, USA

E-mail: Mario.Lafortune@nike.com

Journal of Foot and Ankle Research 2008, **1(Suppl 1)**:K3

The three main needs of athletes are performance, injury protection and comfort. Footwear enhances performance through increases in traction and biomechanical efficiency. Footwear protects the foot at the interface with the ground

and the entire body against the forces resulting from repeated feet-ground impacts. Footwear can also reduce injuries by correcting for the locomotor system static structural misalignments. Footwear uppers, insoles or sockliners being considered upper elements, are responsible to maintain the feet over the shoe soles. Uppers fit is most important to athletes' comfort. Athletes' needs as well as their relative importance are defined by the 'critical' maneuvers performed during sporting activities. 'Critical' maneuvers are maneuvers that must be performed to succeed in a sport and/or maneuvers that have been linked to the highest incidence of injury observed in that sport. Focus group research and surveys help to identify critical maneuvers. 3D motion capture systems, force plateforms and pressure insoles are used to study the critical maneuvers associated to different sporting activities. The results of these studies lead to design criteria that are shared with designers and developers. Prototypes are created and evaluated using the same batteries of biomechanical tests to assess how well they meet the design criteria. Therefore, footwear designed for different sporting activities can readily be differentiated. Gender, skill level, and environmental conditions add further requirements upon footwear design thus allowing for differentiation even within a given sporting activity.

Footwear intended for use in multiple sporting activities represent non-trivial design challenges. Typically, such designs lead to shoes that feature some level of compromise to address the competing requirements of each different sporting activity. This holds true even within a sport when injury protection and performance needs conflict, or when different injury protection needs require somewhat contradictory solutions. Considering running footwear as an example, it is generally believed that shoes currently designed to offer maximal cushioning lack rearfoot stability and vice-versa, shoes designed to resist injury inducing excessive rearfoot motion lack cushioning. Yet, recent research and novel design approaches have shown that the magnitude of the compromises in footwear design can be significantly reduced if not eliminated.

K4

Biomechanical factors in diabetic foot disease

PR Cavanagh¹, A Erdemir², M Petre³, TM Owings⁴, G Botek⁴, S Chokhandre² and R Bafna²

¹Department of Orthopaedics and Sports Medicine, University of Washington, Seattle, USA

²Department of Biomedical Engineering, Cleveland Clinic, OH, USA

³Department of Anaesthesiology Research, Cleveland Clinic, OH, USA

⁴Department of Orthopaedics, Cleveland Clinic, OH, USA

E-mail: cavanagh@u.washington.edu

Journal of Foot and Ankle Research 2008, **1(Suppl 1)**:K4

Introduction: This presentation will review the evidence that has led to the current understanding of diabetic foot complications, discuss some of the authors' current work, and identify unsolved problems for future research and clinical application.

Methods: Although the risk of vascular disease is markedly increased in diabetes [1], it is the combination of altered vascular status and nerve damage that often leads to ulceration and amputation [2]. Important early studies by Brand and colleagues [3] focused on elevated stress in a deformed, neuropathic limb as a

causative factor in tissue breakdown and this has been a constant theme of experimental and analytical studies to the present day. The stress component normal to the foot (usually called plantar pressure) has typically been available for study [4] and this quantity is associated with the risk of future ulceration [5]. We have shown it to be useful, together with foot shape, in the design of pressure relieving footwear [6] and others have derived quantities such as pressure gradient to indicate risk [7]. Recent studies of plantar shear stress [8] have reported higher neuropathic/control ratios than for plantar pressure, suggesting that shear stress may have an important role in tissue damage. The measurement of pressure between the foot and the footwear is potentially very useful clinically [9]. If the patient is compliant with footwear use, the stresses measured using in-shoe techniques reflect the influence of anatomical structure, lower extremity function, lifestyle, and footwear construction. Finite element modelling of the foot, and in some cases footwear, has been explored by a number of groups [10–12] to provide estimates of quantities that cannot be directly measured or to perform simulations that would be onerous or dangerous for human subjects. Our own recent work has been directed towards the development of more realistic soft tissue models utilizing detailed deformation measurements of foot structures [13] and an attempt to reduce the burden of mesh development by the use of morphing techniques to modify stock meshes.

Conclusion: More effort needs to be directed towards the application of biomechanics research to benefit the patient. This will require clear demonstration of improved outcomes when biomechanically based interventions are conducted.

Acknowledgements

We acknowledge support from NIH Grants 5R01 HD037433 and T32 AR50959.

References

1. Mazzone T, et al: *Lancet* 2008, **371**:1800–9.
2. Kles KA and Vinik AI: *Curr Diabetes Rev* 2006, **2(2)**:131–45.
3. Bauman J, et al: *J Bone Joint Surg Am* 1964, **45-B(4)**:652–73.
4. Bus SA, et al: *Diabetes Metab Res Re* 2008, **Suppl 1**: S162–80.
5. Crawford F, et al: *QJM* 2007, **100(2)**:65–86.
6. Owings TM, et al: *Diabetes Care* 2008, **31(5)**:839–44.
7. Mueller MJ, et al: *Diabetes Care* 2005, **28(12)**:2908–12.
8. Yavuz M, et al: *J Biomech* 2008, **41(3)**:556–9.
9. Guldemond NA, et al: *Diabetes Res Clin Pract* 2007, **77(2)**:203–9.
10. Cheung JT and Zhang M: *Med Eng Phys* 2008, **30(3)**:269–77.
11. Actis RL, et al: *Med Biol Eng Comput* 2008, **46(4)**:363–71.
12. Yarnitzky G, et al: *J Biomech* 2006, **39(14)**:2673–89.
13. Petre M, et al: *J Biomech* 2008, **41(2)**:470–4.

K5

Advances in image-based biomechanics of the human ankle

Sorin Siegler

Department of Mechanical Engineering, Drexel University,
Philadelphia, PA, USA

E-mail: ssiegler@cbis.ece.drexel.edu

Journal of Foot and Ankle Research 2008, **1(Suppl 1)**:K5

Introduction: Medical imaging techniques including CT, MRI, Micro-CT and micro-MRI have matured over the last years into

affordable, practical and accessible observational tools to the Biomechanics community. These tools provide unique opportunities to expand the knowledge of the biomechanics of the human foot and ankle. The purpose of this presentation is to demonstrate the potential of these imaging techniques through three specific applications from our current research.

Image-based models: The morphology of the bones, articular surfaces and ligaments and the passive mechanical characteristics of the ankle complex were reported to vary greatly among individuals. The later were often presumed to be associated with variations in experimental conditions. MRI-based models of various individuals were used to test the hypothesis that the variations observed in the passive mechanical properties of the ankle complex are strongly influenced by morphological variations. Confirmation of this hypothesis suggests that individualized subject-specific treatment procedures for ankle complex disorders are potentially superior to a one-size-fits-all approach. It suggest that, in the future, MRI-based subject-specific models of the hindfoot could be used as individualized surgical planning tools for improvement of clinical outcome.

Characterization of passive structural properties: The passive structural properties of the hindfoot are assessed from measurements of the displacements produced at the hindfoot in response to applied loads. Current in vivo and in vitro techniques have shortcomings that limit their scientific and clinical usefulness. In vitro conditions fail to account for phenomena such as tissue remodeling or partial damage effects. The in vivo approach, based on external observations has been shown to be inaccurate due to soft tissue and skin interference and the inaccessibility of the talus to external markers. The MRI-based technique referred to as “3D stress MRI” and abbreviated as 3D sMRI, solves many of the problems associated with present in vivo and in vitro techniques. 3D sMRI does not require exposure to harmful radiation, it is non-invasive, and internal bone kinematics can be derived without soft tissue interference. The technique can also provide direct visualization of the level of integrity of the underlying structures. The 3D sMRI technique may be used in the future to expand fundamental knowledge of the biomechanics of the hindfoot in vivo and for developing sensitive and reliable clinical diagnostic and evaluation procedures for a variety of ankle pathologies such as chronic ankle instability. However, as with any new technology, considerable further development is needed to take sMRI from its current state to a stage where it can be routinely used in the clinic.

Skeletal development in clubfoot treatment: Congenital clubfoot is a common foot deformity often treated using serial manipulations and casting such as the Ponseti Technique. It provides a unique natural occurring experiment to observe the mechanisms of tissue adaptation under external loads. These mechanisms of adaptations including cartilage and bone adaptation as well as osteogenesis can be observed through multiple MRI observations of the treated clubfoot. Using this observational tool some unique observations on cartilage adaptation and osteogenesis were made.

Conclusion: Image-based biomechanics, although still in its infancy, has the potential to evolve into a major field that can deepen and expand biomechanical knowledge lead to improved clinical management of hindfoot disorders.

Acknowledgements

These studies were partially supported by NIH grants #AR46902, and #AR053255.

References

1. Imhauser, et al: *J Biomech* 2008, **41/6**:341–1349.
2. Siegler, et al: *J Biomech* 2005, **38/3**:567–578.
3. Ringleb, et al: *J Ortho Sur* 2005, **23**:743–749.
4. Brand, et al: *J Med Hypoth* 2006, **66**:653–659.

K6

Multiscale modelling and team science: the future of orthopaedic biomechanics

Marco Viceconti

Laboratorio di Tecnologia Medica, Istituto Ortopedico Rizzoli, Bologna, Italy

E-mail: viceconti@tecno.ior.it

Journal of Foot and Ankle Research 2008, **1(Suppl 1)**:K6

Introduction: Some of the most exciting developments in recent biomechanics research regard topics that lay at boundaries: boundaries between dimensional scales (i.e. cell-tissue interaction), between sub-systems (i.e. cardiovascular and musculoskeletal), or between different domains of biomedical knowledge (i.e. biology and engineering). This is a trend that we are observing in the entire biomedical research field, and undergoes the name of biomedical Integrative Research [1]. In order to follow this trend, every researcher needs to add to her tool chest two new tools: multiscale modelling, and team science.

Multiscale modelling: This term indicates the ability to models capable of predicting the physical behaviour of a complex system, which is regulated by multiple phenomena observable at radically different dimensional and/or temporal scales.

Given the level of complexity that integrative research involves, mathematical/numerical modelling appears the only viable option. However, this requires modelling methods that are not only multi-physics, but also multiscale.

The trivial declination of multiscale modelling are problems where all scale are regulated by exactly the same physics: if you need to model a single bolt whose loading is defined by the deformation of the entire car body, you have a significant difference in dimensions, but both models describe the elastic behaviour of a solid continuum; nowadays these problems are trivially solved with methods such as sub-structuring [2].

The true challenge is when each sub-model is a truly independent model, representing different physical behaviours, and most of the times using different mathematical approaches for the modelling. No off-the-shelf tool can currently solve this problem, but intense research activity is being conducted [3].

Team science: While multiscale modelling can help in integrating across sub-systems and across dimensional scales, to integrate across different domains of knowledge we need something else: team science. “Team science” refers to multi-partnered and multi-disciplinary research partnerships designed to bring together specialized researchers to work on specific facets of a larger project or study. In the context of integrative research the need for team science is being addressed in three directions: the development of consensus processes involving stakeholders from very different sub-domains of biomedical research, such as the one we developed in STEP [1]; to create Internet communities specifically oriented to team science and its support, such as Biomed Town [4]; and to develop specialised

pre-post processing environments for the multiscale modelling that help in capturing and exchanging knowledge across domains. This latter activity it is still in its infancy, but some seminal work is being done in the context of the MAF framework [5].

References

1. STEP Consortium: **Seeding the EuroPhysiome: A Roadmap to the Virtual Physiological Human.** (<http://www.europhysiome.org/roadmap>), [Online] 5 July 2007.
2. Feng F, et al: **The mechanical and thermal effects of focused ultrasound in a model biological material.** *J Acoust Soc Am* 2005, **117(4 Pt 1)**:2347–55.
3. Viceconti M, et al: **Multiscale modelling of the skeleton for the prediction of the risk of fracture.** *Clin Biomech in press*, 2008 Feb 25. PMID: 18304710.
4. **Biomed Town: on-line Community for Integrative Research.** (<http://www.biomedtown.org>).
5. Viceconti M, et al: **The multimod application framework: a rapid application development tool for computer aided medicine.** *Comput Methods Programs Biomed* 2007, **85(2)**:138–51.

ORAL PRESENTATIONS

Pathological Foot

O1

Energetics of the intrinsic foot muscles in plantar fasciitis

R Chang¹, R Larsen², J Kent-Braun² and J Hamill¹

¹Biomechanics Laboratory,

University of Massachusetts, USA

²Muscle Physiology Laboratory,

University of Massachusetts, USA

E-mail: ryan.chang.umass@gmail.com

Journal of Foot and Ankle Research 2008, **1(Suppl 1)**:O1

Introduction: Intrinsic foot muscles and the plantar fascia provide mechanical support for the medial longitudinal arch in gait [1]. In an injury to the plantar fascia (i.e. plantar fasciitis), there may be an increase in load on the intrinsic foot muscles resulting in increased metabolic demand. Phosphorus magnetic resonance spectroscopy (³¹P MRS) has shown that the ratio of inorganic phosphate to phosphocreatine ([Pi]/[PCr]) within a muscle increases proportionately with muscle work at low to moderate levels [2]. The purpose of this study was to determine whether walking elicits a relatively higher increase in activity of the intrinsic foot muscles of feet with plantar fasciitis relative to healthy feet.

Methods: Three female subjects (mean age: 43 yrs; arch index: 0.299) with unilateral chronic plantar fasciitis (>3 months) participated.

A 4-Tesla MRS system (Bruker, Germany) was used to obtain concentrations of [PCr] and [Pi] before (PRE) and after (POST) walking. Subjects were positioned supine in the MRS system with a ¹H and ³¹P coplanar surface coil under the medial arch. ³¹P free induction decays (FIDs) were captured for 3 mins (100 μs, 60° nominal flip angle, TR = 2 s, 2048 data points, spectral width = 8000 Hz).

Subjects walked barefoot on a treadmill for 7 mins at 1.35 ms⁻¹. To preserve the intracellular metabolic state of the intrinsic foot muscles induced by walking, a cuff was inflated around the ankle within the last step. In less than 4 min, subjects were repositioned into the magnet for POST measurement. Both the healthy (H) and plantar fasciitis (PF) feet were studied with > 25 min between tests. Pi and PCr peaks were integrated and [Pi]/[PCr] was calculated.

Results: Walking caused a depletion of [PCr] and an accumulation of [Pi] (Figure 1) which resulted in an increased [Pi]/[PCr] with walking (Table 1). The increases in [Pi]/[PCr] from PRE to POST were similar in PF and H.

Conclusion: In this novel approach to the study of intrinsic foot muscles, we used MRS to measure metabolic activity non-invasively and *in vivo*.

The data showed that walking caused an increased use of ATP in the intrinsic foot muscles, indicating that these muscles were activated to produce force along the plantar aspect of the foot. Although increases in [Pi]/[PCr] of PF and H were similar, more information is required to conclude that both feet performed equal force output. Subsequent studies will examine whether there is PF and H asymmetry in forefoot-rearfoot kinematics, muscle size and mitochondrial function.

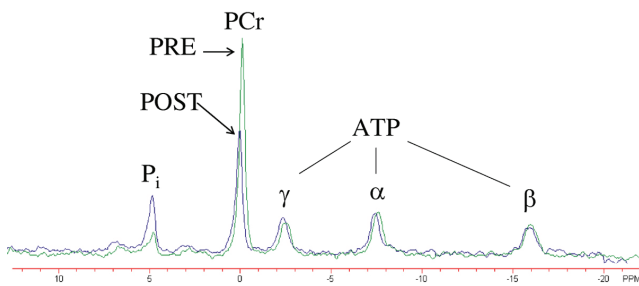
Acknowledgements

We thank the International Society of Biomechanics and Kintex Footlabs for funding, and the Yale Magnetic Resonance Research Center.

References

- Mann R, et al: *J Bone Joint Surg Am* 1964, **46**:469–481.
- Kent-Braun JA: *J Appl Physiol* 1993, **75**(2):573–580.

Figure 1 (abstract O1)



Exemplar PRE and POST spectra.

Table 1 (abstract O1) [Pi]/[PCr] before (PRE) and after (POST) walking

Subject	PF		Healthy	
	PRE	POST	PRE	POST
S1	0.12	0.17	0.12	0.18
S2	0.10	0.25	0.14	0.18
S3	0.11	0.45	0.10	0.46
Mean	0.11	0.29	0.12	0.27

O2

Clawed toes in the diabetic foot: neuropathy, intrinsic muscle volume, and plantar aponeurosis thickness

William R Ledoux^{1,2,3}, Jason Schoen¹, Matthew Lovell¹ and Elizabeth Huff¹

¹RR&D Center of Excellence, Department of Veterans Affairs, Seattle, WA, USA

²Departments of Mechanical Engineering, University of Washington, Seattle, WA, USA

³Orthopaedic & Sports Medicine, University of Washington, Seattle, WA, USA

E-mail: wrledoux@u.washington.edu

Journal of Foot and Ankle Research 2008, 1(Suppl 1):O2

Introduction: Clawed toes, defined as extension of the metatarsophalangeal joint (MTPJ) and flexion of the proximal and distal interphalangeal joints (IPJ), have been associated with the diabetic foot. One theory states that this deformity is caused by an imbalance between the extrinsic and intrinsic foot muscles [1, 2]. However, Bus et al. found a 73% decrease in intrinsic muscle cross sectional area between diabetic neuropathic patients and controls, but only 2 of 8 neuropathic patients had toe deformities [3]. Anderson et al. found that diabetic neuropathic patients had a little more than 50% of the intrinsic muscle volume of either controls or non-neuropathic diabetic patients, but none of the diabetic neuropathic patients had toe deformities [4]. Others have found a link between plantar apo-neurosis (PA) dysfunction and clawed toes [5, 6] and between diabetes and a thicker PA [7–9]. The purpose of this study was to explore the relationship between claw toes, neuropathy, intrinsic muscle volume and PA thickness.

Methods: We enrolled 40 diabetic subjects in 4 groups: G1) neuropathic, claw toes, G2) neuropathic, no claw toes, G3) non-neuropathic, claw toes, and G4) non-neuropathic, no claw toes. We have analyzed a subset for this abstract (G1: n = 6, G2: n = 4, G3: n = 6, G4: n = 4). The presence of claw toes was determined via clinical exam and neuropathy was defined as insensitivity to a 10 g monofilament. Partial weight-bearing CT scans were taken for each foot. Intrinsic muscle volume was determined by segmenting each foot using MultiRigid; data were normalized to total foot volume. PA thickness was measured at 1/5 the distance from the heel to the base of the first metatarsal using ImageJ. A two-way analysis of variance was used to test for interaction and significance (p < 0.05).

Results: There was significant interaction between foot deformity and neuropathy (p = 0.02). Feet with both neuropathy and foot deformity had lower mean volume than all the other groups, i.e., volume was reduced only when feet were both neuropathic and had deformity (Table 1).

Mean PA thickness was significantly higher for feet with foot deformities than those without (p = 0.019) (Table 2). Thickness was also higher in neuropathic feet than in non-neuropathic feet, but this difference was not significant (p = 0.14). While the data

Table 1 (abstract O2) Intrinsic muscle volume (mean ± SD)

	claw toes yes	claw toes no
neuropathy yes	0.130 ± 0.037	0.191 ± 0.008
neuropathy no	0.198 ± 0.018	0.192 ± 0.034

Table 2 (abstract O2) PA thickness (mean ± SD)

	claw toes yes	claw toes no
neuropathy yes	4.57 ± 1.19	2.96 ± 0.22
neuropathy no	3.51 ± 0.99	3.00 ± 0.20

suggests that thickness was highest in feet that had both neuropathy and deformity beyond the additive effects of each factor separately, the interaction between deformity and neuropathy was not significant ($p = 0.2$).

Conclusion: Our pilot study demonstrates that neuropathic feet with claw toes have less intrinsic muscle volume than the other groups. The same feet also had thicker PA, suggesting that both intrinsic muscle atrophy and PA dysfunction are required for the development of claw toes. The specific mechanism of clawing with a thicker PA (as opposed to a ruptured PA, as seen previously [5, 6]) is not yet understood.

Acknowledgements

The Department of Veterans Affairs.

References

1. Boulton: *M Clin NA* 1988, **72**:1513–30.
2. Myerson and Shereff: *JBJS-Am* 1989, **71**:45–9.
3. Bus, et al: *Dia Care* 2002, **25**:1444–50.
4. Andersen, et al: *Dia Care* 2004, **27**:2382–5.
5. Pardiwala and Henry: *Ft & Ank Sur* 2001, **7**:197–200.
6. Taylor: *JBJS-Br* 1951, **33-B**:539–542.
7. Bolton, et al: *Cl Biom* 2005, **20**:540–6.
8. D’Ambrogi, et al: *Dia Med* 2005, **22**:1713–9.
9. Giacomozzi, et al: *Cl Biom* 2005, **20**:532–9.

O3

The role of shear stress in the aetiology of diabetic neuropathic foot ulcers

C Giacomozzi¹, Z Sawacha², L Uccioli³, E D’Ambrogi³, A Avogaro⁴ and C Cobelli²

¹Dept of Technology and Health, Italian National Institute of Health (ISS), Rome, Italy

²Dept of Information Engineering, University of Padova, Padova, Italy

³Dept of Internal Medicine, University of Tor Vergata, Rome, Italy

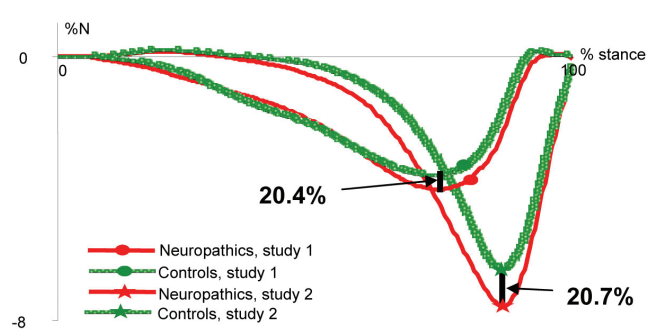
⁴Dept of Clinical Medicine and Metabolic Disease, University Polyclinic, Padova, Italy

E-mail: claudia.giacomozzi@iss.it

Journal of Foot and Ankle Research 2008, 1(Suppl 1):O3

Introduction: Several biomechanical studies have been conducted in the last decade to investigate the aetiology of plantar ulcers in presence of Diabetes (D) and Peripheral Neuropathy (PN) [1]. Great renewed interest has been lately showed towards shear stresses during gait [2, 3]. In this case, the major difficulty lays in technology, since it is still hard to obtain reliable and meaningful measurements by using the available measurement systems. The authors’ validated methodology [4] is here re-proposed, and the results of its further applications to the analysis of PN shear stress are here briefly reported.

Figure 1 (abstract O3)



Lateral shear forces under the metatarsal region.

Methods: A compound instrument was made at ISS (Rome, Italy) by superimposing a resistive pressure platform (4 sensors/cm²; pressure resolution 15.2 kPa; 100 Hz) on a Bertec force plate (force resolution 2 N, moment resolution: 0.3 Nm), and a mathematical model was implemented whose input are local vertical forces and global shear forces. Output of the model are estimated local shear forces and free moment [4]. The measurement system was used to investigate 61 barefoot D patients (34 PN, 21 matched controls = C). Three subareas – heel, metatarsals and hallux – were geometrically identified by making reference to the lines at 40% and 70% of the total length perpendicular to the bisecting line of the foot [3].

A similar prototype was then developed at the University of Padova (Italy), and the mathematical procedure replicated. In this case a 6-camera BTS motion capture system (60–120 Hz) synchronized with two Bertec force plates and integrated with two Imago resistive pressure platforms (1.56 sensors/cm²; 150 Hz) were used. The foot subareas were defined by projecting the anatomical landmark positions onto the plantar pressure footprint [5]. 38 patients were analyzed: 10 C, 14 diabetics (D), 14 PN. Three subareas were again selected, rearfoot, midfoot, forefoot [5].

Results: There was a good agreement between the main results of the two studies, the most interesting finding being the increased peak of the lateral component of shear force under the metatarsal region (LMR, Figure 1). In the first study, mean values and SD for LMR (%N) were 4.4 ± 2.1 for PN patients and 3.9 ± 2.1 for C. In the second study the mean and SD values (%N) were 7.7 ± 3.0 for PN patients and 6.7 ± 2.7 for C. The relative increase with respect to C was 20.4% in the first study and 20.7% in the second one.

Conclusion: The above studies confirm the need of a deep biomechanics analysis of the diabetic foot including vertical and shear forces during gait. The results from the two studies were in a good agreement, absolute differences mainly due to partially different subarea selection and adopted technologic solution. Further reliable measurement instrumentation and foot models should be validated and applied, also including in-shoe measurements, and the analysis of motor tasks more demanding than level walking.

References

1. Cavanagh P, et al: *The Diabetic Foot*, St. Louis: Bowker JH, Pfeifer MA 2001, 125–196.
2. Ledoux WR: *Foot and Ankle Motion Analysis* CRC Press: Harris GF, et al: 2008, 317–345.

3. Giacomozzi C, et al: *Diabetes Care* 2002, **25**:1451–1457.
4. Giacomozzi C and Macellari V: *IEEE Trans On Rehab Eng* 1997, **5(4)**:322–330.
5. Sawacha, et al: *Gait & Posture* 2006, **24**:S2–S3.

O4

Plantar fascia thickness and first metatarsal mobility in patients with diabetes and neuropathy

Smita Rao¹, Charles L Saltzman² and H John Yack³

¹Ithaca College-Center for Foot and Ankle Research, Rochester, NY, USA

²Department of Orthopaedics, University of Utah School of Medicine, Salt Lake City, UT, USA

³Department of Physical Therapy and Rehabilitation Science, The University of Iowa, IA, USA

E-mail: srao@ithaca.edu

Journal of Foot and Ankle Research 2008, **1(Suppl 1)**:O4

Introduction: Individuals with Diabetes Mellitus and Neuropathy (DN) are at increased risk for ulcer development at sites exposed to repetitive, high plantar loading. Limited joint mobility may contribute to increased forefoot loading by limiting foot flexibility and restraining the forward progression of body weight during the stance phase of gait. However data substantiating the causes and consequences of limited mobility in forefoot loading is limited. The purpose of this study was to compare plantar fascia thickness, passive and active 1st metatarsal (Met) mobility and loading in patients with and without DN.

Methods: All procedures were approved by the Institutional Review Board at the University of Iowa Hospitals and Clinics. 15 subjects with DN and 15 non-diabetic, age and gender matched control subjects participated in this study. Sagittal T1 scans were acquired using a 3T Trio scanner (Siemens Corp). Plantar fascia thickness was measured using ImageJ. Passive 1st Met mobility and stiffness were measured using the device described by Glasoe et al. [1] Foot mobility during walking was captured using a two-segment model tracking the 1st Met and calcaneus. Kinematic data were collected at 120 Hz, using 3 iReds on each segment (Optotrak, NDI, CAN), plantar loading data were collected at 50 Hz using a pedobarograph (EMed, Novel Inc). Kinematic data were low-pass filtered using a fourth order butterworth filter with cut-off frequencies of 6 Hz and processed using Visual3D (C-motion Inc., MD). Motion of the distal segment was expressed relative to the proximal segment using Euler angles. For kinematic data, stance phase mean was subtracted from pattern to correct for systematic offsets.

Statistical Analysis: A two sample t test was used to assess differences between the two groups ($\alpha = 0.05$). Pearson product moment correlation (r) was used to assess the relationship between variables of interest.

Results: Subjects with DN showed increased plantar fascia thickness, decreased passive 1st Met mobility and increased passive 1st Met stiffness. Subjects with DN showed reduced 1st metatarsal sagittal, transverse and frontal motion and increased medial forefoot loading (Table 1).

Plantar fascia thickness was negatively associated with passive 1st Met mobility ($r = -0.40$, $p < 0.05$) when considering both groups together ($n = 30$). In subjects with DN, 1st Met sagittal motion was negatively associated with peak pressure sustained under the medial forefoot ($r = -0.42$ and -0.06 , DN and Ctrl respectively, $p = 0.02$).

Table 1 (abstract O4) Plantar fascia thickness, foot mobility and loading, expressed as. Mean (SD)

Dependent Variable	DN	Ctrl	P value
Plantar fascia thickness (mm)	2.78 (0.64)	1.51 (0.33)	<0.001
Passive 1 st Met mobility (mm)	3.78 (0.63)	5.54 (2.13)	0.004
Passive 1 st Met Stiffness (N/mm)	10.69 (1.63)	8.13 (2.67)	0.003
1 st Met sagittal motion (deg)	13.0 (2.5)	15.8 (3.3)	0.047
1 st Met transverse motion (deg)	7.1 (3.1)	9.6 (3.6)	0.026
1 st Met frontal motion (deg)	9.8 (3.6)	12.3 (3.1)	0.029
Medial forefoot peak pressure (N/cm ²)	82.4 (29)	49.8 (10)	<0.001

Conclusion: Our results indicate that increased plantar fascia thickness limits passive first Met mobility. However we did not find evidence that passive 1st Met mobility or stiffness influences 1st Met mobility during gait. In individuals with DN, loss of sagittal 1st Met mobility correlated with increased medial forefoot loading, highlighting the importance of 1st Met mobility during functional activities.

Reference

1. Glasoe, et al: *Foot Ankle Int* 2000, **21(3)**:240–6.

O5

Evolution of foot manifestations in children with Charcot-Marie-Tooth disease

Joshua Burns¹, Monique M Ryan² and Robert A Ouvrier¹

¹Institute for Neuromuscular Research, The Children's Hospital at Westmead/Discipline of Paediatrics and Child Health, Faculty of Medicine, The University of Sydney, NSW, Australia

²Neurosciences Department, Royal Children's Hospital/ Murdoch Children's Research Institute, Melbourne, Victoria, Australia

E-mail: joshuab2@chw.edu.au

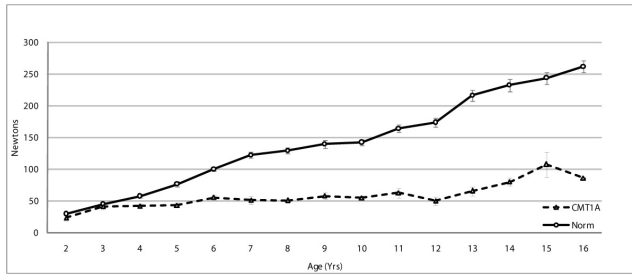
Journal of Foot and Ankle Research 2008, **1(Suppl 1)**:O5

Introduction: Charcot-Marie-Tooth disease (CMT) is the most common genetic nerve disorder. The most prevalent form, CMT1A, is characterised by demyelinating neuropathy with progressive foot and ankle weakness, contractures and deformity. The wide range of foot/ankle manifestations in CMT1A complicates the assessment, diagnosis and therapy. We aimed to characterise foot and ankle strength, flexibility, morphology and symptoms in children with CMT1A.

Methods: 81 children aged 2–16 y with CMT1A were objectively assessed for strength (dorsiflexion, plantarflexion, inversion, eversion) with hand-held dynamometry [1], ankle dorsiflexion flexibility using the weight bearing lunge [2] and foot morphology with the Foot Posture Index (FPI) [3]. We also looked for difficulties in heel or tip-toe walking, foot drop during gait, and questioned about foot/ankle pain, cramps, ankle instability, trips and falls during walking.

Results: Mean strength was: dorsiflexion 55N (SD, 20), plantarflexion 175N (SD, 49), inversion 76N (SD, 29), eversion 63N (SD, 24). While age ($r = 0.65$ – 0.80 , $p < 0.001$) correlated with foot strength, compared to age-equivalent norms, mean strength was lower in all ages of childhood CMT1A. This disparity was most evident for dorsiflexion (Figure 1).

Figure 1 (abstract O5)



Foot dorsiflexion weakness in CMT.

Ankle dorsiflexion ranged from 7–41° (mean 25°, SD 7). Compared to normal, ankle flexibility was lower in children at all ages with CMTIA. Interestingly, there were no significant correlations between ankle flexibility and age, height or body weight.

Foot morphology ranged from a FPI of -12 to +11 (mean 2, SD 5). 35% of children exhibited pes cavus, 39% had normal feet and 26% had pes planus. There was a significant correlation between FPI and age ($r = -0.47, p < 0.001$), indicating the evolution of pes cavus during growth (Figure 2).

Compared to norms, foot morphology in preschool children with CMTIA did not differ, but from the age of 5 years, deviated from normal towards a more cavoid appearance.

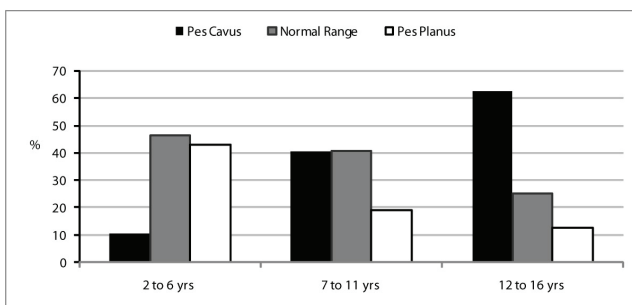
Difficulty heel walking occurred in 82% of children, 4% had difficulty tip-toe walking and 4% exhibited foot drop. 27% reported foot pain, 36% reported cramps, 72% described ankle instability, 63% reported frequent trips and 47% falls. Foot pain, cramps, toe-walking and foot drop worsened with age ($p < 0.05$).

Conclusion: Children with CMTIA experience foot weakness, contracture and deformity from an early age. These manifestations are expected to impact negatively on daily function. Early intervention targeting the foot and ankle may prevent long-term disability in CMTIA.

References

- Rose KJ, et al: *Muscle Nerve* 2008, **37(5)**:626–631, doi: 10.1002/mus.20961.
- Burns J, et al: *Foot* 2005, **15(2)**:91–94.
- Redmond AC, et al: *Clin Biomech* 2006, **21(1)**:89–98.

Figure 2 (abstract O5)



Age-related foot morphology in CMT.

O6

Comparison of the clinical heel rise test in subjects with Stage II PTTD and healthy controls

Chris Neville^{1,2}, Jeff Houck¹ and A Sam Flemister²

¹Ithaca College-Center for Foot and Ankle Research, Rochester, NY, USA

²University of Rochester, Rochester, NY, USA

E-mail: christopher_neville@urmc.rochester.edu

Journal of Foot and Ankle Research 2008, 1(Suppl 1):O6

Introduction: The heel rise test is commonly used as a strength test for the triceps sura muscle group but has also become widely used as a functional task to aid in the diagnosis of Posterior Tibial Tendon Dysfunction (PTTD) [1, 2]. Although failure to invert the hindfoot during the heel rise test is reported to be a sign of failure in the posterior tibial muscle, posterior tibialis function may also contribute to forefoot plantar flexion, assisting with raising the heel off the floor. Midfoot collapse associated with weakness of the posterior tibialis muscle may limit a PTTD subjects' ability to plantar flex the forefoot during the heel rise test. The purpose of this study was to compare sagittal plane ankle and midfoot kinematics as well as HF frontal plane kinematics in subjects with stage II PTTD and healthy controls during a bilateral heel rise test.

Methods: 30 stage II PTTD subjects (age; 59.2 (11.3) years, BMI; 29.8 (4.8)) and 15 healthy controls (58.6 (7.7) years, BMI; 30.5 (3.6)) were included in this study. While subjects performed a bilateral heel rise task, kinematic data was collected (sampled at 60 Hz, filtered at 6 Hz) from the shank, calcaneus (HF), and first metatarsal (FF) using an Optotrak Motion Analysis System (Northern Digital Inc, CAN) and Motion Monitor Software (Innsport Training Inc, USA). Kinematic data were used to calculate Cardan angles (Z-X-Y sequence) including ankle plantar flexion/dorsiflexion (HF relative to the shank), ankle inversion/eversion (HF relative to the shank) and midfoot plantar flexion/dorsiflexion (FF relative to the HF). Statistical Analysis: To compare groups a mixed design ANOVA model with a repeated factor of phase (three levels: start position, peak heel rise position, and ending position) and a fixed factor of group (two levels: PTTD and healthy controls) was utilized.

Results: There was no significant difference ($p = 0.11$) in sagittal plane ankle motion between subjects with PTTD and healthy controls across all phases of the heel rise test. Interestingly, although subject with PTTD began the heel rise test with greater eversion compared to controls (5 degrees difference $p < 0.001$) they achieved a position of inversion equal to controls at peak heel rise (1.7 degrees difference $p = 0.15$). A significant difference between groups in sagittal plane midfoot motion was found to be dependent on phase of the heel rise task (interaction $p = 0.05$). Pairwise comparisons between groups at each phase revealed a significant ($p = 0.03$) decrease in midfoot plantar flexion in subjects with PTTD (6.5 degrees) compared to healthy controls (12.1 degrees) at the peak heel rise position.

Conclusion: Raising the heel off the floor during the heel rise test is accomplished with both ankle plantar flexion and midfoot plantar flexion. Significantly reduced midfoot plantar flexion (midfoot collapse) was observed in PTTD subjects compared to healthy controls despite normal HF inversion. Hindfoot inversion may provide some stability to the midtarsal joint limiting midfoot collapse but this relationship is only partially able to protect

secondary ligaments. Summary: In this first investigation of the heel rise test failure to plantar flex the midfoot while completing the heel rise test was more common in subjects with stage II PTTD than failure to invert the hindfoot. The ability to stabilize the midfoot with muscle control or joint stability is compromised in subjects with stage II PTTD placing increased demand on support ligaments.

Acknowledgements

Collaborators in the Center for Foot and Ankle Research at Ithaca College-Rochester.

References

1. Alvarez RG, et al: *Foot and Ankle International* 2006, **27(1)**:2–8.
2. Flanagan SP, et al: *Journal Aging and Physical Activity* 2005, **13**:160–171.

O7

The effects of taping and exercise on ankle joint movement in subjects with functional instability (FI) of the ankle joint during a jump down

Eamonn Delahunty¹, Jeremiah O'Driscoll² and Kieran Moran³

¹School of Physiotherapy and Performance Science, University College Dublin, Republic of Ireland

²Mount Carmel Hospital, Republic of Ireland

³School of Health and Human Performance, Dublin City University, Republic of Ireland

E-mail: eamonn.delahunty@ucd.ie

Journal of Foot and Ankle Research 2008, **1(Suppl 1)**:O7

Introduction: Ankle joint taping is a common prophylactic measure used by individuals involved in sports. Little information is available on the effects of ankle joint taping on biomechanical parameters in subjects with FI during functional activities such as jump landing. [1] Thus the aim of this study was to examine the effects of ankle joint taping and exercise on ankle joint frontal and sagittal plane movement in subjects with FI while they performed a jump landing technique.

Methods: Eleven (7 male and 4 female) subjects with a history of unilateral FI volunteered to participate in the study. FI was defined as a score of ≤ 24 of 30 on the Cumberland Ankle Instability Tool (CAIT). [2] Each subject performed three single leg sagittal plane jump landings under three conditions; condition 1 (no tape), condition 2 (tape), condition 3 (post-exercise tape). The exercise protocol between testing of condition 2 and 3 consisted of a series of hopping, ladder and cutting drills. Joint movement was measured at 250 Hz using a 12 camera motion analysis capture system (Vicon Oxford Metrics, UK), while initial contact with the ground was identified using the vertical component of ground reaction force. Ankle joint frontal and sagittal plane motion was measured at 50 ms prior to and at initial contact (IC) with the ground.

Results: There was no significant effect on ankle joint inversion, either at 50 ms prior to [$F_{2,18} = 1.2$, $P = 0.32$] or at IC with the ground [$F_{2,18} = 0.4$, $P = 0.68$]. However, there was a significant effect on the angle of ankle joint plantar flexion, both at 50 ms prior to IC [$F_{2,18} = 29.4$, $P < 0.001$] and at IC [$F_{2,18} = 16.1$, $P < 0.001$]. Post hoc analysis revealed that condition 1 (no tape) resulted in significantly greater plantar flexion at 50 ms prior to IC than condition 2 (tape) [$7.7 \pm 3.0^\circ$; $P < 0.002$] and condition 3 (post-exercise tape) [$8.3 \pm 4.8^\circ$; $P = 0.001$]. Similarly,

condition 1 (no tape) resulted in significantly greater plantar flexion at IC than both condition 2 (tape) [$5.3 \pm 3.2^\circ$; $P = 0.002$] and condition 3 (post-exercise tape) [$5.3 \pm 4.4^\circ$; $P = 0.01$]. No significant differences were evident between condition 2 (tape) and condition 3 (post-exercise tape) [$P > 0.05$].

Conclusion: These results indicate that taping acted to reduce the degree of plantar flexion at both 50 ms prior to and at IC with the ground, and that these reductions were retained even after exercise.

Acknowledgements

This study was supported by the CPSM bursary of the Irish Society of Chartered Physiotherapists.

References

1. Cordova ML, et al: *J Athl Train* 2002, **37**:446–457.
2. Hiller CE, et al: *Arch Phys Med Rehabil* 2006, **87**:1235–1241.

Foot and Ankle Surgery

O8

Preliminary results of a biomechanics driven design of a total ankle prosthesis

A Leardini¹, JJ O'Connor², F Catani^{1,2,3}, M Romagnoli³ and S Giannini^{1,2,3}

¹Movement Analysis Laboratory, Istituti Ortopedici Rizzoli, Italy

²Engineering Science, University of Oxford, Oxford UK

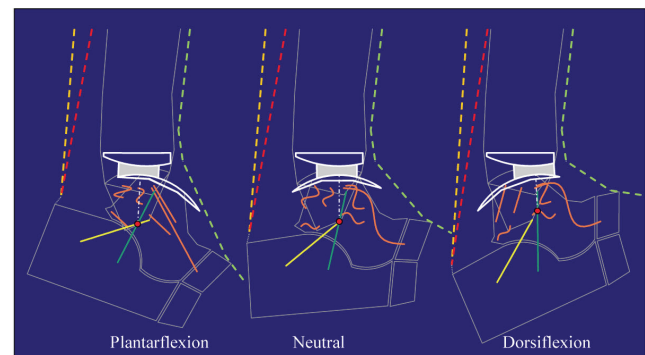
³Department of Orthopaedic Surgery, Istituti Ortopedici Rizzoli, Italy

E-mail: leardini@ior.it

Journal of Foot and Ankle Research 2008, **1(Suppl 1)**:O8

Introduction: A new design of total ankle replacement [1] was developed according to extensive prior biomechanical research [2–5]. A linkage-based mathematical model was used to design for the first time ligament-compatible shapes of the prosthesis components in the sagittal plane (Fig. 1). The radius of the metal talar component in the sagittal plane is about 50% longer than that of the normal talus, the metal tibial component is spherically convex. A fully conforming meniscal bearing is interposed between them and free to move. Experiments in cadaver specimens confirmed the mathematical prediction that the bearing moves forwards on both metal components during dorsiflexion and backwards during plantarflexion. FEA models [6]

Figure 1 (abstract O8)



Model-based mobility of the replaced ankle in the sagittal plane.

and experiments with a wear simulator [7] confirmed that the risk of wear is minimised. Preliminary clinical results are here reported as support to the biomechanical claims.

Methods: Between July 2003 and May 2007, the prosthesis was implanted in 189 patients at 7 hospitals in Northern Italy. Mean age was 59.4 years. The diagnosis was post-traumatic OA in 79.3%, primary OA in 6.9%, RA in 8.0%. At one hospital, range of motion was measured in the operating theatre before and after implantation in 90 ankles, and meniscal motion in lateral radiograms at maximum plantar- and dorsi-flexion in 30 ankles.

Results: At September 2007, the mean follow-up was 21 months. The mean pre-operative AOFAS score of 41.1 rose to 80.2, 79.7, 77.9, and 79.0 respectively at 18, 24, 36, 48 months. Mean dorsi-flexion increased after implantation from 0.1° to 9.7°, plantar-flexion from 15.1° to 24.6°. From radiographic measurements, the range of full motion, 14°–53°, was significantly correlated to the range of bearing movement on the tibial component, 2–11 mm ($r^2 = 0.37$, $p < 0.0005$), as predicted. Two revision operations had been performed, respectively for obvious surgical and indication errors. There were no device related revisions (loosening, fracture, dislocation). The Kaplan-Meier survival rate (components removal as end-point) at 4 years was 97% (Confidence interval 92–100).

Conclusion: The shapes of the three components are compatible with physiologic ankle mobility and with the natural role of the ligaments. The survival rate at four years compares well with multi-centre 5-year rates published by the Swedish (531 cases, survival 78%), Norwegian (257, 89%) and New Zealand (202, 86%) registries and with a recent meta-analysis [8]. The early clinical results have demonstrated safety and efficacy and encourage a widening of the clinical trial.

References

1. Leardini A, et al: *Clin Orth Rel Res* 2004, **424**:39–46.
2. Leardini A, et al: *J Biomech* 1999, **32**:111–118.
3. Leardini A, et al: *J Biomech* 1999, **32**:585–591.
4. Leardini A, et al: *Med Biol Eng Comp* 2001, **39**:168–175.
5. Leardini A, et al: *Gait Post* 2002, **15**:220–229.
6. Reggiani B, et al: *J Biomech* 2006, **39**:1435–1443.
7. Affatato S, et al: *J Biomech* 2007, **40**(8):1871–6.
8. Stengel D, et al: *Arch Orth Trau Surg* 2005, **125**:109–119.

O9

Pressure profile changes after cartilage biopsy at the postero-medial rim of the talar dome

Giovanni Arnoldo Matricali¹, Ward Bartels², Luc Labey², Greta Dereymaeker², Frank Luyten¹ and Jos Vander Sloten²

¹Department of Musculoskeletal Sciences, Katholieke Universiteit Leuven, Belgium

²Division of Biomechanics and Engineering Design, Katholieke Universiteit Leuven, Belgium
E-mail: giovanni.matricali@uzleuven.be

Journal of Foot and Ankle Research 2008, 1(Suppl 1):O9

Introduction: Autologous chondrocytes implantation is a promising technique to treat joint surface defects of the talar dome, especially when it is considered that a complete

arthroscopic procedure is available yet [1]. However, the exact biopsy site as source of the cells to be expanded remains an issue of debate. Recently we showed that a limited biopsy can be harvested reliably and consistently at the postero-medial rim of the talar dome by arthroscopy [2]. Further research must establish if this location is indeed a “lesser weight bearing area”. This study aims to determine the changes occurring in the pressure profile across the aforementioned site after a biopsy has been harvested.

Methods: Ten fresh frozen ankle specimens were tested. An anterior and posterolateral arthrotomy were used. Reference points just next to the articular cartilage were created. A template of the talar dome was made to shape the custom-made units of sealed pressure sensitive film. Specimens were mounted in a testing machine, the foot fixed on a custom-made tilting platform to allow positioning of the tibio-talar joint in neutral (N), 10° of plantar flexion (PF) or 10° of dorsiflexion (DF). Applied loads consisted of 2.5 times body weight in N and DF, and 1.5 times bodyweight in PF. The tests were performed before and after harvest of a postero-medial cartilage biopsy of 5 × 11 mm. The images were further analysed in the ImageJ environment. Digital photographs of the posterior side of the joint in each position were taken after harvest to study the relationship of the created defect to the tibial plafond. The pressure profile at the biopsy site was determined by scanning the stains across this zone in an antero-posterior direction and converting the grey values in pressures with aid of a calibration curve. The plots of each pre and post biopsy situation were analysed for significant changes. The photographs were analysed to determine the amount of coverage of the biopsy by the tibial plafond. Pre and post biopst stains were macroscopically analysed to detect any change in shape and any possible outline of the biopsy visible. Finally, all results were compared to cross-check for significant findings.

Results: Possibly significant changes in the pressure profile were noted twice in N and 5 times in PF, consisting of a lower pressure across the biopsy site after harvest. The pressure change ranged from 0.4–1.3 MPa. A rebound effect with pressures exceeding the pre biopsy level was never seen. In all other tests the pressure plots run parallel, although in some cases not superimposed. In the latter the highest pressure was seen both pre and post biopsy, the difference never exceeding 0.5 MPa. The biopsy site resulted (partially) covered by the tibial plafond 3 times in N and 8 times in PF. A change in the shape of the contact area or in the outline of the biopsy was seen 7 times in PF. After comparing all results a limited effect of the biopsy on the pressure profile was seen in PF in 6 specimens.

Conclusion: In only a part of the specimens a change in the local pressure profile was seen, after harvesting a postero-medial cartilage biopsy of 5 × 11 mm. All changes consisted in a lower pressure registered across the biopsy site and no peak pressures near to the biopsy site developed. Moreover all changes were in PF. In this position the joint is loaded only a short time during the stance phase and only in a limited way [3]. Therefore, currently the investigated biopsy site seems safe to be used in clinical practice.

References

1. Giannini S, et al: *Am J Sports Med* 2008, doi: 10.1177/0363546507312644.
2. Matricali GA, et al: *Arthroscopy* 2006, **22**(11):1241–1245.
3. Reggiani B, et al: *J Biomechanics* 2006, **39**:1435–1443.

O10**Robotic cadaver testing of a new total ankle prosthesis model (GERMAN ANKLE SYSTEM)**

Martinus Richter¹, Stefan Zech¹, Ralf Westphal²,
Yvonne Klimesch³ and Thomas Gosling³

¹Department for Trauma, Orthopaedic and Foot Surgery,
Coburg Medical Center, Germany

²Institute for Robotics and Process Control, Technical
University Braunschweig, Germany

³Trauma Department, Hannover Medical School,
Hannover, Germany

E-mail: info@foot-trauma.org

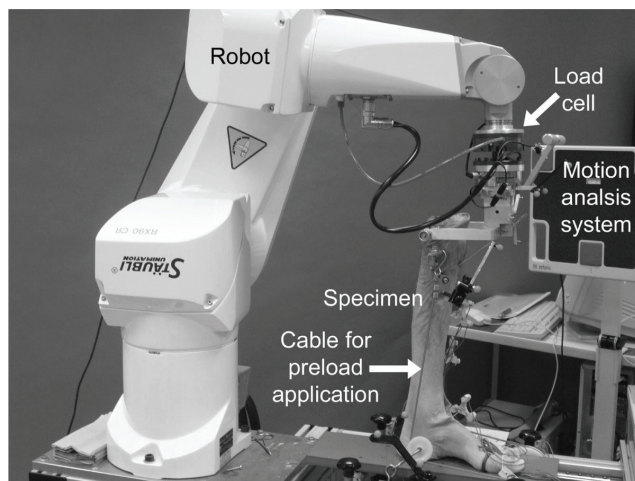
Journal of Foot and Ankle Research 2008, 1(Suppl 1):O10

Introduction: An investigation should be carried out into possible increased forces, torques and altered motions during motion of a load-bearing ankle after implantation of two different total ankle prostheses. A robot-based cadaver test was developed for the study. We hypothesized that the parameters investigated would not differ in relation to the two implants compared.

Methods: We included two different ankle prostheses (Hintegra, Newdeal SA, Vienne, France; German Ankle System, Small Bone Innovations, Morrisville, PA, USA). The prostheses were implanted in seven paired cadaver specimens (sides and testing sequence randomized). The specimens were mounted on an industrial robot (RX 90, Stäubli Tec-Systems, Bayreuth, Germany, Figure 1).

The robot was guided by a navigation system (VectorVision™, BrainLAB Inc., Kirchheim-Heimstetten, Germany). The robot detected the load-bearing (30 kg) motion of the specimens without prostheses during 100 cycles and mimicked that exact motion after the prostheses were implanted for another 100 cycles. The resulting forces and torques were recorded by an integrated load cell (model FT Delta SI-660-60; Schunk, Lauffen, Germany). The spatial orientation of the tibia, fibula, and foot plate was recorded via an ultrasound measurement system

Figure 1 (abstract O10)



Setting with robot, specimen, and motion analysis system. Specimen mounted to the robot and footplate and equipped with ultrasound transducers.

(model CMS HS; Zebris Inc., Tuebingen, Germany). The differences of the measured parameters were compared between prosthesis types.

Results: No shifting or dislocation of the tibial or talar components in relation to the specimen was observed after the testing by radiological assessment. No significant differences of forces, torques and motions (parameters as described below) occurred between the cycles 6–10 with the cycles 96–100 with prosthesis (paired-t-test for all parameters, $p > 0.05$).

The Hintegra and German Ankle System, significantly increased the forces and torques in relation to the specimen without prosthesis with one exception [One-sample-t-test, each $p \leq 0.01$ (exception, parameter lateral force measured with the German Ankle System, $p = 0.34$)]. The force, torque and motion differences between the specimens before and after implantation of the prostheses were lower with the German Ankle System than with the Hintegra (unpaired t-test, each $p \leq 0.05$).

Conclusion: In conclusion, the German Ankle System prosthesis had less of an affect on resulting forces and torques during partial-weight bearing ankle motion than the Hintegra prosthesis. This might improve function and minimize loosening during the clinical use.

References

1. Leardini A, O'Connor JJ, Catani F and Giannini S: **Mobility of the human ankle and the design of total ankle replacement.** *Clin Orthop* 2004, 39–46.
2. Valderrabano V, Hintermann B, Nigg BM, Stefanyshyn D and Stergiou P: **Kinematic changes after fusion and total replacement of the ankle: part 3: Talar movement.** *Foot Ankle Int* 2003, 24:897–900.

O11**Ankle morphometry in the Chinese population**

Chien-Chung Kuo^{1,2}, Guan-Ying Lee¹, Chia-Min Chang¹,
Horng-Chaung Hsu², Alberto Leardini³ and Tung-Wu Lu¹

¹Institute of Biomedical Engineering, National Taiwan
University, Taipei, Taiwan

²Department of Orthopedics, China Medical University
Hospital, Taichung, Taiwan

³Movement Analysis Laboratory, Istituto Ortopedici Rizzoli,
Italy

E-mail: twlu@ntu.edu.tw

Journal of Foot and Ankle Research 2008, 1(Suppl 1):O11

Introduction: Modern designs are now contributing to a remarkable renewed interest in total ankle arthroplasty (TAA), but TAA is still not as successful as total hip and total knee arthroplasty [1]. Among the remaining issues there is the design of the prosthesis components, which are often claimed to be 'anatomical' or compatible with the bony and ligament structures. However, very little is reported in the literature about the morphology of the distal tibia and proximal talus. Not a single is dedicated to the ankle morphological parameters in the Chinese population, which are expected to be addressed particularly in prosthesis designs dedicated to meeting the requirements of oriental life style. The purpose of the current study was to bridge the gap.

Methods: Ten ankle/foot cadaver specimens without any trauma or disease (mean foot length: 22 cm) were used in the current study. Each specimen was positioned at the neutral position and fixed to a plastic frame before receiving a

Table 1 (abstract O11) Mean, standard deviation, maximum, minimum, median values for all 8 measurements of the ankle joint for the 10 subjects analysed

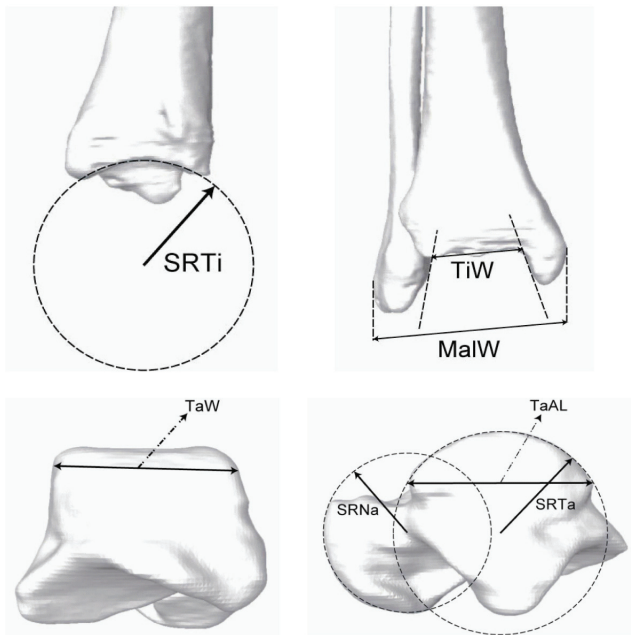
	Mean	S.D.	Max	Min	Median
Volume(cm ³)	30.01	3.88	35.74	25.55	29.81
SRTa(cm)	2.21	0.27	2.67	1.83	2.09
SRNa(cm)	1.70	0.14	1.88	1.49	1.75
TaW(cm)	2.99	0.21	3.35	2.63	2.96
TaAL(cm)	3.23	0.29	3.76	2.85	3.20
SRTi(cm)	2.98	0.79	4.75	2.00	2.92
MalW(cm)	6.15	0.28	6.64	5.82	6.08
TiW(cm)	3.19	0.24	3.67	2.82	3.17

computerized tomography (CT) scan at a slice thickness of 0.6 mm. The CT data were then used to reconstruct the 3D model of the bones and a MATLAB program was implemented with Geomagic STUDIO to obtain the morphological parameters of the distal tibia and proximal talus, Figure 1.

Results: The morphometrical measurements obtained (Table 1) are all smaller than those in a recent study [1], except for TaW, SRTi and Tiw. The observed relatively smaller bone mass of the distal tibia in the Chinese population suggests that the current tibial components might not be suitable for this bone in this population, and that stress fractures at the medial and lateral malleoli [2] may occur more frequently.

Conclusion: The success of an ankle prosthesis design depends largely on the morphological data from the ankle joints of its

Figure 1 (abstract O11)



Morphological parameters measured: talar width (TaW), tibial width (TiW), radii of the trochlea tali (TaAL) and the tibial mortise (SRTi), trochlea tali length (TaAL), inter-malleolus distance (MaIW).

targeted population. The measurements in the current study are expected to contribute to the design of surgical instruments and in particular of the dimensions for the different prosthesis component sizes, which were revealed to be under dimensioned. This is particularly true in post-traumatic ankles, where bones are larger than in normal ankles.

References

1. Stagni R, et al: *J Biomech* 2004, **37(7)**:1113–8.
2. Kumar Arun and Dhar Sunil: *Foot and ankle surgery* 2007, **13**:19–23.

O12

In-vivo first metatarsophalangeal joint mechanics following cheilectomy: MRI and gait alterations

Deborah A Nawoczenski¹, John Ketz², Josh Tome¹ and Judith F Baumhauer²

¹Ithaca College-Center for Foot and Ankle Research, Rochester, NY, USA

²Department of Orthopaedics, University of Rochester School of Medicine and Dentistry, USA

E-mail: dnawoczenski@ithaca.edu

Journal of Foot and Ankle Research 2008, **1(Suppl 1)**:O12

Introduction: Cheilectomy surgery has been shown to provide pain relief for patients with hallux rigidus [1], however limited data exists regarding the effectiveness of this surgery in re-establishing normal first metatarsophalangeal (1st MTP) joint kinematics. A recent dynamic gait study has reported only modest improvement in 1st MTP motion following surgery, thus implicating the persistence of altered joint mechanics [2]. The purpose of this study was to evaluate *in vivo* joint motion changes using MRI under 1st MTP loaded conditions in patients who received cheilectomy surgery. These data were compared to dynamic alterations during gait measured in a second cohort of subjects who previously underwent surgery.

Methods: 20 subjects were enrolled for the MRI analysis. Pre- and post-operative data of 10 subjects with hallux rigidus (HR) were compared to a healthy control group of 10 subjects. Using a validated loading harness, all subjects underwent an MRI evaluation at varying angles of 1st MTP dorsiflexion, pre and post surgery (>3 months). Image J software was used to derive MRI measurements: 1st MTP dorsiflexion, instant centers of rotation, and sagittal translations of the proximal phalanx/ 1st metatarsal. Outcome measures were assessed using the Foot Function Index (FFI). MRI changes were compared to 3D gait analysis previously acquired on a second cohort of 20 surgical subjects using a magnetic tracking device.

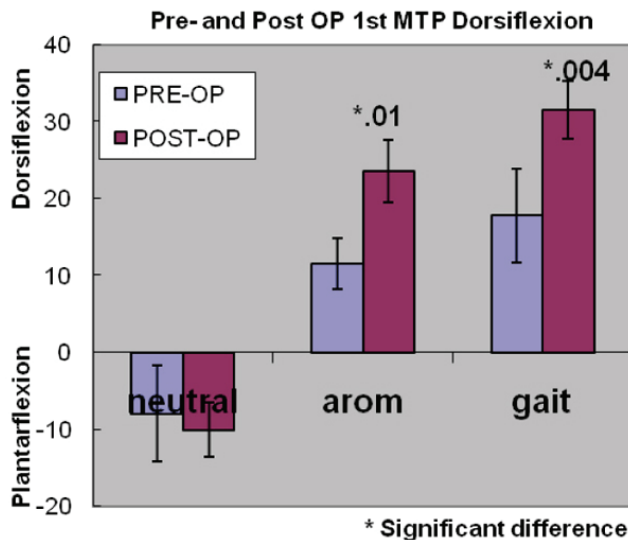
Results: All subjects had a significant decrease in FFI scores indicating an improvement in pain relief and function (p < .01). Table 1 shows pre- and post-op data compared to the control subjects. No significant differences were found between pre- and post-op measures for peak 1st MTP dorsiflexion, instant center of rotation (ICR), and sagittal translations of the hallux relative to the first metatarsal. Values for the cheilectomy group all remained significantly different from the control group (p < 0.001 for all variables).

These data can be compared to kinematic changes during gait, measured on a second cohort of subjects. Differences were found between pre- and post-op values, although still significantly less than normative values for 1st MTP motion [2]. Figure 1.

Table 1 (abstract O12) Controls, Pre- and post-op MRI values

Variable	Pre-op	Post-op	Controls
1 st MTP dorsiflexion	35.0° ± 8.8°	31.3° ± 10.0	64.4° ± 7.8°
ICR	8.9 ± 1.3 mm	8.6 ± 1.6 mm	4.2 ± 0.6 mm
Sagittal translation	1.6 ± 0.8 mm	1.5 ± 0.7 mm	5.5 ± 0.9 mm

Figure 1 (abstract O12)



1st MTP dorsiflexion during neutral/rest, active motion and gait.

Conclusion: Joint mechanics are significantly altered in patients with hallux rigidus. Although cheilectomy resulted in favorable outcomes as measured by FFI scores, surgery did not re-establish normal 1st MTP joint kinematics. Long term follow up of these patients will determine if altered kinematics lead to progressive arthritis over time and may suggest alternative intervention strategies.

References

1. Coughlin, et al: *J Bone Jt Surg* 2003.
2. Nawoczenski, et al: *Foot Ankle Int* 2008.

Shoes, Sport & Performance

O13

Effects of different shoe lacing patterns on perceptual variables and dorsal pressure distribution in heel-toe running

Marco Hagen, Ann-Kathrin Hömme, Tim Umlauf and Ewald M Hennig
 Biomechanics Laboratory, University of Duisburg-Essen, Germany
 E-mail: marco.hagen@uni-due.de

Journal of Foot and Ankle Research 2008, 1(Suppl 1):O13

Introduction: Foot movement in heel-toe running is influenced by various shoe lacing patterns [1]. Different shoe lacing systems and techniques also offer the possibility to improve shoe

fit and shoe comfort. The purpose of this study was to investigate the effects of different lacing patterns on dorsal foot pressures during running. Furthermore, perceived comfort and shoe stability ratings were recorded.

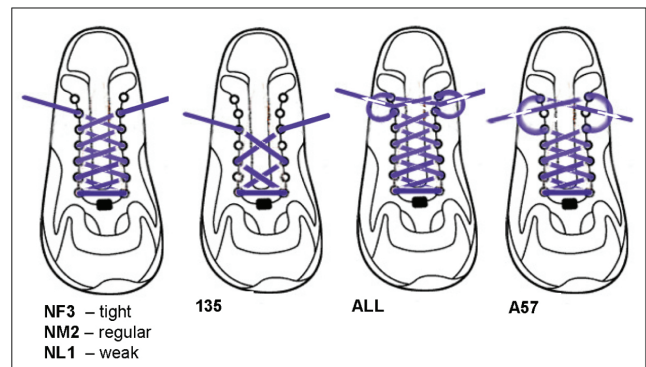
Methods: 14 experienced male rearfoot runners ran with the same running shoe (Nike Air Pegasus) in 6 different lacing conditions (randomized order) across a Kistler force platform at a speed of 3.3 m/s. Using pedar insoles (Novel) plantar and dorsal pressure distributions were measured. The dorsal sole was attached to the inside of the shoe’s tongue. The 54 active sensors on the foot dorsum were divided into 8 masks. The anatomical locations of the pressure sensors were identified by MRT-scans. One typical subject, wearing the test shoe and a modified sole with MRT-markers was scanned. The markers were placed on the sole at identical locations of the 54 sensors. Figure 1.

The lacing conditions differed in the number of laced eyelets and individually chosen lacing tightness (weak – NL1; regular – NM2; tight – NF3). Subjectively perceived comfort and stability within the shoe were identified on a perception scale. Shoe lacing comparisons were carried out using one-way repeated measures ANOVA with post hoc t-tests ($p < 0.05$). Average perceptual ratings were related to peak dorsal pressures with correlation and regression analyses.

Results: The subjects perceived the tightest six-eyelet lacing NF3 and the seven-eyelet lacings (A57, ALL) as the most stable conditions. The most comfortable lacing was A57, followed by the regular 6-eyelet lacing (NM2). Lacing ALL was perceived slightly less comfortable than NM2. The highest peak dorsal pressures were localized on the medial side of the foot dorsum: the talus and navicular, the medial cuneiform bone, and first metatarsal head. In the lower (135) and weaker (NL1) lacings peak dorsal pressures were significantly reduced on the tarsal bones and the extensor tendons compared to most other conditions. Compared to ALL, leaving out the sixth eyelet in A57, resulted in significantly lower ($p < 0.05$) peak dorsal pressures on the talus and navicular bone and lower peak pressures on the extensor tendons. Peak plantar heel pressures were significantly ($p < 0.05$) reduced in ALL and A57.

The correlation analyses revealed a highly significant ($p < 0.01$) relationship between perceived stability and peak dorsal pressures on the talus and navicular bone ($r^2 = 0.89$) and the extensor tendons ($r^2 = 0.97$). No significant relationship was found between perceived comfort and dorsal pressure data.

Figure 1 (abstract O13)



Lacing conditions.

Conclusion: The perception analyses indicate that a certain amount of lacing tightness is necessary to feel comfortable in the running shoe. Both 7-eyelet lacing techniques enhance perceived stability and can be recommended as very well foot-to-shoe-coupling techniques – with highest comfort in A57. The knowledge of the location of the peak dorsal pressures is useful for new tongue constructions and lacing systems to improve comfort in running shoes.

Reference

1. Hagen M and Hennig EM: *J Sports Sci* 2008 in press.

O14

Therapeutic efficiency and biomechanical effects of sport insoles in female runners

H Baur¹, A Hirschmüller², M Jahn³, S Müller¹ and F Mayer¹

¹Institute of Sports Medicine and Prevention, University of Potsdam, Germany

²Department of Orthopedics and Traumatology, University Hospital Freiburg, Germany

³IETEC Orthopädische Einlagen GmbH & und Produktions KG, Künzell, Germany

E-mail: hbaur@uni-potsdam.de

Journal of Foot and Ankle Research 2008, 1(Suppl 1):O14

Introduction: Orthopaedic insoles are used in sports medicine practice to treat overuse injuries although clinical evidence is still lacking. There are only few randomized controlled trials with male cohorts available [1]. Moreover, biomechanical effects of insoles remain unclear. Besides mechanical effects (“alignment of the skeleton”), sensorimotor effects are discussed suggesting an influence on neuromuscular control mechanisms by altering afferent input [2]. The purpose was therefore twofold: 1. To analyze the clinical efficiency of an insole intervention in female runners with overuse complaints, 2. To assess possible neuromuscular adaptation mechanisms by wearing insoles.

Methods: 48 female runners with running related overuse symptoms were randomly assigned to a control group (CO: age 35 ± 10 years, height: 1,66 ± 0,04 m, weight: 56 ± 5 kg, training km per week: 41 ± 25 km) and an insole therapy group (IN: age: 39 ± 10 years, height: 1,66 ± 0,06 m, weight: 58 ± 8 kg, training km per week: 37 ± 17 km). IN received an individually accustomed insole out of special polyurethane foam (molded, longitudinal arch support, bowl-shaped heel). All insoles were accustomed by the same orthopaedic technician. CO continued their regular training regimen without therapy, while IN used the insole for every run for 8 weeks. Both groups were analyzed on a treadmill at 12 km·h⁻¹ pre and post intervention. Surface EMG of the lower leg muscles (M. tibialis anterior, M. peroneus longus, M. gastrocnemius medialis) was measured while subjects ran (in random order) barefoot with a reference shoe and with the individually accustomed insoles. Mean amplitude quantities (normalized to barefoot running condition) in preactivation, weight acceptance and push-off phase were extracted from EMG [3]. Functional disabilities resulting from running related injury symptoms were examined using the Pain-Disability-Index (PDI). Pain Experience Scale (SES) was used to assess current pain rating [1]. The main outcome measure (PDI sum score) was analyzed by repeated measures ANOVA ($\alpha = 0.05$). SES values as well as EMG quantities were descriptively evaluated.

Results: PDI sum score decreased in IN (-40%) compared to CO (+3%) after 8 weeks ($p < 0.001$, $R_{sq} = 0.81$). SES values

showed a decrease in subjective pain rating in IN mainly in the first two weeks of therapy. Descriptive analysis of EMG amplitudes showed no changes in M. tibialis anterior and M. gastrocnemius medialis activity. M. peroneus longus amplitudes in preactivation phase showed an increase of about 30% after intervention in IN compared to CO.

Conclusion: Orthopaedic insoles molded out of polyurethane foam with longitudinal arch supports and bowl-shaped heels are able to reduce functional disabilities resulting from running related overuse injury symptoms. Therefore insoles can be used as an efficient non-surgical treatment option in female runners. Altered preactivation of the M. peroneus longus after therapy may result in optimized joint stability. This could possibly underline the concept of sensorimotor effects of orthopaedic insoles in sports.

Acknowledgements

This study was supported by the Federal Institute of Sports Science, Germany (VF 0407/01/49/2003–2005). Insoles were supplied by IETEC Orthopädische Einlagen GmbH & Produktions KG, Künzell, Germany.

References

1. Mayer F, et al: *Br J Sports Med* 2007, **41**(7):e6.
2. Nigg BM: *Clin J Sports Med* 2001, **11**:2–9.
3. Winter: *Biomechanics and Motor Control of Human Gait* 1991, 1–150.

O15

Rearfoot and knee coupling over a prolonged run in runners with patellofemoral pain syndrome

Irene S Davis¹ and Tracy A Dierks²

¹University of Delaware, Newark, DE, USA

²Indiana University, Indianapolis, IN, USA

E-mail: mcclay@udel.edu

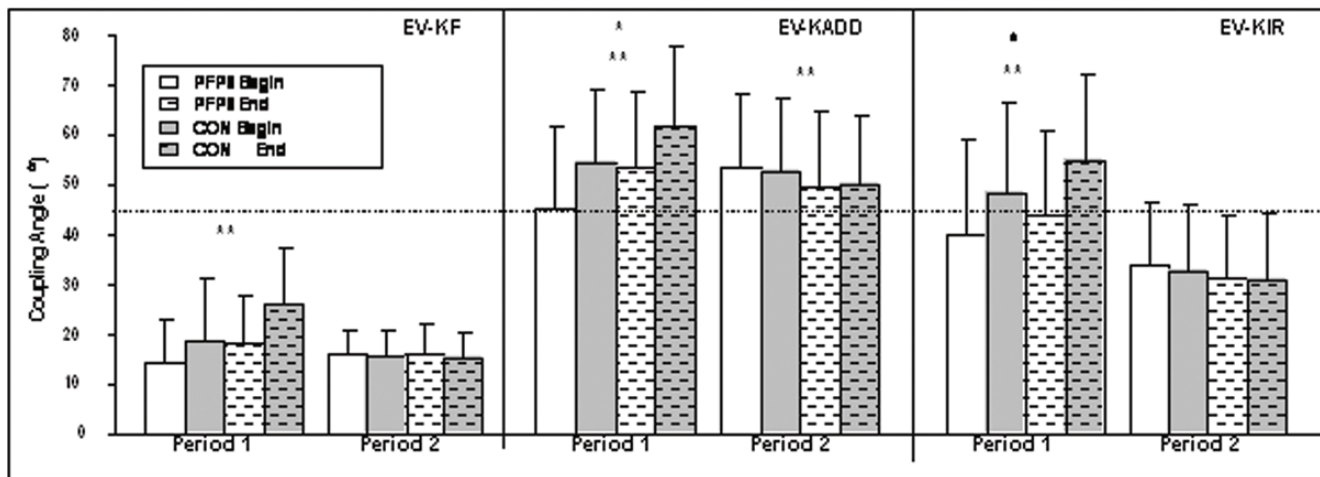
Journal of Foot and Ankle Research 2008, 1(Suppl 1):O15

Introduction: Patellofemoral pain syndrome (PFPS) is common in runners and is often related to excessive rearfoot eversion. Increased eversion is known to be associated with increased knee flexion, internal rotation, and reduced adduction [1]. Therefore, our purpose was to investigate coupling between the foot and knee in runners with PFPS. We hypothesized that the PFPS group would display larger coupling angles at baseline, due to relatively greater eversion. We also expected that these angles would increase to a greater degree in the PFPS group at the end of a prolonged run.

Methods: 20 runners (18–40 yrs) with PFPS and 20 controls (CON) participated in a prolonged treadmill run averaging 30–45 min. The run was stopped when preset criteria of heart rate, perceived exertion or knee pain were reached. 3D kinematic data were collected at the beginning and end of the run. A vector coding method [2] was used to assess the following joint couplings: rearfoot eversion (EV) with knee flexion (KF), adduction (KADD), and internal rotation (KIR). Coupling angles of 45° indicate equal joint excursions. Increasing values indicate more eversion, decreasing values indicate more knee motion. Values were averaged over the first half of stance: Period 1 (initial loading): footstrike to vertical impact peak (VIP) and Period 2 (maximal loading): VIP to vertical propulsive peak. A 2-factor ANOVA (group by time) was used ($p = 0.05$).

Results: There were no group by time interactions. During period 1, all coupling values were unexpectedly lower in the

Figure 1 (abstract O15)



Coupling angle group means during the 2 loading periods of stance at the beginning and end of the run.

* Significant main effect for group in a period. ** Significant main effect for time in a period. Horizontal dashed line at 45° indicates point of equal amounts of EV and knee excursion.

PFFS group, with EV-KADD and EV-KIR couplings being significantly lower (Figure 1). This relatively reduced eversion may have been a compensatory control strategy to minimize the abnormal knee mechanics that often accompany excessive eversion. This period of early loading is important, as the patella is not yet well seated into the femoral trochlea and is vulnerable to malalignment. By period 2, coupling angles were similar between the 2 groups for all relationships. As this is the period of maximal loading, the PFFS group may not have been able to maintain the relatively reduced EV seen in early loading. Over the course of the run, both groups increased their coupling angles in period 1 at the end of the prolonged run compared to the beginning. This may be an indication of fatigue, as EV has been shown to increase over the course of prolonged running [3].

Conclusion: Coupling angles are lower at initial loading in the PFFS group. During maximal loading, coupling is generally similar between groups. Finally, both groups increased their coupling angles over the course of the prolonged run.

References

- McClay I, et al: *Clin Biom* 1998, **13**:195–203.
- Sparrow A, et al: *J Mot Beh* 1987, **19**:115–129.
- Derrick T, et al: *MSSE* 2002, **34**:998–1002.

O16

Heel strike angle and foot angular velocity in the sagittal plane during running in different shoe conditions

Jens Heidenfelder, Thorsten Sterzing, Manuel Bullmann and Thomas L Milani

Department of Human Locomotion, Chemnitz University of Technology, Chemnitz, Germany

E-mail: jens.heidenfelder@phil.tu-chemnitz.de

Journal of Foot and Ankle Research 2008, 1(Suppl 1):O16

Introduction: Runners change their running style, e.g. heel strike strategy, to adapt to different shoe conditions [1]. Various

mechanisms for adaptation are discussed [2, 3]. Alteration of stiffness of the ankle joint at heel strike by dorsiflexion or plantarflexion of the foot seems to be disregarded as mechanism of adaptation.

In this study, alterations of heel strike angle (HSA) and plantarflexion velocity (PFV) in the sagittal plane due to wearing different shoe conditions was examined. By this, adaptation in running style as a mechanism of shock attenuation should be investigated.

Methods: Twenty-four male, injury-free recreational runners (age: 24.8 ± 2.5 years, height: 177.7 ± 5.8 cm, weight: 73.1 ± 7.1 kg) participated in this study. Three running shoes differing in heel height and cushioning properties were used: S1 = low heel, less cushioning; S2 = low heel, medium cushioning; S3 = high heel, medium cushioning.

Subjects performed five repetitive running trials across a force plate (Kistler 9287BA) at a speed of 3.5 ± 0.1 m/s. Kinetic parameters like peak vertical impact force (PVFI) and corresponding force rising rate (FRR) were obtained at a sampling rate of 1 kHz. Kinematic data of the foot and the shank were collected using a nine camera motion capture system (Vicon MX 3) at a sampling rate of 240 Hz. HSA in the sagittal plane and average corresponding PFV during touch down were calculated. A one-way repeated measures ANOVA was performed for each parameter in order to compare effects of the three shoe conditions. Furthermore, intraindividual variability across all subjects and shoes was quantified by the coefficient of variation (COV_{θ}).

Results: For kinematic and kinetic parameters highly significant differences were found between shoe conditions (Figure 1). Comparing progression of heel angle around touchdown ± 30 ms increased cushioning conditions (S2, S3) resulted in higher HSA (Figure 2).

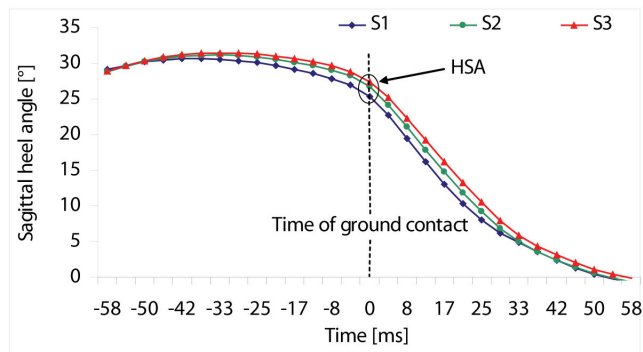
HSA and PFV show an individual range from 15.3° to 36.1° and $377^{\circ}/s$ to $664^{\circ}/s$ between subjects and shoes. Low intraindividual variability of subjects was found for all shoe conditions ($COV_{\theta HSA} = 5.4\%$, $COV_{\theta PFV} = 5.6\%$).

Figure 1 (abstract O16)

shoe	HSA [°]	PFV [°/s]	PVF1 [BW]	FRR [BW/s]
S1	26.7 (4.1)	484 (54)	1.92 (0.22)	84.5 (13.9)
S2	28.1 (3.6)	513 (59)	1.76 (0.23)	63.5 (10.8)
S3	28.7 (3.8)	488 (50)	1.73 (0.26)	58.3 (7.7)
p	<.01	<.01	<.01	<.01

Means (SD) of kinematic and kinetic parameters for the three shoe conditions.

Figure 2 (abstract O16)



Progression of heel angle.

No correlation was observed between HSA, PFV, and the kinetic impact parameters for individual subjects.

Conclusion: Significant differences of HSA and PFV between shoes support the assumption that heel strike angle and plantarflexion velocity in the sagittal plane are used to adapt to different shoe conditions independent from impact parameters. Furthermore, due to small intraindividual variability, it seems that magnitude of HSA and PFV is a characteristic feature of individual running style.

Acknowledgements

This research was supported by Puma Inc., Germany.

References

1. Nigg BM: HumanKinetics, Champaign, IL; 1986.
2. Frederick EC: *J Sports Science* 1986, **4**:169–184.
3. Mercer JA, et al: *Eur J Appl Physiol* 2002, **87**:403–408.

**O17
Biomechanical analysis of an inciting event of ankle sprain on basketball players**

MA Castro^{1,3}, MA Janeira², O Fernandes⁴ and LM Cunha⁵

¹ESTESC IPC, Portugal (Escola Superior Tecnologia da Saúde – Instituto Politécnico de Coimbra)

²FADE UP, Portugal (Faculdade Desporto – Universidade do Porto)

³FMH UTL, Portugal (Faculdade Motricidade Humana – Universidade Técnica de Lisboa)

⁴FD EU, Portugal (Faculdade Desporto – Universidade de Évora)

⁵FC UP, Portugal (Faculdade Ciências – Universidade do Porto)
E-mail: macastro@netcabo.pt

Journal of Foot and Ankle Research 2008, 1(Suppl 1):O17

Introduction: Lateral ankle sprains are very common among basketball players and are responsible for great time lost in

practice. Nevertheless, having the same exposure to risk by playing basketball, some athletes never sprain their ankles while others do. The aim of this study is to understand the main kinematics an electromyography differences in basketball players during the dynamic activity that causes more sprained ankles in basketball: jump to unstable surface.

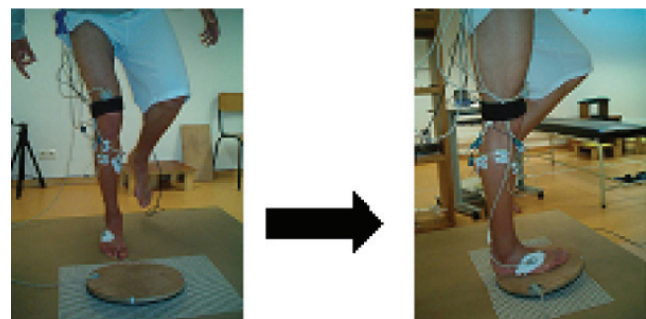
Methods: 24 elite basketball players, (12 females, and 12 males) underwent the same test procedures consisting of five consecutive jumps in unipodal support. Barefoot athletes with (NS) healthy (n = 17) and already sprained (S) ankles (n = 28) were asked to jump from the floor to an unstable surface in all directions (round Freeman board) placed 50 cm in front of them. Three experimental jumps were executed before data collection to familiarize the subject with the protocol and maximize the height of the jump (figures 1ab). This design aimed to reproduce the most vulgar mechanism of ankle sprain in Portuguese basketball players: landing in another player’s foot, which temporarily becomes an unstable surface. EMG data (1600 Hz) was recorded using bipolar, pre-amplified surface EMG electrodes (Daisy Lab), placed over four lower leg muscles (Tibialis Anterior TA, Peroneus Longus PL, Gastrocnemius Lateral GL and Medial GM). Motion data (100 Hz) was recorded using an electromagnetic tracking device with 3 sensors located in each segment (foot, shank and thigh) of lower limb.

Data was analyzed in four phases of movement: prepare to jump, push-off; ascending flying and descending flying that culminate on the contact moment.

Results: During jump athletes with already sprained ankles showed less flying time ($-p < 0,01$), probably leading to less preparation for contact and load (NS: $-0,111 \text{ sec} \pm 0,043$; S: $0,103 \text{ sec} \pm 0,030$). This could be the result of less accurate anticipatory postural adjustments by central nervous system of athletes that already sprained their ankle, which wouldn’t anticipate the equilibrium disturbance caused by the whole sequence of movements [1]. Konradsen [2] findings suggest a risk for ankle sprains when there is an ankle-position error. Regarding to landing kinematics, we found that knee and ankle angles at contact did change significantly with previous ankle sprain (table 1).

Although differences on landing moment are far more obvious for the ankle, they also become visible for knee flexion. Healthy subjects showed more knee flexion and less ankle plantar flexion on contact which gives them a better arrangement for lower limb impact absorption and creates a safer position for ankle load. They also showed lower muscle activity for all muscles with

Figure 1 (abstract O17)



Athletes jumping a) from a stable surface to b) an unstable board.

Table 1 (abstract O17) Knee and ankle angles on landing (deg)

	Healthy	Sprained	P Ancova
Knee Flexion	17,49 ± 12,52	14,63 ± 10,77	p < 0,05
Ankle planta flexion	-3,38 ± 10,04	-9,75 ± 14,18	p < 0,01

exception of TA which contraction is significantly different on both groups on landing.

Conclusion: This study identified different movement behaviour for the lower leg of healthy versus previous sprained ankles during the jump, which could possibly prevent the athlete from preparing for contact and supporting moment, leading to an ankle sprain, especially because of an ankle position in greater risk. Healthy athletes take more time preparing lower limb for contact moment and further load. These findings also suggest that healthy athletes manage to arrange a better position for lower limb to land, which may be a sign that there might be necessary to train athletes' jumps in "safe positions" in order to prevent ankle sprains.

Acknowledgements

Authors would like thank Prof. Gil Pascoal & IDP & PRODEP.

References

1. Le Pellec A and Maton B: *J Electromyogr Kinesiol* 2000, **10(3)**:171–8.
2. Konradsen L: *J Athl Train* 2002, **37(4)**:381–385.

O18

Impact of 90 minutes running exercise on plantar loading of the forefoot: a prospective study on symptom-free athletes

P-A Deleu¹, G Matricali², T Leemrijse¹ and K Deschamps²
¹Department of Orthopaedic Surgery, St Luc University Hospital, UCL, Belgium

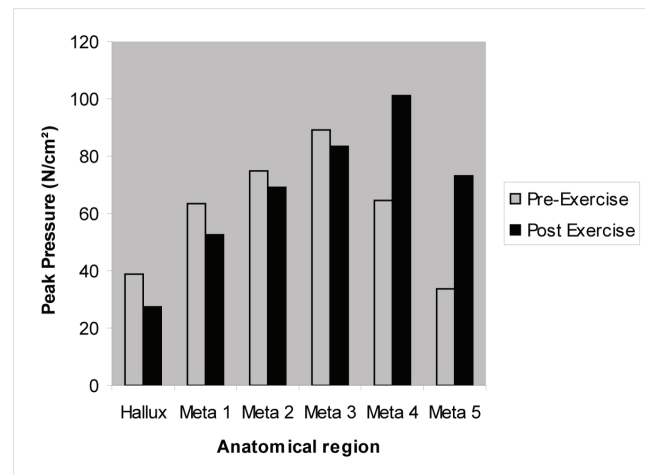
²Division of Musculoskeletal Disorders, University Hospital-Leuven, KU-Leuven, Belgium

E-mail: kevin.deschamps@uz.kuleuven.ac.be

Journal of Foot and Ankle Research 2008, **1(Suppl 1)**:O18

Introduction: Many studies have demonstrated that individuals who engage in running exercises appear to develop musculo-skeletal injuries more frequently [1]. Considering the foot, the most common injuries include stress fractures of the metatarsals, plantar fasciitis, tibialis posterior lesions and ankle sprains. Studies have been conducted who analysed the loading characteristics of the foot in repeated measurement designs – before and after exercise – in order to find a pathomechanical pathway for metatarsal stress fractures [2–4]. The published studies evaluated the in-shoe plantar pressure during treadmill running [2, 3] or barefoot after a marathon [4]. To date, no investigation have been conducted who evaluated the impact of a regular training session onto the forefoot loading characteristics. The objective of this investigation was therefore to identify changes in loading characteristics of the foot after a 90 minute running exercise.

Methods: Thirty-two volunteer athletes (4 women, 28 men) were recruited to participate in this study and gave their informed consent. During the pre-training session, participants were asked to run barefoot at a self-selected speed across a plantar pressure platform (RScan International, 0,5 m × 0,4 m, 4 sensors/cm², 300 Hz) that was embedded in a 16 meter walkway (EVA foam, shore 60). The post-training measurements

Figure 1 (abstract O18)

Changes in Peak Pressure between pre-and post-exercise in one patient.

were performed in the same location and according to the same method. Three left and three right steps were captured for each session and each participant. One observer localised 6 anatomical regions on the footprints using the multimask function of the software (Scientific version 7.0). For these regions (the five metatarsal heads and the hallux) the following dependent variables were analyzed: Peak Pressure, Impulse, Time to Peak, Start Time and End Time.

Intra-individual differences between both conditions were tested for significance with the paired student T-test.

Results: The contact time of the whole foot was not significantly different between the pre-and post training sessions, which indicates repeatable gait.

Also, no significant differences were found between the various parameters of the two sessions, and this for all the 6 regions under investigation.

However, in some participants a clear different Peak Pressure pattern (Figure 1), was found in the pre-and post exercise situation.

Conclusion: The results of this study show no significant changes in the loading characteristics as reported by other publications.

References

1. Fredericson M: *Sports Med* 1996, **21**:49–72.
2. Wilson JD, et al: *Med Sci Sports Exerc* 1999, **31(12)**:1828–1834.
3. Weist R, et al: *American Journal of Sports Medicine* 2004, **32(8)**:1893–1898.
4. Nagel A, et al: *Gait & Posture* 2008, **27**:152–155.

O19

Efficacy of an ankle orthosis with a subtalar locking system in restricting ankle kinetics and kinematics in lateral cutting

Songning Zhang, Michael Wortley, Qingjian Chen, Julia Freedman and Casey Riley

Biomechanics/Sports Medicine Lab, The University of Tennessee, Knoxville, TN, USA

E-mail: szhang@utk.edu

Journal of Foot and Ankle Research 2008, 1(Suppl 1):O19

Introduction: The ankle joint is the most injured joint during sports participation [1]. Ankle orthoses have been shown to be effective in reducing ankle inversion injuries and are often prescribed for rehabilitation and prevention of lateral ankle sprains. Efficacy of ankle orthoses is often assessed by comparing reduction of passive inversion ROM as well as ankle kinematics between braced and unbraced movements [2, 3]. However, joint kinetic responses in lateral cutting were rarely examined. Therefore, the objective of this study was to examine the effectiveness of a new semi-rigid ankle orthosis with a subtalar joint locking mechanism in restricting ankle kinetics and kinematics during a lateral cutting movement.

Methods: Ten female and ten male subjects performed five lateral cutting trials in each of four conditions wearing no brace (NB), a semi-rigid Element ankle brace with a calcaneal and subtalar locking system (AB1, DeRoyal), a semi-rigid Functional ankle brace with a hinge joint (AB2, DeRoyal), and a soft ASO lace-up ankle brace (AB3, Medical Specialties). A seven-camera motion analysis system (240 Hz, Vicon Motion Analysis Inc.) and a force platform (2400 Hz, AMTI) were used to obtain the three-dimensional kinematics and ground reaction force data respectively. A one-way repeated measures ANOVA was used to evaluate differences among the brace conditions on selected variables ($p < 0.05$) with post hoc comparisons conducted to detect specific differences among the braces using a Bonferroni adjustment (SPSS, Inc.).

Results: For the angular velocity, the peak contact inversion velocity (On_Y) was significantly reduced for AB1 compared to the control group (Table 1). No significant differences were seen in the peak lateral impact GRF (Min_X) among the brace conditions. However, the peak vertical GRF (Max_Z) for AB1 was significantly smaller than no brace and AB3. In addition, the peak ankle eversion joint moment (Min_Y) did not show significant differences among the brace conditions (Table 1).

Conclusion: The ankles did not reduce peak horizontal GRF data which is consistent with the findings of Cordova and his colleagues [2] in a shuffle movement. However, the peak vertical GRF was reduced with the Element brace compared to the ASO and control condition. Furthermore, the results showed that the Element ankle brace provides restriction of ankle inversion at early contact and pushoff. These results suggest that the Element brace is more effective in the lateral cutting. In addition, the tested orthoses also accommodate movement requirements that are commonly desired of an effective ankle orthosis.

Acknowledgements

Funded by DeRoyal Industries, Inc.

References

- Hootman JM, et al: *J Athl Train* 2007, **42(2)**:311–319.

- Cordova ML, et al: *Med Sci Sports Exerc* 1998, **30(9)**: 1363–1370.
- Gross MT, et al: *J Orthop Sports Phys Ther* 1997, **25(4)**: 245–252.

Pedography

O20

From “first” to “last” steps in life – pressure patterns of three generations

Kerstin Bosch, Arne Nagel, Lars Weigend and Dieter Rosenbaum

Movement Analysis Lab, Orthopaedic Department, University Hospital Muenster, Germany

E-mail: boschk@uni-muenster.de

Journal of Foot and Ankle Research 2008, 1(Suppl 1):O20

Introduction: The human foot has to bear loads during all kinds of bipedal locomotion throughout the whole life. Rapid developmental changes of foot morphology and foot function occur during the first years of walking [1]. Furthermore, disease dependent modifications can also have an influence on plantar loading [2]. Therefore, it is reasonable to assume that foot function alters in life [3]. However, the main differences between the pressure patterns in young and elder humans have not been well described? The aim of the present study was to evaluate age-dependent pressure patterns and their differences between new-walkers, 7-year olds, adults and seniors.

Methods: Dynamic foot pressure measurements were analysed in 104 healthy humans of 4 different age groups; each with 26 participants: New-walkers (1.0 yr. \pm 0.2); 7-year olds (7.0 yrs. \pm 0.4); adults (31.9 \pm 2.1); seniors (68.4 \pm 3.2). The participants walked barefoot with self selected speed over the emed x pressure platform (Novel, Munich). Mean values of either 5 left or 5 right foot trials were randomly selected and analysed. The foot was divided in 5 regions (heel, midfoot, forefoot, hallux, toes 2–5). Peak pressure (PP), Maximum force (MF), contact time (CT), contact area (CA) and arch index (AI) were evaluated. Local CT, CA and MF were normalised. ANOVA ($p < 0.05$) and the Tuckey as Post Hoc Test were used.

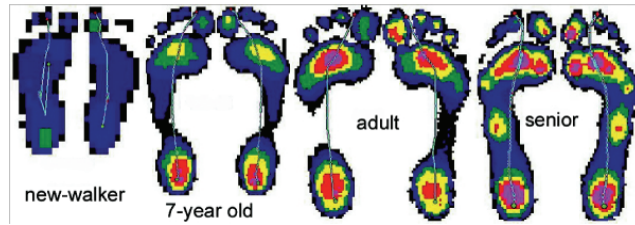
Results: Significant differences were found for each parameter between almost every age group. The most significant differences were observed for the new-walkers. Regarding the heel significantly lower PP were seen in the new-walkers. This is based on the fat pad, a lower body-weight to foot CA ratio and the non-existing initial heel contact in many new-walkers [1, 4]. Scott [3] found significantly lower pressures under the heel in elderly in comparison to young adults, which cannot be proven with our findings. However, a significantly reduced MF under the heel of the seniors could also be demonstrated in another study [3]. During the roll-over process the seniors' midfoot was loaded with 87% body-weight. This is twice as much as for the new-walkers, about 8 times more than in adults and 6 times more than for the 7-year olds. The seniors and new-walkers showed longer loading times in the mid- and forefoot in contrast to the other age groups, which can be explained by step length and foot structure differences [3]. The significantly higher PP under the seniors' midfoot can be attributed to the decreasing fat pad under the 5th ray. It cannot be ascribed to a flattened arch because no significant differences concerning the AI and the

Table 1 (abstract O19) Selected kinematic and kinetic variables: Mean \pm STD.

Cond	On_Y (deg/s)	Min_X (BW)	Max_Z (BW)	Min_Y (Nm/kg)
NB	322.3 \pm 103.7 ¹	-1.05 \pm 0.24	1.71 \pm 0.29 ¹	-0.58 \pm 0.19
AB1	263.6 \pm 113.6	-0.98 \pm 0.21	1.58 \pm 0.20 ³	-0.60 \pm 0.16
AB2	257.5 \pm 128.6	-1.02 \pm 0.27	1.67 \pm 0.28	-0.62 \pm 0.19
AB3	295.7 \pm 129.9	-1.04 \pm 0.23	1.68 \pm 0.24	-0.60 \pm 0.18

¹significantly different from AB1, ³significantly different from AB3.

Figure 1 (abstract O20)



Pressure patterns of each age-group.

midfoot CA between the seniors and the 7-year olds and adults were found. Only the new-walkers, with their developing arch showed a significantly higher AI with a larger midfoot CA in comparison to the others. Regarding the seniors and the new-walkers the CT, CA, AI and the MF values of a number of foot regions are comparable. Figure 1.

Conclusion: Significant differences of pressure patterns were found for every age group. The new-walkers showed the most differences in contrast to the others. The less significant differences were found between the adults and seniors. It can be assumed that with increasing age the pressure pattern develops again new-walker characteristics.

Acknowledgements

We are grateful to the participants and the DFG for funding (RO 2146/3-4).

References

1. Bosch, et al: *Gait Posture* 2007, **26**:238–47.
2. Schmiegel, et al: *Gait Posture* 2008, **27**:110–4.
3. Scott, et al: *Gait Posture* 2007, **26**:68–75.
4. Hennig, et al: *Foot & Ankle* 1991, **11**:306–11.

O21

Foot joint pressures during dynamic gait simulation

W Brent Edwards¹, Erin D Ward² and Timothy R Derrick¹

¹Department of Kinesiology, Iowa State University, Ames, IA, USA

²Central Iowa Foot Clinic, Perry, IA, USA

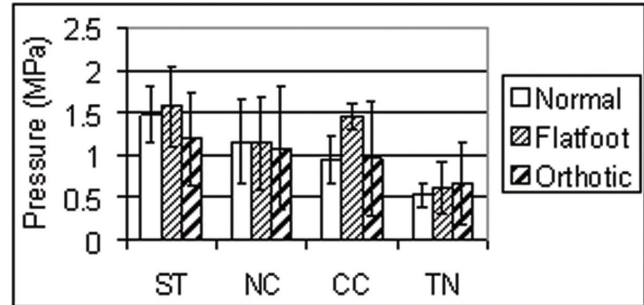
E-mail: edwards9@iastate.edu

Journal of Foot and Ankle Research 2008, 1(Suppl 1):O21

Introduction: Adult acquired flatfoot deformity is a progressive loss of normal function of the entire foot. A limited number of studies concerning joint pressures [1, 2] with adult acquired flatfoot exist. Custom orthotics [3, 4] are often used for conservative treatment of adult acquired flatfoot.

Methods: 5 fresh cadaveric specimens were connected to a dynamic gait simulator. I-scan #6900 sensors[®] were calibrated and surgically inserted into the subtalar (ST), naviculocuneiform (NC), calcaneocuboid (CC), and talonavicular (TN) joints using a joint spreader. Each foot was walked multiple trials across a force platform for three conditions (normal, flatfoot, flatfoot-orthotic). The flatfoot condition was created by detaching the posterior tibial tendon from the simulator and surgically releasing the spring ligament complex and the plantar fascia. Joint pressure data were collected at 100 Hz. Peak pressures were averaged within subjects and effect sizes were calculated between conditions.

Figure 1 (abstract O21)



Mean joint pressures. Pressures for CC and TN were only available for two feet.

Table 1 (abstract O21) Measurements of effect size

	ST	NC	CC	TN
Normal vs Flatfoot	-0.43	0.60*	-2.62**	-0.19
Normal vs Orthotic	3.40**	1.26**	-0.46	-0.03
Flatfoot vs Orthotic	2.17**	0.75*	3.96**	0.11

*medium effect, **large effect.

Results: Mean joint pressures ranged between 0.5 and 1.5 MPa (Figure 1).

According to Cohen [5], effect sizes of .20, .50 and .80 represent small, medium and large differences, respectively.

Medium and large effect sizes were observed for the ST, NC, and CC joint (Table 1). Compared to the normal condition: ST pressures were lower during the flatfoot and orthotic condition, NC pressures were lower during the flatfoot and orthotic conditions, and CC pressures were higher during the flatfoot condition. Compared to the flatfoot condition: ST, NC, and CC pressures were all lower during the orthotic condition.

Conclusion: Adult acquired flatfoot deformity appears to increase pressure at the CC joint, and slightly decrease pressure at the NC joint. The use of orthotics may be an effective method to reduce joint pressures in both the normal foot and flatfoot. The TN joint does not appear to be substantially affected by flatfoot deformity or the use of orthotics.

Acknowledgements

Tekscan, Inc., South Boston, MA, USA. KLM Orthotics Laboratory, Valencia, CA, USA.

References

1. McCormack AP, et al: *Foot Ankle Int* 1998, **19(7)**:452–461.
2. Reeck J, et al: *Foot Ankle Int* 1998, **19(10)**:674–682.
3. Leung AK, et al: *Prosthet Orthot Int* 1998, **22(1)**:25–34.
4. Imhauser CVW, et al: *Foot Ankle Int* 2002, **23(8)**:727–737.
5. Cohen J: *Psychol Bull* 1992, **112**:155–159.

O22

Correlation between plantar pressure and Oxford Foot Model kinematics

J Stebbins¹, C Giacomozzi² and T Theologis¹

¹Oxford Gait Laboratory, Nuffield Orthopaedic Centre, Oxford, UK

²Istituto Superiore di Sanita, Rome, Italy
E-mail: julie.stebbins@noc.anglox.nhs.uk

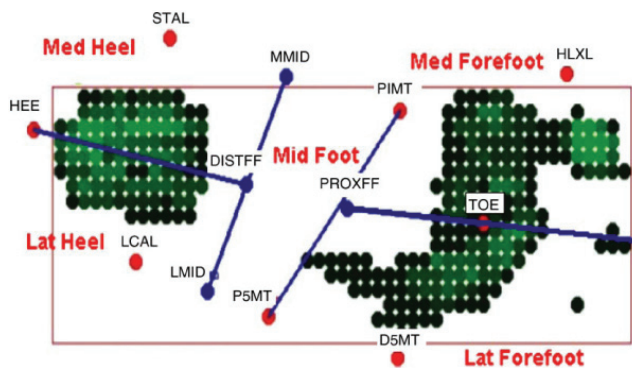
Journal of Foot and Ankle Research 2008, 1(Suppl 1):O22

Introduction: Plantar pressure measurement is widely used to assess foot deformity and plan treatment. However, measurement is notoriously variable, and the outcomes of questionable clinical relevance. The aim of this study was to provide an objective, comprehensive and clinically relevant measure of foot deformity by correlating pressure measurement with multi-segment foot model kinematics.

Methods: 35 children with hemiplegic cerebral palsy were assessed (19 male, 16 female, age 10.8 ± 3.2 yrs). Each child had 29 markers attached to both legs and the affected foot, according to the Oxford Foot Model (OFM) [1]. Data were collected with a 12 camera Vicon 612 system (Oxford, UK) and a prototype, piezo-resistive pressure plate (Istituto Superiore di Sanita, Rome, Italy) with a spatial resolution of 5 mm [2]. The positions of the markers on the foot were superimposed onto the pressure footprint at a time corresponding to mid-stance. The coordinates of each marker were then projected vertically onto the footprint (Figure 1). This provided the means to automatically divide the foot into five sub-sections on the basis of anatomical landmarks, and to correlate pressure findings with the output from the OFM. Peak force and area from each subdivision was correlated with clinically relevant variables from the OFM.

Results: No significant correlation was found between hindfoot varus and the medial/lateral distribution of force at the hindfoot (Table 1). This was presumed to be due reduced ground contact at the heel. There was also only minimal correlation between hindfoot varus and midfoot force and contact area. The force in the midfoot tended to be higher than that of the healthy population, regardless of whether the hindfoot was in varus or valgus. In the case of a varus hindfoot, this was due to weight bearing on the lateral border, while in the valgus hindfoot, it was due to a flattening of the arch. Dividing the midfoot into medial and lateral sections could have shown a more significant correlation. Interestingly, an inverse correlation was found between forefoot supination (in relation to the hindfoot) and lateral force at the forefoot. The direct correlation between hindfoot varus and forefoot lateral loading (0.64) indicates that the hindfoot varus is responsible for increased lateral forefoot

Figure 1 (abstract O22)



Pressure footprint showing five sub-areas. The labelled circles represent the projected positions of markers on the foot.

Table 1 (abstract O22) Correlation between OFM and pressure plate results

Foot Model	Pressure Plate	Corr
HF Varus	Lat:Med heel force	0.07
HF Varus	Lat:Med heel area	-0.11
HF Varus	Midfoot force	0.29
HF Varus	Midfoot area	0.15
FF supination	Lat:Med FF force	-0.54
FF supination	Lat:Med FF area	-0.48
FF/Tibia supination	Lat:Med FF force	0.41
FF/Tibia supination	Lat:Med FF area	0.43
HF Varus	Lateral FF force	0.64
HF Varus	Lat:Med FF force	0.59
HF dorsiflexion	Heel force	0.30
FF dorsiflexion	FF force	-0.45
FF/Tibia dorsiflex	FF force	-0.63

FF = forefoot, HF = hindfoot, Corr = correlation.

loading. Therefore, high loading of the lateral forefoot may not always be attributable to forefoot supination.

A significant correlation was found between increased forefoot dorsiflexion and decreased forefoot force as expected.

Conclusion: Correlating pressure measurements with multi-segment foot angles provides valuable insight into foot pathomechanics.

References

1. Stebbins J, et al: *Gait & Posture* 2006, **23(4)**:401–10.
2. Stebbins J, et al: *Gait & Posture* 2005, **22(4)**:372–6.

O23

Metatarsal fracture mechanism: accelerating loads the fifth ray more than cutting

Michael Orendurff¹, Eric Rohr², Ava Segal², Jonathan Medley², John Greenll³ and Nancy Kadel⁴

¹Movement Science Laboratory, Texas Scottish Rite Hospital for Children, Dallas, Texas, USA

²Motion Analysis Laboratory, VAPSHCS, Seattle, Washington, USA

³Orthopedics & Sports Medicine, University of Washington, Seattle, Washington, USA

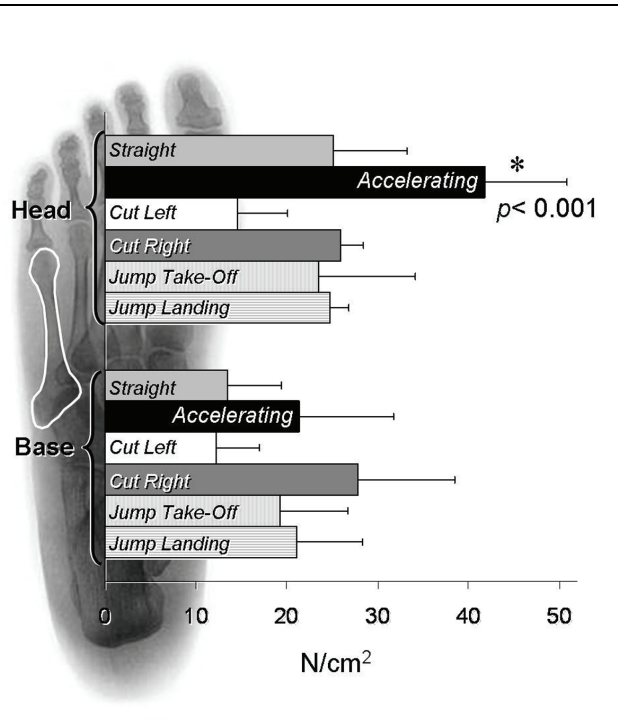
⁴Orthopaedic Surgery, University of California San Francisco, California, USA

E-mail: Michael.Orendurff@tsrh.org

Journal of Foot and Ankle Research 2008, 1(Suppl 1):O23

Introduction: Metatarsal fractures, especially of the 5th metatarsal are an increasingly common orthopedic problem among athletes [1]. Sports with a substantial amount of sprint and cutting movements appear to be at greater risk for both stress and acute fractures of the fifth metatarsal. One mechanism of injury is proposed to be the cumulative effect of the many bending moments applied to the fifth ray during cutting maneuvers, specifically to the foot on the inside of the turn [2]. This hypothesis has been bolstered by observing several athletes fracturing their 5th metatarsal during cutting maneuvers in games recorded on video, but no rigorous evidence exists to support cutting as the cause of the fracture. The purpose of this study was to identify the loading pattern of the fifth metatarsal

Figure 1 (abstract O23)



Peak plantar pressures (N/cm²) at the head and base of the fifth metatarsal during running straight, accelerating, cutting left, cutting right, jump take-off and jump landing.

during several typical sport maneuvers to determine if a bending moment is likely to occur.

Methods: Foot pressure was recorded using a Pedar (Novel, GmbH, München) insole system (99 Hz) on ten male college-aged athletes while they ran a course that included running straight, cutting left, cutting right, accelerating, jumping and landing. Using a videotape, each footstep was matched to a step processed in Emedlink to identify which maneuver was being performed. Seven regions of the foot were evaluated for peak pressure with specific focus on the fifth metatarsal head and fifth metatarsal base. The purpose was to determine which maneuver had the highest pressure on the fifth metatarsal head, and which maneuver had the greatest pressure differential between the base and the head of the fifth metatarsal – a corollary to a bending moment. A mixed-effects 2-way ANOVA (2 regions × 6 maneuvers) with Scheffe's tests post hoc were used for statistical analysis.

Results: The highest peak pressure occurred at the head of the fifth metatarsal during accelerating (41.8 ± 9.0 N/cm²; $p < 0.001$), 61% higher than the pressure during all other maneuvers (see Figure 1). Accelerating also had the greatest difference between the pressure at the head and the base of the fifth metatarsal (30 N/cm²), indicating the largest bending moment across the length of the fifth metatarsal during this maneuver.

Conclusion: Based on the pressure data from this study, bending moments applied to the fifth metatarsal appear highest when attempting to increase running speed (accelerating). Sudden increases in training load, especially activities involving sprint starts, should be tempered with adequate rest. Athletes

may be able to continue light work in practice if rapid changes in running speed are avoided.

References

1. Fetzter GB and Wright RW: *Clin Sports Med* 2006, **25**(1): 139–50.
2. Orendurff MS, et al: *Am J Sports Med* 2008, **36**(3):566–71.

O24

Pedographic findings in 461 patients in a foot and ankle outpatient clinic – definition of standard pedographic patterns for typical pathologies

Martinus Richter¹, Stefan Zech¹ and Axel Kalpen²

¹Department for Trauma, Orthopaedic and Foot Surgery, Coburg Medical Center, Germany

²Novel Inc., Munich, Germany

E-mail: info@foot-trauma.org

Journal of Foot and Ankle Research 2008, **1**(Suppl 1):O24

Introduction: Pedography is the most sophisticated method for biomechanical analysis in foot and ankle. Standard force distribution patterns for physiologic (normal) conditions had been defined on the basis of a sufficient number of examined individuals. However, standard force distribution patterns for certain pathologic conditions have not been established so far. Consequently, pedographic data could be compared with physiologic data only but not with standard pathologic data. The goal of this study was to create a basis for a definition of standard pedographic force distribution patterns for different typical pathologic conditions.

Methods: Patients who visited a foot and ankle outpatient clinic from October 1, 2006 to December 31, 2007 were included. Demographic data, clinical and radiological findings were registered. Standardized pedography (three trials, walking, third step, bilateral) using an EMED™ platform and software (Novel Inc., Munich, Germany) was performed. The patients were grouped regarding different typical pathologies such as Hallux valgus or flatfoot. The pedographic data were analyzed and compared between and within groups (ANOVA). Standard pedographic patterns were extracted from the data for the different pathologies. The definition of a standard was considered to be possible if no statistical differences within one group was found ($p > 0.05$), and if the power of this special analysis adequate (>0.8). The defined standard data for the different pathologies were also compared with known physiologic pedographic patterns (ANOVA). The null hypothesis at the $p < 0.05$ level means there is no difference between groups, and the defined standard data for the different pathologies and known physiologic pedographic patterns.

Results: 461 patients were included. 312 were female and 149 male. The mean age was 53 years. The patients were grouped as follows (n = 192 (42%) individuals in more than one group): forefoot/isolated Hallux valgus, n = 113 (25%); forefoot Hallux valgus & claw toes, n = 58 (13%); forefoot others, n = 110 (24%); midfoot deformity, n = 36 (8%); midfoot others, n = 40 (9%); hindfoot varus deformity, n = 18 (4%); hindfoot valgus deformity, n = 36 (8%); hindfoot others, n = 79 (17%); ankle deformity, n = 56 (12%); ankle instability, n = 15 (3%); flatfoot, n = 73 (16%); cavus foot, n = 19 (4%).

The standard pedographic parameters (contact time, contact area, maximum force, mean force, etc.) differed between groups

(ANOVA, $p < 0.05$). These parameters differed not within the groups (ANOVA, $p \geq 0.05$) for all groups except forefoot others, midfoot deformity, midfoot others, ankle deformity, hindfoot others. The power of this analysis was >0.8 for all subgroups except ankle instability and cavus foot. "Mean" pedographic patterns were defined if possible (see definition in methods). The null-hypothesis was rejected for the comparison between pathological groups, and between the defined standard data for the different pathologies and known physiologic pedographic patterns.

Conclusion: Typical pathologic foot and ankle conditions show a specific and typical force distribution pattern that differs from known physiologic data. A basis for the comparison of pedographic data with standard data for pathologic conditions was established patients with the following pathologies, isolated Hallux valgus, Hallux valgus & claw toes, hindfoot varus deformity, hindfoot valgus deformity, flatfoot, cavus foot. This data may serve as a valuable tool in foot and ankle diagnostics.

O25

New insights into stance phase foot biomechanics using pedobarographic statistical parametric mapping

Todd C Pataky¹, John Y Goulermas², Paolo Caravaggi¹ and Robin H Crompton¹

¹School of Biomedical Sciences, University of Liverpool, UK

²Department of Electrical Engineering and Electronics, University of Liverpool, UK

E-mail: tpataky@liv.ac.uk

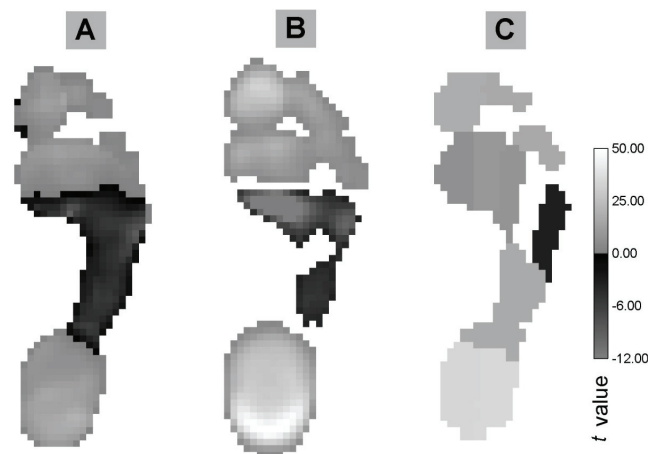
Journal of Foot and Ankle Research 2008, 1(Suppl 1):O25

Introduction: There is disagreement in the literature regarding the peak plantar pressure correlates of walking speed. Some studies report generalized increased pressures across the entire plantar surface [1] while others report decreases in lateral forefoot pressures and infer a medial shift in load with increased walking speeds [2]. The purposes of this study were: (a) To use statistical parametric mapping (SPM), a high resolution statistical technique, to clarify the pressure correlates of walking speed and (b) To corroborate SPM results with those of a traditional ten-region subsampling technique.

Methods: Ten subjects performed twenty trials of each of slow, normal, and fast walking in a fully randomized design. Plantar pressure data were collected using a Footscan 3D system (RSscan, Belgium). Walking speed was recorded with a six camera ProReflex system (Qualisys, Sweden). Peak pressure images were registered [3] using an optimal rigid body transform, and then between-subjects registration was performed using an optimum affine transform to ensure homologous structure overlap. The registered images were analyzed using pedobarographic SPM (pSPM), an adaptation of an established cerebral fMRI technique [4]. A parametric mass univariate general linear statistical model blocked SUBJECT effects and yielded a generalized SPEED regression statistic having the Student's t distribution. The original peak pressure images were also subsampled over ten anatomical regions using commercial software (Footscan 7, RSscan). These data were analyzed using the same linear model.

Results: pSPM analyses produced smooth and continuous statistical maps that exhibited positive correlation with walking speed over the heel and distal forefoot, but which also exhibited

Figure 1 (abstract O25)



(A) pSPM results for an example subject, unmasked. (B) Between-subjects pSPM results, masked at $p < 0.001$; data were qualitatively identical even after a Bonferroni correction of $p < 5 \times 10^{-5}$. (C) Subsampling results, masked at a Bonferroni-corrected $p < 0.005$.

broad negative correlation over the midfoot and proximal forefoot (Figure 1A). The significance of these trends was confirmed across subjects (Figure 1B). Subsampling obscured these data, exhibiting negative correlation only in the lateral forefoot, and reversing the midfoot trend (Figure 1C).

Conclusion: pSPM analyses revealed novel information regarding stance phase foot biomechanics, suggesting that longitudinal arch collapse is actively reduced as a function of walking speed and that such prevention may be beneficial to propulsion, possibly through increased plantar aponeurosis tension. The data also demonstrate, critically, that traditional subsampling techniques can distort or reverse statistical trends due to regional conflation, procuring erroneous conclusions regarding foot function. Foot pressure image analyses should incorporate all pixel data wherever possible.

References

1. Taylor AJ, et al: *Foot* 2004, **14**:49–55.
2. Rosenbaum D, et al: *Foot Ankle Surg* 1997, **3**:1–24.
3. Maintz JBA, et al: *Med Image Anal* 1998, **2**(1):1–37.
4. Friston KJ, et al: *Hum Brain Mapp* 1995, **2**:189–210.

Motion Analysis

O26

Foot motion in children and adults

Sebastian Wolf

Department of Orthopedic Surgery, University of Heidelberg, Germany

E-mail: Sebastian.Wolf@ok.uni-hd.de

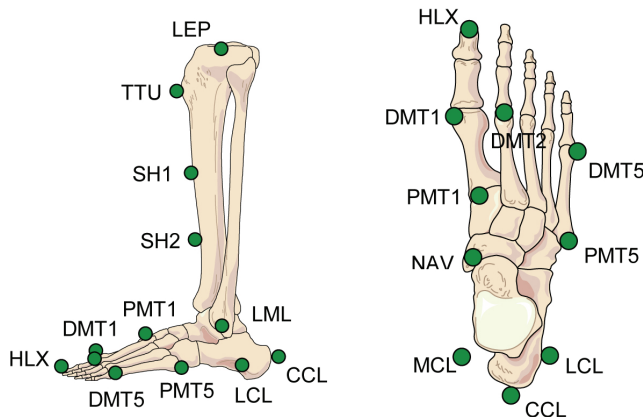
Journal of Foot and Ankle Research 2008, 1(Suppl 1):O26

Introduction: When studying the function of the human foot, foot pressure measurements offer some insight into the biomechanics of the growing foot [1] and models have been proposed to measure the foot kinematics especially of children [2]. Aside from ankle kinematics however [3], little is known

about differences in foot motion between children and adults. This ongoing study therefore examines the foot kinematics of normal subjects in a large age range.

Methods: Normal feet of 30 children aged 4–11 years (mean 7.8 yrs) and of 24 adults aged 19–51 years (mean 32.4 yrs) have been examined by instrumented gait analysis using the Heidelberg foot measurement method (HFMM) [4] with the marker set illustrated in Figure 1. In this method, the motion of the hind foot is described relative to the tibia by tibio-talar (ankle) flexion and subtalar rotation. For mid- and forefoot motion, functional parameters are evaluated which are relevant for a clinical evaluation

Figure 1 (abstract O26)



Marker set.

Table 1 (abstract O26) Comparison of foot parameters

	Children	Adults	p
ROM Tib.-talar flexion	19 ± 4	25 ± 6	0.000
ROM Ankle flexion	30 ± 5	34 ± 7	0.017
ROM Subtalar evers	11 ± 2	11 ± 3	0.504
ROM Medial arch	17 ± 4	17 ± 4	0.789
ROM Medial arch tilt	19 ± 7	17 ± 7	0.393
ROM Lateral arch	13 ± 3	13 ± 3	0.634
ROM Fore/Hindf. add.	9 ± 3	10 ± 3	0.109
ROM Foref./Ankle add	12 ± 3	14 ± 4	0.042
ROM Foref./Ankle supi	10 ± 2	14 ± 4	0.000
ROM Fore/midf. supin	6 ± 2	6 ± 2	0.463
ROM MT1–5 Angle	10 ± 3	13 ± 4	0.003
ROM Hallux abduct	8 ± 3	6 ± 2	0.029
ROM Hallux extens	46 ± 8	48 ± 8	0.379
ROM Foot Alignment	15 ± 5	13 ± 5	0.377
MSw Subtalar evers	7 ± 6	8 ± 6	0.607
MSw Medial arch	122 ± 8	129 ± 10	0.009
MSw Medial arch tilt	-3 ± 7	0 ± 9	0.131
MSw Lateral arch	-1 ± 7	-4 ± 6	0.119
MSw Fore/Hindf. add.	-13 ± 4	-13 ± 6	0.839
MSw Foref./ankle add.	-6 ± 4	-4 ± 4	0.015
MSw Foref./Ankle supi	7 ± 4	9 ± 4	0.073
MSw Fore/midf. supi	-12 ± 5	-12 ± 4	0.847
MSw MT1–5 angle	0 ± 5	6 ± 5	0.000
MSw Hallux abduct	-14 ± 5	-15 ± 6	0.286
MSw Hallux extens	21 ± 8	19 ± 6	0.430
MSw Foot Align. (ARO)	2 ± 5	5 ± 4	0.008

forming together a standardized set of 12 angles. The ROM in each angle has been determined across the gait cycle as a “dynamic” evaluation. Further, these parameters have been evaluated in mid swing to find “static” differences with respect to age in the geometry of the unloaded foot. A student T-Test was used to evaluate differences between the feet of children and adults.

Results: Data are summarized in Table 1. We find a smaller ROM across the gait cycle in (conventional) ankle flexion for children in agreement with [3] and specifically a smaller ROM in tibio-talar flexion. Further, children show smaller ROMs in forefoot supination and adduction. Most prominent “static” findings in mid swing were a higher cavus (smaller medial arch angle) and less divergent metatarsals (MT 1–5 angle) with also a smaller ROM in children compared to adults.

Conclusion: In normal walking, foot motion in children differs significantly to foot motion in adults with respect to forefoot and hind foot motion.

References

1. Bosch K, Gerss J and Rosenbaum D: *Gait Posture* 2007, **26** (2):238–47.
2. Stebbins J, et al: *Gait Posture* 2006, **23**(4):401–10.
3. Ganley KJ and Powers CM: *Gait Posture* 2005, **21**(2):141–5.
4. Simon J, et al: *Gait Posture* 2006, **23**(4):411–24.

O27

Shoe inserts alter inter-segmental foot motion and provide symptomatic relief in patients with midfoot arthritis

Smita Rao¹, Judith F Baumhauer², Josh Tome¹ and Deborah A Nawoczenski¹

¹Ithaca College-Center for Foot and Ankle Research, Rochester, NY, USA

²Department of Orthopaedics, University of Rochester, Rochester, NY, USA

E-mail: srao@ithaca.edu

Journal of Foot and Ankle Research 2008, 1(Suppl 1):O27

Introduction: Patients with midfoot arthritis present with disabling pain, which limits their participation in walking and other physical activity. The primary aim of treatment is to afford pain relief and is often attempted using shoe inserts. The custom-molded three-quarter insert (3Q) is recommended as the first line of treatment; however clinical experience shows that patients continue to report pain. Recent reports indicate that the full length carbon graphite insert (FL) may offer symptomatic relief in patients with midfoot arthritis. However the mechanisms by which the FL may be effective remain unknown. The purpose of this study was to examine the effects of four-week intervention with the FL on self-reported outcomes and in vivo inter-segmental foot motion in patients with midfoot arthritis.

Methods: 17 patients with midfoot arthritis participated in this study. Mean age: 62 ± 4 years, Mean BMI: 29.6 ± 5.4) 13/17 patients were previous users of the 3Q orthosis. In accordance with IRB and HIPAA guidelines, Informed Consent was sought prior to initiating study procedures. Patients’ self-reported outcomes were documented using the Foot Function Index – Revised (FFI-R) prior to and after four week intervention with the FL orthoses.

In vivo segmental foot motion was examined using a 5 segment foot model with previously established validity, as patients walked at self-selected monitored speed (0.82 ± 0.25 and 0.89 ± 0.19 m/s, 3Q and FL respectively, p = 0.49). Modified shoes, with

Table 1 (abstract O27) Summary of kinematic variables

Dependent variable	3Q	FL	P value
Calcaneal eversion	2.5 ± 3.0	3.9 ± 4.2	0.05
Forefoot abduction	5.9 ± 8.6	8.3 ± 9.7	0.10
Arch dorsiflexion	12.8 ± 8.2	15.6 ± 8.1	0.02
1 st MTP dorsiflexion	16.3 ± 10.9	14.4 ± 8.2	0.10

cut-out windows to accommodate the sensors were worn during walking. Local co-ordinate systems were established by digitizing anatomical landmarks of interest. Kinematic data were low pass filtered using a fourth-order Butterworth filter with a cutoff frequency of 6 Hz and analyzed using MotionMonitor™ software. Euler angles, representing three sequential rotations (Z-Y-X) were used to describe joint motion. Peak values for all dependent variables were referenced to subtalar neutral: calcaneal eversion, forefoot abduction, arch dorsiflexion, 1st metatarso-phalangeal (MTP) dorsiflexion. Paired-t tests were used to examine differences between orthoses conditions.

Results: Four week intervention with the FL orthosis provided symptomatic relief evidenced as 17 and 15% decrease in pain and activity limitation scores. Improvements were also reflected in total FFI-R score (36 ± 10 and 32 ± 9, baseline and after four week intervention respectively, p = 0.02). Compared to the 3Q orthosis, use of the FL orthosis resulted in increased calcaneal eversion, forefoot abduction and arch dorsiflexion as well as decreased 1st MTP dorsiflexion. (Table 1).

Change in pain score was correlated with arch dorsiflexion available in the FL condition (r = 0.60, p < 0.05).

Conclusion: The findings of this study demonstrate that four-week intervention with the FL affords symptomatic relief in patients with midfoot arthritis. Use of the FL was accompanied by distinct kinematic changes, all of which allowed the foot to assume a lower arched position. Arch dorsiflexion explained a third of the variance in change in pain score. Our findings suggest that kinematic changes, occurring independently or in combination, when using the FL orthoses, result in favorable short-term response to intervention. We hypothesize that kinematic changes in inter-segmental foot motion may influence articular loading and mediate relief of symptoms in patients with midfoot arthritis.

Acknowledgements

The carbon foot plates used in this study were donated by Wrymark Inc. This work is also supported in part by the Arthritis Foundation and the AOFAS.

O28

Use of the Oxford Foot Model in clinical practice

Jennifer McCahill, Julie Stebbins and Tim Theologis
Oxford Gait Laboratory, Nuffield Orthopaedic Centre,
Oxford, UK

E-mail: jennifer.mccahill@noc.anglox.nhs.uk

Journal of Foot and Ankle Research 2008, 1(Suppl 1):O28

Introduction: The Oxford Foot Model (OFM) [1] has been used routinely in clinical practice to assess foot deformity during gait in our laboratory since 2004. Over this time, 163 patients with various pathologies have been assessed. The aim of this study was to determine the OFM's clinical relevance in defining dynamic foot deformity thereby assisting management decisions in two populations: idiopathic clubfoot and cerebral palsy/hemiplegia.

Methods: Idiopathic Clubfoot – 24 patients (7 female and 17 male, age range 6 to 24 years) have been seen – 12 bilateral, 7 right and 5 left clubfeet for a total of 36 feet. All patients were surgically treated to correct foot deformity at an early age with a posterior-medial release. Ankle range of motion and weight bearing foot posture were assessed in a standardised clinical examination (CE) and compared with foot model kinematics.

Cerebral Palsy – Hemiplegia – 70 patients (34 male and 36 female, age range 6 to 38 years) have been assessed. Six of these subjects were measured bilaterally.

Results: Idiopathic Clubfoot – The findings from the OFM were used to identify the level of foot deformity in order to specify the type of surgery required, justify the type of casting appropriate to correct foot deformity, clarify the source of foot rotation (ie tibial, hindfoot, forefoot), and to corroborate clinical findings. The OFM influenced future management in 45% of the patients seen (Table 1).

The CE and OFM had best agreement in hindfoot plantarflexion and inversion, and forefoot adduction in relation to the tibia. Arch height was increased in 7 feet (cavus) and reduced in 8 feet (planus); clinically cavus was described in 16 feet and planus in 16 feet. Hindfoot internal rotation was present in 64% of feet post-surgically and was the sole cause of forefoot adduction in relation to the tibia in 33% of feet.

Cerebral Palsy – Hemiplegia: The OFM was used to assess dynamic foot motion to define indications and assess the outcome of surgical or orthotic management, Botulinum Toxin treatment and serial casting. The model was also used to monitor the progression of foot deformity, to clarify controversial findings from conventional lower limb kinematics, to determine the level of foot drop, and to corroborate clinical findings. The OFM directly influenced management in 71% of cases. Figure 1 summarises the findings of the foot model in this population.

Conclusion: Understanding the foot's dynamics during gait adds crucial information compared to the CE alone. The information gained from the OFM has become gradually more influential in the decision-making process. As with conventional gait analysis in its first steps, multi-segment foot kinematics is becoming increasingly important in clinical practice; in planning management and assessing results.

Reference

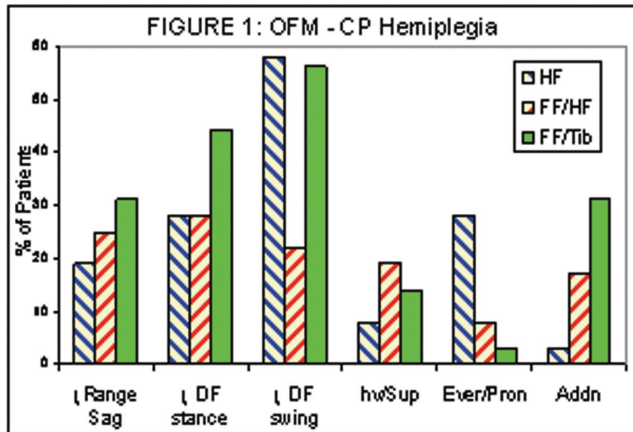
1. Stebbins, et al: *Gait & Posture* 2006, 23(4):401–10.

Table 1 (abstract O28) Results of CE and OFM data

Hindfoot							
	↓ DF	↑ DF	↑ PF	Inversion	Eversion	IR	ER
CE	0	22	7	8	18	4	0
OFM	6	3	5	9	10	23	4
Forefoot							
	↓ DF	Supn (Tib)	Addn (HF)	Addn (Tib)	Abdn (HF)	Abdn (Tib)	
CE	0	6	0	25	0	0	
OFM	11	15	11	22	6	3	

Key: ↓df-inadequate dorsiflexion; ↑df-excessive dorsiflexion; ↓pf-restricted plantarflexion; IR-internal rotation; ER – external rotation; supn (Tib) – supination related to tibia; addn/abdn (HF)-adduction/abduction related to hindfoot; addn/abdn (Tib) – adduction/abduction related to tibia.

Figure 1 (abstract O28)



Oxford Foot Model Findings – CP hemiplegia. Key: ↓Range Sag = reduced range in sagittal plane, ↓DF stance – reduced dorsiflexion in stance, ↓DF swing = reduced dorsiflexion in swing, Inv/Sup = excessive inversion/supination, Ever/Pron = excessive eversion/pronation, Addn = excessive adduction. HF = hindfoot with respect to tibia, FF/HF = Forefoot with respect to hindfoot, FF/Tib = Forefoot with respect to tibia.

O29

Validation of windows for examining kinematics of the foot with respect to the shoe using a multi-segment foot model

Rebecca Shultz, Trevor Birmingham and Thomas R Jenkyn
 Wolf Orthopaedic Biomechanics Laboratory, Fowler Kennedy Sport Medicine Clinic, The University of Western Ontario, London, ON, Canada
 E-mail: rshultz2@uwo.ca

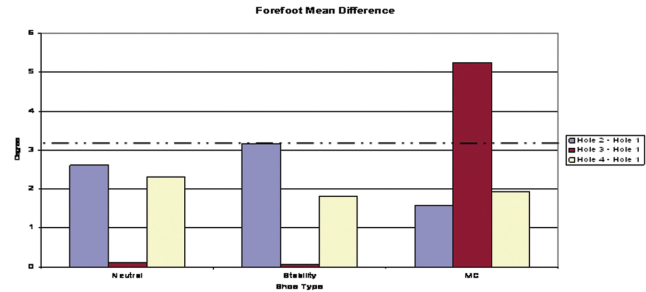
Journal of Foot and Ankle Research 2008, 1(Suppl 1):O29

Introduction: Shoes designed for specific foot types are speculated to decrease running injuries by encouraging different foot kinematics. One method to test this hypothesis is to track reflective markers affixed to the foot via windows cut in the shoe. The window size should be small enough to maintain the shoe’s structural integrity. Only one study had a detailed description of the method used to validate window sizes in the hindfoot [1]. The objective of this study was to validate window sizes for five different locations in the shoe: calcaneus, navicular, first metatarsal, fifth metatarsal and hallux using an optical tracking system.

Methods and procedures: One subject was tested under 3 different shoe conditions (motion control, stability and cushioning) with standard gait analysis using an 8-camera system motion capture system (Eagle camera, EvaRT system, Motion Analysis Corporation, Santa Rosa, CA). For the first 10 trials, the shoe was intact with a heel and toe markers affixed to the shoe. For the next four conditions, windows of increasing size were cut into the shoe above the calcaneus, navicular, first metatarsal, fifth metatarsal and hallux bone. Triad marker clusters were affixed to the skin of the foot via the windows.

A neutral trial was collected in quiet standing and digitization of bony landmarks were collected for each condition [2]. The subject then walked at a self-selected pace over an 8 m runway. The deformation of the shoe was assessed using the toe and heel markers on the shoe, and lateral malleolus marker. The foot was

Figure 1 (abstract O29)



All mean differences for the 2.5 cm hole are below 3°.

tracked as five individual segments [2]. The forefoot and hindfoot with respect to the midfoot (frontal plane) and the height/length ratio of the medial longitudinal arch were measured and compared for each window size [2].

Shoe deformation was assessed by mean differences between window sizes each compared to the intact shoe at the instant of heel raise. Foot kinematics differences were compared as mean differences between the first hole size and the following three hole sizes at heel raise. Sensitivity of the system was considered to be less than 3°. Any mean difference below 3° was considered insignificant.

Results: Both the shoe and the foot calculations demonstrated that a window size of less than 2.5 cm diameter was appropriate for all three shoes. Window sizes above this deviated from the original motion of the foot. Shoe motion generally remained constant. The forefoot graph is shown in Figure 1 as an example.

Discussion: Results show that the 2.5 cm holes were a valid window sizes in the three shoes. The first marker size was not chosen since larger windows increased camera visibility of the markers on the foot and the decreased the possibility of marker-shoe contact. The study was limited by the fact that only one subject was tested, using one shoe per condition. Future investigation of different shoes during different movements should be conducted since window size is speculated to depend on shoe type, shoe brand and activity.

Acknowledgements

This research was made possible by generous contributions from Saucony.

References

1. Stacoff, et al: *Med Sci Sports Exerc* 1991, **23(4)**:482–90.
2. Jenkyn TR, et al: *J Biomech* 2007, **40(14)**:3271–8.

O30

A new protocol for complete 3D kinematics analysis of the ankle foot complex in stroke patients

MG Benedetti¹, M Manca², G Ferraresi², G Cervigni², L Berti¹ and A Leardini¹
¹Movement Analysis Laboratory, Istituto Ortopedici Rizzoli, Bologna, Italy
²Movement Analysis Laboratory, Dept. Rehabilitation Medicine, Arcispedale S. Anna, Ferrara, Italy
 E-mail: benedetti@ior.it

Journal of Foot and Ankle Research 2008, 1(Suppl 1):O30

Introduction: Most widespread clinical gait analysis protocols for lower limb kinematics provide information about the ankle

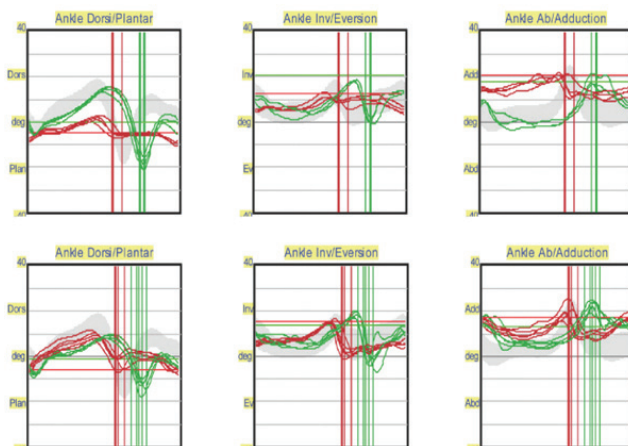
motion only in the sagittal plane. Behavior of the foot in the coronal plane during gait is usually determined just through the measure of the foot angle of progression. In the clinical practice most of the patients, particularly with upper motor disease, present a complex deformity of the foot in the three anatomical planes, most frequently in equinus, varus, supinated foot. Adequate kinematic analysis requires full consideration of the 3D ankle-foot complex position and motion on the basis of appropriate biomechanical conventions. The aim of the present work is to test the efficacy of current kinematic protocols for gait analysis in the measurement of 3D motion in stroke patients with foot deformities before and after surgery.

Methods: Ten stroke patients with equinus-varus foot deformity were analysed. Patients were evaluated by means of a clinical examination including: leg and foot alignment, range of motion, spasticity, strength and selectivity, and observational gait analysis of foot during gait. Patients were assessed by means of the Vicon system (8 TVC) during gait using Total 3D Gait protocol (T3DG) [1]. Five subjects were assessed over the same gait cycles by means of Plug in Gait protocol (PIG) [2] sharing common markers. Five subjects were evaluated before and after surgery for foot deformities.

Results: Data obtained in the ten patients with the T3DG protocol provided a complete 3D measure of the deformity consistent with clinical measure of alignment and of range of motion. In the five patients evaluated during the same gait cycle by means of the two protocols, it was evident the added value of the T3DG protocol in providing information on the coronal and transverse planes. Data on operated patients provide evidence of changes induced by surgery. Figure 1.

Conclusion: Total 3 D Gait protocol, based on anatomical references and on the ISB convention [3] for the biomechanical reconstruction of movement, provides reliable 3D kinematics data of the ankle foot complex during gait, consistent with clinical findings. This offers greater support to clinicians in patients with severe foot deformities, such as stroke patients, for which the instrumental analysis is relevant for dynamic deformity measure, clinical decision making and outcome assessment, particularly after surgery.

Figure 1 (abstract O30)



Ankle-foot complex rotations before (top row) and after (bottom) surgery.

References

1. Leardini A, et al: *Gait Posture* 2007, **26(4)**:560–71.
2. Davis RB III, et al: *Hum Mov Sci* 1991, **10**:575–87.
3. Wu G, et al: *J Biomech* 2002, **35(4)**:543–8.

O31

3D foot joints angle description using projected lines on anatomical planes

Hossein Rouhani¹, Julien Favre¹, Xavier Crevoisier², Brigitte M Jolles² and Kamiar Aminian¹
¹Ecole Polytechnique Fédérale de Lausanne (EPFL-LMAM), Lausanne, Switzerland

²Centre Hospitalier Universitaire Vaudois & University of Lausanne, Lausanne, Switzerland

E-mail: hossein.rouhani@epfl.ch

Journal of Foot and Ankle Research 2008, **1(Suppl 1)**:O31

Introduction: An increasing trend for 3D kinematic analysis of multi-segment foot has emerged both in clinical and biomechanical studies [1, 2]. Nevertheless, existence of several joints among tiny bones of foot causes difficulties both for joint angle definition and their measurement. Unlike with the larger lower limbs bone, it is hardly possible to put three reflective markers over each foot bone. Subsequently, it is not practical to define local coordinate systems (LCS) for all foot segments bounding foot joints. This work proposed a simple method for foot joints angle description which is easy to interpret.

Methods: Since it is hardly possible to have LCS based on three rigid markers per foot segment, many of standard joint angle description methods (e.g. JCS) might not be suitable for many foot joints. Moreover, such conventional methods might not be efficient for some foot joint angles descriptions in clinical applications.

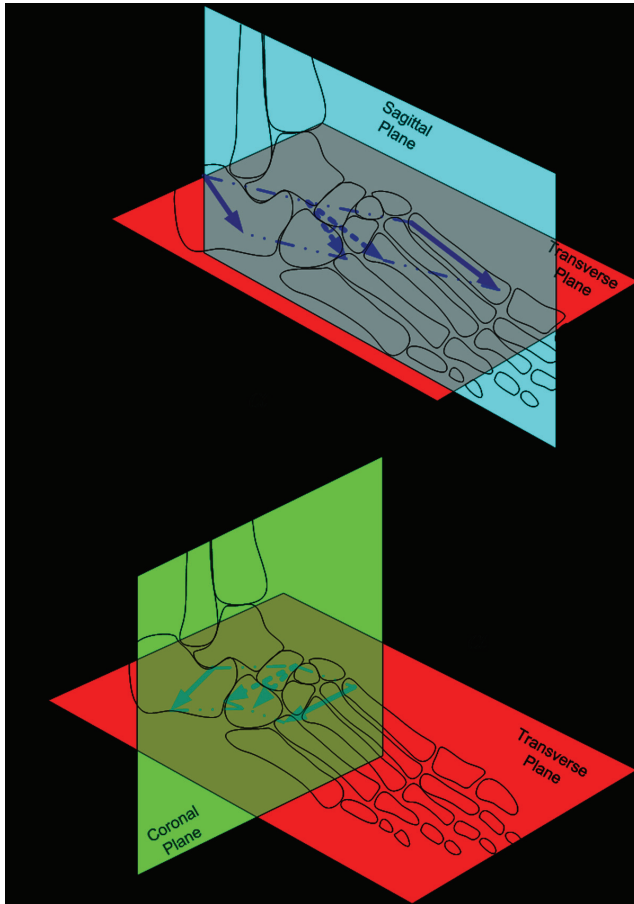
Recently, Simon et al [2] proposed a new foot joint angle description where each joint angle is defined by the rotation angle between two lines corresponding to two segments about a rotation axis on the third segment. The defined joint angle is equal with the angle between projections of two lines on the normal plane of the rotation axis. The results were repeatable and reliable. Nevertheless, there was a need for defining one axis for each considered joint which complicates the 3D kinematic model of foot. We proposed to define all foot joint angles by projection on three common anatomical planes.

Sagittal, coronal and transverse planes of whole foot were defined based on [3]. For each considered foot joint, one line per each of two segments bounding the joint was defined between captured anatomical landmarks (AL). As an example, Figure 1 depicts this method for the case of angle calculation for the considered joint between calcaneus and metatarsals.

Results: The proposed method was applied for foot kinematic analysis of 6 subjects with 21 tiny markers on ALs of foot. The 3D joint angle patterns and ranges were comparable to those of the other methods [1]. For similar angles, repeatability and sensitivity to measurement errors were showed to be in the same range as other angle representation methods.

Conclusion: A method to describe 3D angles of foot joints was suggested with an easy clinical interpretation. Without use of LCS, the method had also the similar performance as other conventions. Yet, the movement of foot's anatomical planes can induce error which can be avoided by definition of rotation axis on the same joint segments and not others. The suitability of method will be soon assessed in clinical applications.

Figure 1 (abstract O31)



Definition of calcaneus-metatarsals joint angles: a) Lines defined for sagittal projection b) Lines defined for coronal projection.

References

1. Leardini A, et al: *Gait & Posture* 2007, **25**:453–462.
2. Simon J, et al: *Gait & Posture* 2006, **23**:411–424.
3. Cappozzo A, et al: *Clinical Biomechanics* 1995, **10**(4): 171–178.

O32

Comparison of gait data using two different protocols for ankle joint kinematics

I Krauss¹, A Stacoff², D Axmann³, C Ziegler¹, S Grau¹ and T Horstmann¹

¹Medical Clinic, Department of Sports Medicine, University of Tuebingen, Germany

²ETH Zuerich, Institute for Biomechanics, Switzerland

³Dental Clinic, Department of Prosthodontics, University of Tuebingen, Germany

E-mail: inga.krauss@med.uni-tuebingen.de

Journal of Foot and Ankle Research 2008, 1(Suppl 1):O32

Introduction: Gait analysis is an important instrument in various fields of clinical research and its protocols are intended to make kinematics interpretable for clinicians.

Although they use the same nomenclature for joint angles, different protocols produce different results [1]. The purpose of this study was to compare gait events of the ankle joint to determine differences between two protocols.

Methods: Two different protocols were used to quantify distinctive kinematic variables in the stance-phase of barefoot walking at a normal speed:

(1) A functional approach (FA), assuming a ball-and-socket joint at the ankle [2].

(2) A prediction approach (PA) based on anatomical studies [3], differentiating between upper and lower ankle joint.

A single comprehensive marker-set was defined allowing the use of exactly the same gait cycles for both protocols. 10 healthy normal weight subjects (mean = 27 y, s = 5.8) were analyzed on two consecutive days M1 and M2. Landmark definition was done by the same physiotherapist for all subjects. A 12-camera Vicon MX40 system system collected data at 100 Hz. Five force plates were used to detect gait events. Peak eversion, frontal plane range of motion (ROM) and peak plantar flexion of the ankle joint were extracted from the curve data. At least 5 trials were averaged for each subject and measurement day, respectively.

Agreement between the two methods was quantified using the Bland & Altman Plot [4].

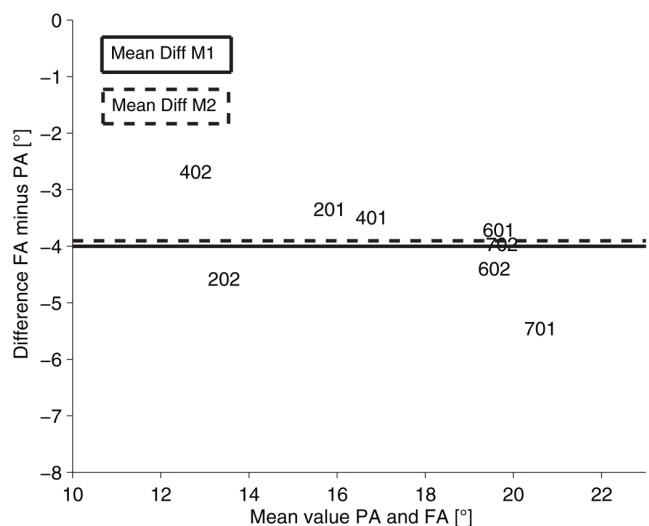
Results (preliminary data of 4 subjects): Figure 1 exemplifies the differences of the peak plantar-flexion between the two methods (y-axis) plotted against their mean values (x-axis). Each subject (2, 4, 6, 7) is represented for M1 (i.e. 201) and M2 (i.e. 202). Mean Diff 1 and 2 display the mean difference between methods for each day.

Based on the preliminary data, there does not seem to be a relation between the magnitude of the mean values of the two protocols and the magnitude of their differences. Furthermore, differences between protocols are similar for both days.

Table 1 shows a smaller peak plantar flexion (see also Figure 1) and peak eversion and frontal plane ROM for FA.

Conclusion: The use of different gait analysis protocols for the description of ankle joint kinematics yields different results for

Figure 1 (abstract O32)



PA vs. FA for peak plantar-flexion.

Table 1 (abstract O32) Mean differences FA-PA in degrees

Variable	Mean Diff (FA-PA)	
	M1	M2
Peak eversion	-1.3	-1.4
Frontal plane ROM	-6.3	-5.9
Peak plantar flexion	-4.0	-3.9

both absolute joint angles and ROM. This should be considered when results from different studies are compared. The Bland & Altman Plot illustrates differences between methods in a very comprehensive way, incorporating diverse information in one single plot. Final results will incorporate limits of agreement to allow an estimate of the range in which 95% of the differences can be expected.

References

1. Ferrari, et al: *Gait Posture* 2008 in press.
2. List, et al: *J Biomech* 2006, **39(S1)**:S550.
3. Inman: *Bul Pros Res* 1969, **Spring**:130-145.
4. Bland and Altman: *Stat Meth Med Res* 1999, **2(8)**:135-60.

Medical Imaging Analyses

O33

In vivo talocrural and subtalar kinematics during nonweightbearing and weightbearing dorsiflexion-plantarflexion activities

S Yamaguchi¹, T Sasho², H Kato³ and SA Banks¹

¹Department of Mechanical and Aerospace Engineering, University of Florida, USA

²Department of Orthopaedic Surgery, Graduate School of Medicine, Chiba University, Japan

³Department of Radiological Technology, Chiba University Hospital, Japan

E-mail: banks@ufl.edu

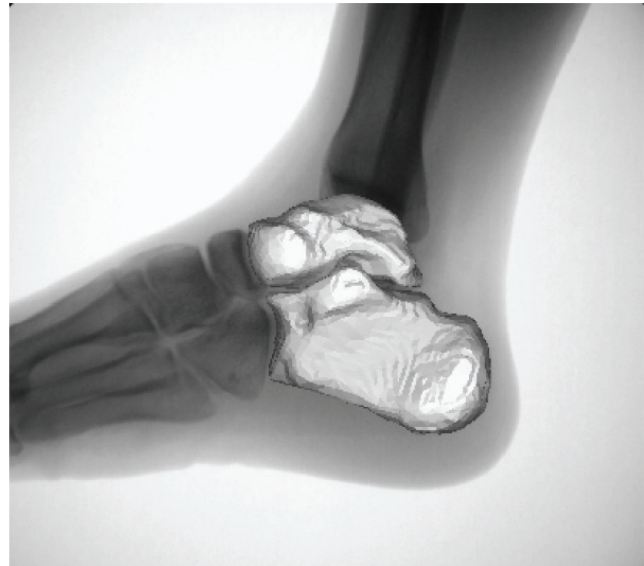
Journal of Foot and Ankle Research 2008, 1(Suppl 1):O33

Introduction: Understanding of the effect of weightbearing on the kinematics of the subtalar and talocrural joints is critical for the diagnosis and treatment of foot and ankle disorders. However, precise kinematics of these joints during dynamic activities in vivo is not well studied. The purpose of this study was to compare in vivo kinematics of these joints during nonweightbearing and weightbearing activities in healthy subjects.

Methods: Seven healthy subjects with a mean age of 32 ± 7 years were enrolled. Nonweightbearing and weightbearing activities from dorsiflexion to plantarflexion were recorded with oblique lateral fluoroscopy at 7.5 frames/sec. Geometric bone models of the tibia/fibula, talus, and calcaneus were created from CT images of the subject. Anatomic coordinate systems were embedded in each bone model. Three dimensional kinematics of the subtalar, talocrural, and ankle joint complex were determined using 3D-2D model registration techniques (Figure 1) [1, 2]. Bone models were projected onto the distortion-corrected fluoroscopic image, and three dimensional positions and orientations of the bones were determined by matching the silhouette of the bone models with the silhouette of the image.

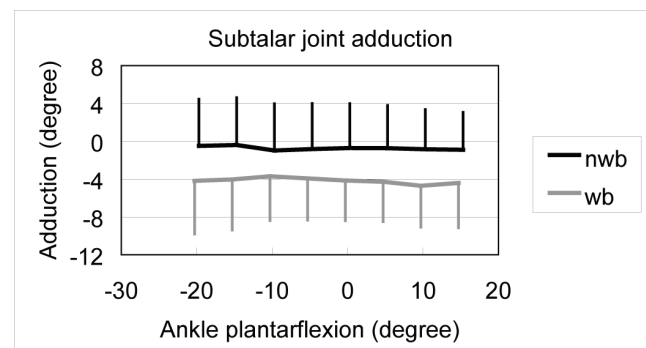
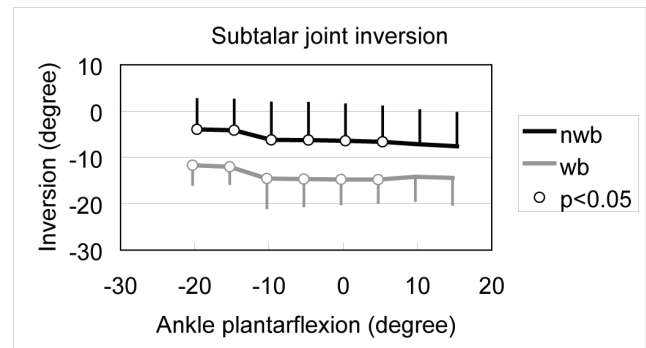
Results: During the nonweightbearing activity from 20° of dorsiflexion to 15° of plantarflexion of the ankle, the subtalar

Figure 1 (abstract O33)



Shape matching of the talus and calcaneus.

Figure 2 (abstract O33)



Subtalar joint inversion and adduction during nonweightbearing and weightbearing activities.

*Significant differences in repeated measures ANOVA. °Significant differences in post-hoc pair-wise comparisons.

joint everted by 4° and dorsiflexed by 2°. The talocrural joint inverted by 3°, plantarflexed by 32°, and adducted by 7°. During the weightbearing activity, the subtalar joint was significantly more everted, (7–8° of difference, Figure 2), dorsiflexed (3–5°), and abducted (3–4°, Figure 2) than during nonweightbearing activity. The talocrural joint was significantly more plantarflexed (7–8°) and adducted (2–5°) during weightbearing activity.

Conclusion: Coupled motion of the subtalar and talocrural joints during weightbearing activity serves to maximize joint contact area and stabilize the subtalar joint. 3D-2D model registration techniques appear to be useful tools for the quantitative analysis of the talocrural and subtalar kinematics during dynamic activities.

References

1. Banks SA, et al: *IEEE Trans Biomed Eng* 1996, **43**(6):638–649.
2. Moro-oka T, et al: *J Orthop Res* 2006, **25**(7):867–872.

O34

The accuracy of a CT-based bone segmentation technique for measuring the range of motion of the joints in the ankle

L Blankevoort^{1,3}, L Beimers^{1,3}, R Jonges², ER Valstar⁴ and GJM Tuijthof^{1,3}

¹Orthopaedic Surgery, Academic Medical Center, Amsterdam

²Medical Physics, Academic Medical Center, Amsterdam

³Orthopaedic Research Center Amsterdam (ORCA),

Academic Medical Center, Amsterdam

⁴Orthopaedic Surgery, Leiden University Medical Center, Leiden, The Netherlands

E-mail: L.Blankevoort@amc.uva.nl

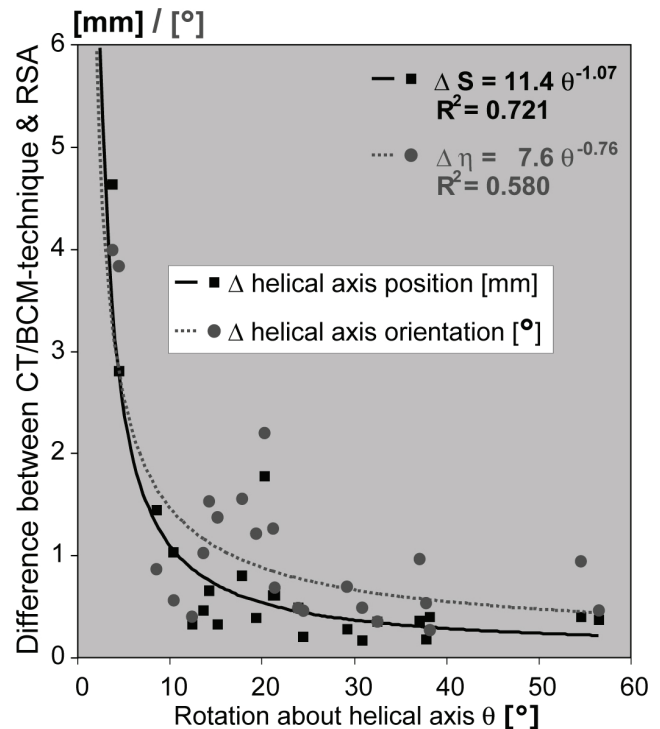
Journal of Foot and Ankle Research 2008, **1**(Suppl 1):O34

Introduction: For measuring the *in-vivo* range-of-motion of the ankle joints, a semi-automated Computer Tomography based bone contour method (CT/BCM) was developed to determine the three-dimensional position and orientation of the bones. To validate this technique, we hypothesized that the range of motion in the ankle is at least equally accurately measured by Roentgen Stereophotogrammetric Analysis (RSA) as by the CT/BCM technique.

Methods: Tantalum beads were placed in the distal tibia, talus and calcaneus of one cadaver specimen. With a fixed lower leg, the cadaveric foot was first held in neutral and subsequently loaded in eight different extreme positions. After acquiring a complete CT-scan with the foot in a position, the specimen was moved through the CT gantry, and two X-ray images were made. Bone contour detection was performed as described by Beimers [1], and RSA was performed according to Valstar [2]. The CT/BCM-data sets and RSA-data sets were transformed into the same coordinate system. Helical axis parameters were calculated for tibiotalar and talocalcaneal joint motion from neutral to the extreme positions and between opposite extreme positions. The differences between CT/BCM and RSA were calculated for rotation around, translation along, the position and the direction of the helical axis.

Results: The difference between the CT/BCM technique and RSA in helical axis position and helical axis rotation was dependent on the amount of rotation (Figure 1). By approximation, this relationship matched the model by Woltring [3]. Compared with RSA, the CT/BCM data registered a RMS difference of 0.26 degree for rotation about the helical axis, and 0.11 mm translation along the helical axis for tibiotalar motion between opposite extreme foot

Figure 1 (abstract O34)



Difference in helical axis position and helical axis orientation between the CT technique and RSA technique as functions of the rotation about the helical axis. Data of the tibiotalar and talocalcaneal joints were pooled.

position. For talocalcaneal motion, these differences were 0.17 degree and 0.23 mm respectively.

Conclusion: A cadaver specimen was used instead of a phantom, mimicking the *in-vivo* situation. A-priori known kinematics could not be applied, but comparison between the two techniques served as a fair estimate of the accuracy of the CT/BCM technique. The data suggest that the CT/BCM technique is as accurate or even more accurate than the RSA technique.

Acknowledgements

The assistance of Ms. S. Bringmann and Mr. M. Poulus in conducting the experiments is gratefully acknowledged.

References

1. Beimers L, et al: *J Biomech*. 2008, **41**:1390–1397.
2. Valstar ER, et al: *J Biomech* 2000, **33**:1593–1599.
3. Woltring HJ, et al: *J Biomech* 1985, **18**:379–389.

O35

Direct in vivo quantification of the 3D talocrural and subtalar finite helical axes

Frances T Sheehan

Physical Disabilities Branch, National Institutes of Health, Bethesda, MD, USA

E-mail: fsheehan@cc.nih.gov

Journal of Foot and Ankle Research 2008, **1**(Suppl 1):O35

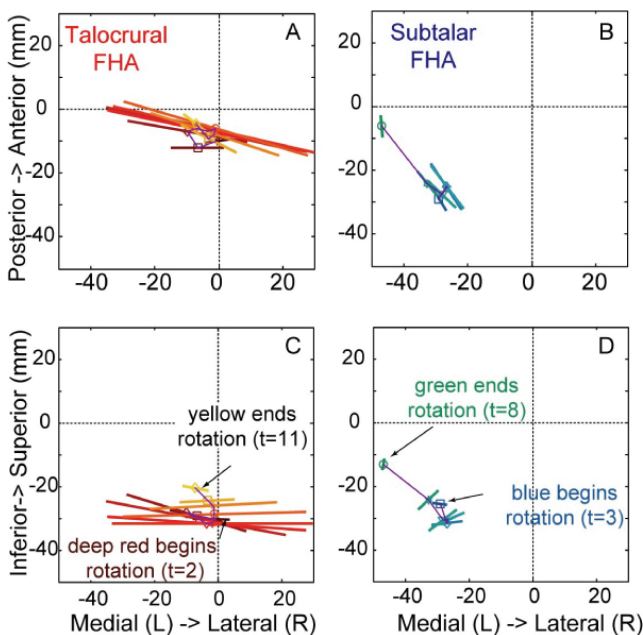
Introduction: In an attempt to understand the etiology of ankle joint injury and degeneration, numerous models have been created

as a means to estimate ankle joint forces. Due to a lack of non-invasive *in vivo* measurement techniques, the kinematics required to drive these models have typically been acquired in cadavers or using external markers to infer internal bone motion. This has left some uncertainty as to the validity of these models. Thus, the purpose of this study was to non-invasively quantify the 3D *in vivo* finite helical axes (FHA) of the subtalar and talocrural joints.

Methods: Twenty healthy subjects (25.9 ± 4.1 years, 70.3 ± 12.8 kg, 174.1 ± 7.7 cm) participated in this IRB approved study. Subjects were placed supine in a 1.5 T MR imager (LX; GE Medical Systems, Milwaukee, WI, USA) after obtaining informed consent. An MRI-compatible device was used to apply a plantarflexion (PF) load. This device allowed natural 3D motion at both joints of the hindfoot. While subjects cyclically plantar-flexed and dorsiflexed their ankle at 35 cycles/min, aided by an auditory metronome, fast-PC MR images (anatomic and x, y, and z velocity images, temporal resolution = 72 ms, imaging time = 2:48) were collected [1]. The sagittal-oblique imaging plane contained the tibia, calcaneus, and talus. The 3D time dependent tibial, talar and calcaneal attitudes were quantified through integration of the velocity data [1]. From these data the FHAs were determined.

Results: The ratio of the talocrural to subtalar angular velocities varied greatly between subjects. This ratio ranged from 1.1 to 4.5. Talocrural joint rotation occurred primarily about the medial-lateral axis (Figure 1A and 1C) during plantarflexion. Yet the FHA was not oriented solely in the M-L direction and rotation of talocrural FHA with minimal displacement during PF was seen across all subjects. The subtalar FHA was directed primarily in the anterior-posterior direction (Figure 1B and 1D).

Figure 1 (abstract O35)



FHAs for subject 9821R. All FHA's are plotted relative to the tibial coordinate system. The talocrural (subtalar) FHA changes from deep red (blue) to yellow (green) as the ankle plantarflexes. The length of the FHA indicates the magnitude of the angular velocity with the center of the line being the closest point the tibial origin (A&C) and talar origin (B&D). Ankle angle for this subject ranged from 1.9° to 39.4°.

The amount of angulation in the M-L and superior-inferior directions varied during PF and was variable across subjects.

Conclusion: The data from this study clearly confirmed that neither joint is a simple hinge joint and that ankle rotation arose primarily from the talocrural joint. The tendency of the subtalar and talocrural FHAs to rotate and translate will impact the calculation of tendon and ligament moment arms and, thus, alter the moment producing capabilities of the force generating structures at the ankle joint. Future modelling studies should investigate the sensitivity of the model outputs to variations in the FHA direction and location.

Reference

1. Sheehan FT, et al: *Foot & Ankle Int* 2007, **28(3)**:323-3.

O36

Validation of a voxel-based 2D to 3D registration method for measuring 3D natural ankle kinematics with single plane fluoroscopy

Tung-Wu Lu¹, Cheng-Chung Lin¹, Po-Hsiang Yu¹, Guan-Ying Li¹, Chien-Chung Kuo^{1,3}, Tsung-Yuan Tsai¹ and Mei-Ying Kuo^{1,2}

¹Institute of Biomedical Engineering, National Taiwan University, Taipei, Taiwan

²School of Physical Therapy, China Medical University, Taichung, Taiwan

³Department of Orthopedics, China Medical University Hospital, Taichung, Taiwan

E-mail: twlu@ntu.edu.tw

Journal of Foot and Ankle Research 2008, 1(Suppl 1):O36

Introduction: *In vivo* three-dimensional (3D) kinematics of the ankle joint is essential for a better understanding of its biomechanics and for many clinical applications. Several measurement techniques are available for this data, but few allow non-invasive measurements with sub-millimetre accuracy. The purposes of the study were to develop further a voxel-based 2D to 3D registration method [1] for measuring 3D ankle kinematics with single plane fluoroscopy, and to determine experimentally the measurement errors *in vitro*.

Methods: An ankle specimen was fixed with a plastic frame of high rigidity at eight different poses, encompassing the ankle range of motion during gait. The CT data and images from 20 fluoroscopy trials (Angiography, Advantx LCA, GE, France) of the specimen were obtained for each pose. 3D voxel-based models were derived from the CT data and then precisely registered to the 2D fluoroscopic images using an improved version of a voxel-based 2D to 3D registration method [1]. With the method, the 3-D poses of the tibia, fibula, talus and calcaneus bones at each fluoroscopic image frame were obtained by searching the poses of the bone models, using an optimization procedure, the DRR of which best matched the fluoroscopic image according to a similarity measure. The poses obtained from a total of 160 fluoroscopic trials were compared to those determined by the CT data for measurement errors.

Results: High accuracies were found for the global poses of the tibia/fibula, talus and calcaneus; and the poses of the ankle and subtalar joints, Tables 1 and 2. The ensemble means (standard deviations) of the global tibial pose errors were less than 0.30 (0.55) mm, 1.10 (1.29) mm, and 0.46(0.79)° for the in-plane translation components, out-of-plane translation component, and all angular components, respectively. The corresponding values for the talus were 0.29 (0.57) mm, 0.07 (1.74) mm, and

Table 1 (abstract O36) Ensemble means (standard deviations) of the global pose errors of the ankle bones

	Tibia/Fibula	Talus	Calcaneus
X(mm)	0.31(0.24)	0.29(0.22)	0.13(0.77)
Y(mm)	0.01(0.55)	0.04(0.57)	-0.39(0.74)
Z(mm)	-1.10(1.29)	0.07(1.74)	0.51(1.29)
$\theta_x(^{\circ})$	-0.46(0.79)	0.07(0.76)	-1.32(0.58)
$\theta_y(^{\circ})$	-0.09(0.64)	-0.15(1.16)	-0.51(0.64)
$\theta_z(^{\circ})$	-0.15(0.50)	0.19(0.62)	0.64(0.72)

Table 2 (abstract O36) The ensemble means (standard deviations) of the pose errors of the ankle and subtalar joints

	Subtalar Joint	Upper Ankle Joint
X(mm)	-0.22(0.78)	0.04(0.27)
Y(mm)	-0.39(0.59)	0.03(0.21)
Z(mm)	0.51(2.22)	0.91(1.50)
$\theta_x(^{\circ})$	1.39(1.03)	-0.53(0.75)
$\theta_y(^{\circ})$	0.37(1.37)	0.06(1.07)
$\theta_z(^{\circ})$	0.44(0.87)	-0.33(0.81)

0.19 (1.16)°, and those for the calcaneus were 0.39 (0.76) mm, 0.51 (1.29) mm, and 1.31 (0.71)°, Table 1.

The ensemble means (standard deviations) of the pose errors for the subtalar joint were less than 0.39 (0.78) mm, 0.50 (2.22) mm, and 1.38 (1.37)° for the in-plane translation components, out-of-plane translation component, and all angular components, respectively. The corresponding values for the ankle joint were 0.04 (0.27) mm, 0.90 (1.50) mm, and 0.53 (1.07)°.

Conclusion: The improved method has been shown experimentally to be accurate for the measurement of the 3D kinematics of the ankle complex with single plane fluoroscopy, the ensemble standard deviations of the errors (indicating the precision) being less than 0.78 mm for the in-plane translations, 2.22 mm for out-of-plane translation, and 1.37° for all rotations. This suggests that the method will be useful for the study of the ankle biomechanics and for relevant clinical applications.

Reference

1. Tsai TY, et al: *Journal of Biomechanics* 2006, **39(Suppl 1)**: S43-S44.

O37

The predictive value of the foot posture index on dynamic function

RG Nielsen¹, M Rathleff¹, UG Kersting³, O Simonsen¹, C Moelgaard³, K Jensen², CG Olesen^{3,6}, S Lundbye-Christensen^{3,4} and S Kaalund⁵

¹Orthopedic Division, North Denmark Region, Aalborg Hospital, part of Aarhus University Hospital, Denmark

²Department of Development and Planning: Division of Geomatics, Aalborg University, Denmark

³Department of Health Science and Technology, Aalborg University, Denmark

⁴Department of Mathematical Sciences, Aalborg University, Denmark

⁵Kaalunds Orthopedic Clinic, Aalborg, Denmark

⁶Department of Mechanical Engineering, Aalborg University, Denmark
E-mail: ragn@rn.dk

Journal of Foot and Ankle Research 2008, **1(Suppl 1)**:O37

Introduction: Keenan et al [1] identified the six-item version of the Foot Posture Index (FPI) as a valid, simple and clinically useful tool. The model combines measures of the standing foot posture in multiple planes and anatomical segments. It provides an alternative to existing static clinical measures when dynamic measures are not feasible. Redmond et al. [2] found the model able to predict 41% of the variation in the complex rotation of the ankle joint, representing inversion/eversion, during mid-stance of walking. To our knowledge no studies have been published on the relationship between the FPI and the movement of the midfoot during walking.

The purpose of this study was to investigate the use of FPI classification as a predictor for dynamic midfoot kinematics during walking.

Methods: Two hundred and eighty participants randomly selected from the Danish Civil Registration System were included in the study (age 43 ± 14, BMI 24.2 ± 3.1). Their foot type was determined using the FPI model. A Video Sequence Analysis (VSA) system was used to quantify midfoot kinematics during walking.

The navicular drop (Δ NH) and minimal navicula height (NHL) were extracted from the stance phase. FPI data were collected as in Redmond et al. [2] Correlations and multiple regression techniques were applied for statistical analysis.

Results: The FPI model predicted 45% of the variation in NHL ($p < 0.001$) and 13.2% of the variation in Δ NH ($p < 0.001$) during walking.

Only few of the individual tests constituting the FPI were significantly correlated with dynamic measures. The significant items were the medial longitudinal arch (MLA) and inversion/eversion of the calcaneus. Some combinations of these measures showed a significant regression (Table 1).

Conclusion: The FPI score is a poor predictor of dynamic navicula drop, as it predicts just above 40% of the variation in minimal navicula height during walking. The visual assessment of medial longitudinal arch and inversion/eversion of the calcaneus are similar compared to the FPI model itself. Other tests such as the Longitudinal Arch Angle [3] were shown to predict midfoot kinematics by explaining over 80% of the variance.

Our results indicate that the FPI as well as its components are relatively poor predictors of midfoot movement during walking. Alternative measures are better predictors of dynamic midfoot function.

Table 1 (abstract O37) Predictive values of different tests on Δ NH and NHL (only significant relationships)

Test	P-value	Determination coefficient, r^2
FPI vs. Δ NH	$p < 0.001$	0.132
Inversion/eversion vs. Δ NH	$p < 0.001$	0.127
FPI vs. NHL	$p < 0.001$	0.450
MLA + inversion/eversion vs. NHL	$p < 0.001$	0.451
MLA vs. NHL	$p < 0.001$	0.415
Inversion/eversion vs. NHL	$p < 0.001$	0.261

References

1. Keenan AM, et al: *Arch Phys Med Rehabil* 2007, **88**:88–93.
2. Redmond AC, et al: *Clinical Biomechanics* 2006, **21**:89–98.
3. McPoil TG, et al: *Journal of the American Podiatric Medical Association* 2007, **97**:102–107.

O38

Objective foot ulcer documentation using 3-D shape analysis: a feasibility study

Burkhard Drerup¹, Xiang Liu², Wangdo Kim³
and Hans Henning Wetz

¹Klinik fuer Technische Orthopaedie, Universitaetsklinikum Muenster, Germany

²School of Mechanical and Aerospace Eng. Nanyang Technological University, Singapore

³Maseeh College of Engineering and Computer Science, Portland State Clinical Department, OR, USA

E-mail: drerup@uni-muenster.de

Journal of Foot and Ankle Research 2008, **1(Suppl 1)**:O38

Introduction: In treating the condition of a diabetic foot with ulcerations need for objective documentation of wound site and wound size is obvious.

There is to our present knowledge no objective method available to document the exact localization of an ulceration with accuracy beyond anatomical description and photographic documentation. In measuring ulcer size, i.e. diameter, area, depth and volume stereoscopic measurement is widely accepted as a most reliable and precise technique [1]. However, it demands for highly skilled computer assisted evaluation making it time consuming and impractical for routine use in clinical practice.

It was the aim of the present study to explore the potential of an automatized evaluation of 3-D measurements of ulcerations of the foot. This should include following steps:

- 3-D data capture of the ulceration and the foot.
- automatized 3-D evaluation of the 3-D data for detection of the wound edges.
- localization of the wound with respect to anatomical landmarks of the foot.

3-D measurement of the foot and establishing a reference system based on anatomical landmarks has been described elsewhere [2]. Here the second step is of special interest. Shape analysis based on differential geometry is used to detect wound edges.

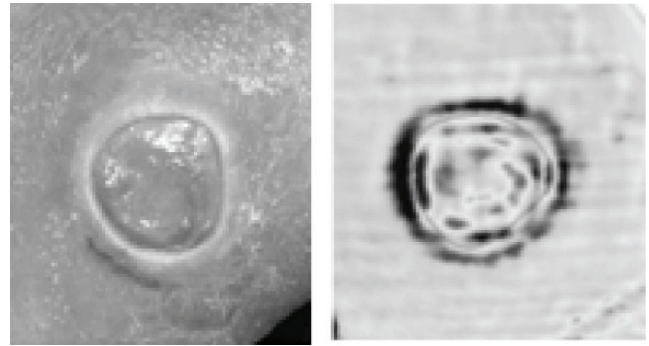
Methods: In a patient with foot ulceration in total 10 3-D scans of the foot have been performed in regular intervals spanning 30 days. Scanning was done with a FastSCAN laser scanner providing after smoothing about 40 points/cm² with a statistical error of 0.02 mm. One special localization of the wand relative to the transmitter was recorded, to use it for the calculation of a virtual image of the calculated wound edge to be overlaid to the true photo of the wound taken from that position [3].

Calculation of the edges is based on analysis of the sum ('mean curvature') and difference ('rim curvature') of the principal curvatures. This allows to calculate a geometric line modelling the wound edge, which can be compared directly with the photographically documented wound edge.

Results: Fig. 1 shows an example of a comparison between a wound photo and the curvature map revealing the wound edges.

Evaluation of 3-D measurement in sequence shows the applicability of this concept for a quantitative documentation of wound size, area and volume.

Figure 1 (abstract O38)



left: wound photo; right: curvature map (difference of principal curvatures) with an automatically generated closed line to model the wound edge.

Conclusion: Use of curvature analysis appears to be a valuable tool in the automatic assessment of wounds. It probably works best together with other techniques, e.g. evaluating the texture.

References

1. Keast DH, et al: *Wound Repair Regen* 2004, **12**:1–17.
2. Liu X, et al: *Real-time imaging* 2004, **10(4)**:217–228.
3. Liu X, et al: *Physiol Meas* 2006, **27**:1107–1123.

Modelling

O39

The calcaneocuboid joint moves with three degrees of freedom

Thomas M Greiner¹ and Kevin A Ball²

¹Department of Health Professions, University of Wisconsin – La Crosse, USA

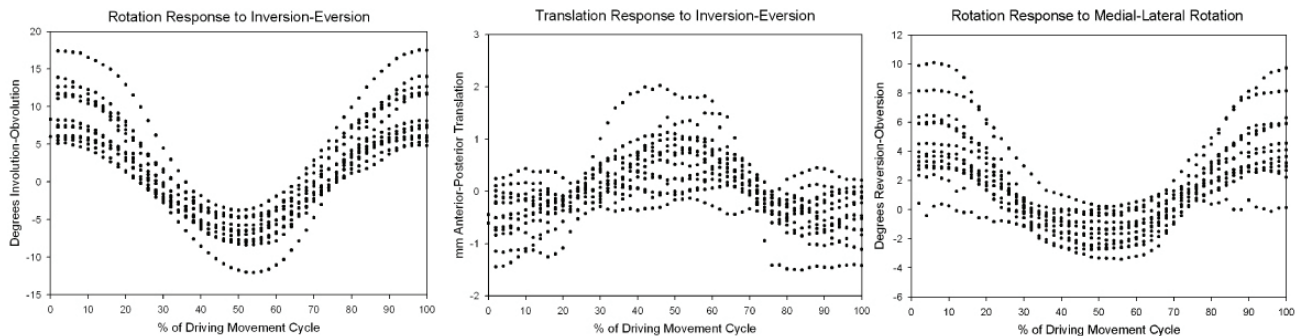
²Department of Physical Therapy, University of Hartford, USA
E-mail: greiner.thom@uwlax.edu

Journal of Foot and Ankle Research 2008, **1(Suppl 1)**:O39

Introduction: Investigations of the calcaneocuboid joint typically find that it is among the least mobile of the intrinsic foot joints [1]. When movement is found, it is shown to be highly variable among individuals [2]. The joint is therefore relegated to the presumably rigid lateral aspect of the foot. The complementary articular surfaces of the two relevant bones are both relatively flat, with some irregular undulations. This joint surface geometry suggests that movement might be limited to a single rotation and perhaps superior and lateral translations in the synovial plane. In this presentation we challenge this expectation by exploring the calcaneocuboid joint in six degrees of freedom through multiple driving actions.

Methods: Data are derived from the legs of 12 non-pathological embalmed cadavers. Legs were prepared by removing all soft tissue, so that only ligamentous structures remained to sustain limb integrity. Each specimen was cycled by moving the leg on the foot through three mutually orthogonal driving actions (Inversion-Eversion, Medial-Lateral Rotation, and Plantarflexion-Dorsiflexion) while monitoring the relative positions of the calcaneus and cuboid with an active-marker tracking system. The Functional Alignment method [3] was used to derive joint axis orientations and motion patterns for three rotational

Figure 1 (abstract O39)



The three movement patterns identified for the calcaneocuboid joint; a rotation and translation as the result of the inversion-eversion driving motion and a rotation produced by the medial-lateral rotation of the leg on the foot.

and three translational degrees of freedom. These results are explored by plotting observed movement patterns against the percentage of the movement cycle.

Results: The movements of the calcaneocuboid joint were explored in all six degrees of freedom for all three driving actions. Figure 1 shows the three clearest movement patterns that were identified. In response to the inversion-eversion driving action the cuboid rotates as much as 25° about an oblique axis – a movement best described as obvolution-involution [4]. The same driving action also produces up to 2 mm of posterior-anterior translation – an actual distraction of the synovial joint. The medial-lateral driving action produced a 6° rotational response about a differently oriented oblique axis, in a movement best described as obversion-reversion [4]. No distinctive movements were produced as a response to the plantarflexion-dorsiflexion driving action.

Conclusion: The calcaneocuboid joint is more mobile than many conventional authorities would suggest. The joint was observed to move in three distinct ways. The largest rotation, occurring only in response to inversion-eversion, meets the expectations based upon surface geometry. However, the other two motions, which require some measure of joint distraction, are not obvious consequences of this geometry.

References

1. Mattingly B, et al: *J Biomech* 2006, **39**:726–733.
2. Nester CH, et al: *J Biomech* 2007, **40**:1927–1937.
3. Ball KB, et al: *Proceedings of ISB 3D. Tampa, FL* 2004.
4. Greiner TM: *Foot Ankle Int* 2007, **28**:109–125.

O40

Reducing rigid-body error in a functional technique to determine ankle joint axes

J Leitch¹, J Stebbins² and AB Zavatsky¹

¹Department of Engineering Science, University of Oxford, Oxford, UK

²Oxford Gait Laboratory, Nuffield Orthopaedic Centre NHS Trust, Oxford, UK

E-mail: amy.zavatsky@eng.ox.ac.uk

Journal of Foot and Ankle Research 2008, 1(Suppl 1):O40

Introduction: Functional methods of finding joint axes of rotation involve tracking the movement of one bone at a joint relative to another and subsequent calculation of the joint axis position and orientation from the locations of skin-mounted

markers. van den Bogert *et al.* [1] proposed a functional method of determining the non-weight bearing axes of the ankle joint complex. Their subjects performed a full range of motion at the ankle with markers on the shank and shoe. The technique implemented an optimisation algorithm to fit a kinematic model of the subtalar and talocrural joints to the experimentally acquired motion data. Soft tissue movement and associated marker movement was reported to be a significant source of error. The aim of the present study was to investigate how this skin movement error might be reduced through a better selection of marker positions.

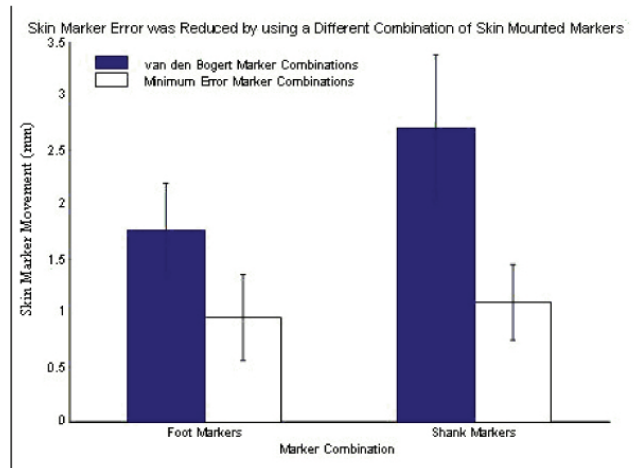
Methods: Seven healthy adult subjects (5 female and 2 male, age range 16–36) with no history of foot or ankle joint problems participated in the study. Spherical reflective markers were located at eleven anatomical landmarks on the shank and foot (without shoe) [1, 2] of ten lower limbs. Three-dimensional spatial data was collected with a 12-camera Vicon MX (Vicon Motion Systems, Oxford, UK) as subjects performed plantar- and dorsi-flexion, pronation-supination, and circumduction [1]. Static trials were performed with the foot in both a weight-bearing and a non-weight bearing condition.

The best-fit rigid-body transformations for the shank and foot segments for all motions were calculated using the method of Söderkvist and Vedin [3]. The reference position for the calculations was taken to be the static trial, first weight-bearing and then non-weight bearing. Skin marker movement during motion was estimated for all combinations of three markers located on the shank and all combinations of three markers located on the foot. This was done by comparing the actual marker positions to those predicted by the best-fit rigid-body transformations [3].

Results: The skin marker movement error, averaged over all time frames and all subjects, varied with different combinations of markers and different static trials (range 0.96–2.55 mm for foot, 1.10–7.83 mm for shank). A reduction in error was achieved when calculations were based on a marker set different from that used by van den Bogert *et al.* (Figure 1). The best combination of markers for the foot in the present study was posterior heel distal, posterior heel proximal (wand marker), and sustentaculum tali, with a non-weight-bearing static reference. For the shank, the best marker combination was head of fibula, anterior tibia, and lateral shank (wand marker), with weight-bearing static reference.

Conclusion: Skin movement error in tracking ankle joint motion can be reduced through a better selection of marker

Figure 1 (abstract O40)



Skin marker movement error during the full range of ankle movement.

positions. This in turn should lead to a more accurate prediction of the motion axes of the ankle joint complex.

References

1. Bogert van den, et al: *J Biomechanics* 1994, **27**:1477–1488.
2. Stebbins, et al: *Gait & Posture* 2006, **23**:401–410.
3. Söderkvist, et al: *J Biomechanics* 1993, **26**:1473–1477.

O41

A biomechanical model of percutaneous distal metatarsal osteotomy: load transmission influencing successful follow-up

R Stagni¹, F Vannini² and S Giannini²

¹Department of Electronics, Informatics, and computer Science, University of Bologna, Italy

²Istituto Ortopedici Rizzoli, Bologna, Italy

E-mail: rita.stagni@unibo.it

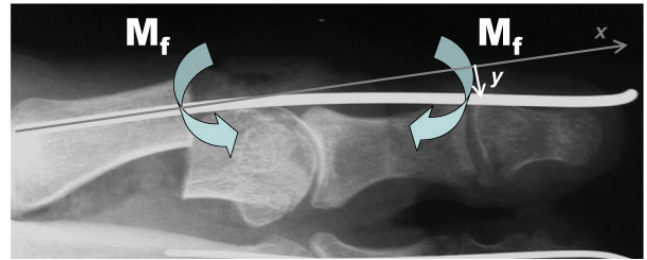
Journal of Foot and Ankle Research 2008, **1(Suppl 1)**:O41

Introduction: Symptomatic hallux valgus is a common clinical problem. Current trends for treatment are toward percutaneous or mini-invasive procedures, among these a mini-invasive distal metatarsal osteotomy (SERI) demonstrated to be effective in correcting the deformity with minimal surgical trauma and satisfactory results [1]. Conflicting with previous clinical studies, a recent paper [2] reported discouraging short-term radiographic results by using a theoretically similar osteotomy and fixation device. The hypothesis of the present study is that conflicting clinical outcomes are associated to different loading conditions imposed by the surgical procedure to the metatarsal. Thus, a biomechanical model of metatarsal osteotomy was designed, in order to investigate relevant biomechanical variables.

Methods: The pin, inserted in the metatarsal to stabilize the osteotomy, was modelled as beam. If a flexion moment M_f is imposed to the beam, a deflection y is observed (Figure 1).

The deflection y results from the applied moment and the geometrical and mechanical characteristics of the beam: Where E is the Young Modulus of the material, and I is the moment of inertia of the section opposing to flexion. For a circular section (radius r) of the beam:

Figure 1 (abstract O41)



Sketch of the deflection y induced to the beam by the flexion moment M_f .

A specific software tool was developed for the quantification of M_f from the radiographic post-op images. The tool was preliminarily used to analyse radiographs from three subjects. The quantified moment corresponds to the reaction moment induced by the pin into the proximal section of the metatarsal. Thus, specific compressive load distribution at the osteotomy interface can be quantified by means of FEM analysis.

Results: The magnitude of compressive force depends on a solid connection of the pin to the phalanx of the toe and to the head of the metatarsal, allowing elastic deflection of the pin. Moreover, the applied moment strongly depends on the radius of the pin: a change of 20% in the radius, results in a reduction of approximately 60% if the moment of inertia, thus of the applied moment.

Conclusion: Although several macroscopic technical differences between the techniques are evident, the biomechanical model proposed pointed out some mandatory characteristics for the efficacy of fixation in SERI procedure: the deflection imposed to the pin implies the generation of a contact load distribution at the interface of the osteotomy, which is likely to induce an appropriate healing of the resection. In this context, the anchorage of the pin to the toe and the head of the metatarsal in appropriate points is of fundamental importance, for load transfer and freedom of deflection, as well as the radius of the pin. The designed software is meant to quantify the induced loads in a large group of subjects, in order to correlate the loading with the outcome.

References

1. Giannini S, et al: *Tech Foot Ankle Surg* 2003, **2**:11–20.
2. Kadakia AR, et al: *Foot & Ankle Int* 2007, **28**(3).

O42

Evidence for early stance phase pre-loading of the plantar aponeurosis

Paolo Caravaggi, Todd C Pataky, Russ Savage and Robin H Crompton

School of Biomedical Sciences, University of Liverpool, UK

E-mail: pacara@liv.ac.uk

Journal of Foot and Ankle Research 2008, **1(Suppl 1)**:O42

Introduction: An inverse dynamics approach has been used to gain an insight into the mechanical behaviour of the plantar aponeurosis (PA) at different walking speeds. Mechanical [1] and finite element models [2] have evaluated its biomechanics in quasi static conditions. To our knowledge only one study has addressed the dynamic behaviour of the PA with relation to the

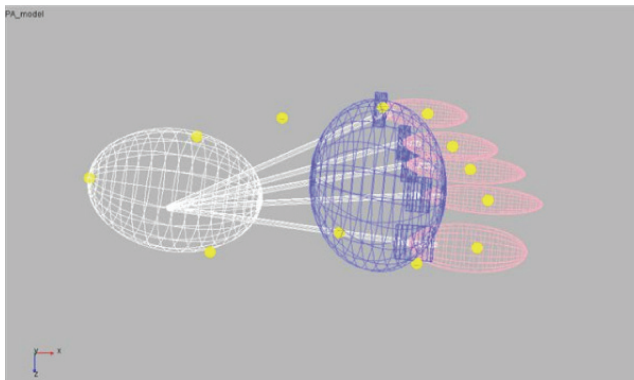
Achilles tendon force [3]. The aims of this study were to create a multibody model to quantify PA tension and to examine how PA tension changes with walking speed.

Methods: Three healthy young subjects with no history of foot injuries or abnormalities participated in this study. A linear ultrasound probe was employed to identify the proximal attachment of the PA onto the plantar heel. An *ad hoc* 12 markers protocol, modification of [4], was designed to record the kinematics of heel, metatarsal bones and toes at different walking speeds.

Commercial software for multibody dynamics analysis (MSC Adams) was used to build the model geometry and to calculate the elongation trajectories for five segments of the PA based on stance phase kinematics data (Figure 1). The metatarsal heads were modelled as cylinders under the metatarso-phalangeal joints. The windlass mechanism of the PA was modelled by contact elements that constrained the PA segments to wrap around the metatarsal heads. Bulk PA stiffness [5] was distributed equally among the five digits and was used to estimate segmental PA tension.

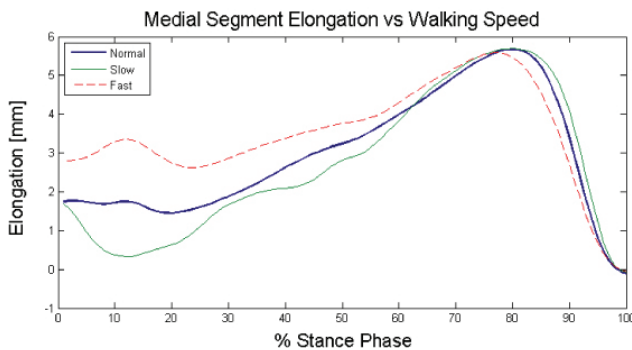
Results: Peak PA tension occurred in late stance phase (~1.5 BW) for all walking speeds and was similar in magnitude to cadaver simulation data [3]. Early stance phase PA tension increased systematically with walking speed (Figure 2).

Figure 1 (abstract O42)



The 7 segments multibody model. In yellow the motion agents driving the segments in the inverse dynamics analysis.

Figure 2 (abstract O42)



Example elongation trajectories for the medial segment of the PA in one subject walking at different speeds.

Conclusion: Preliminary results demonstrate model validity and reveal an interesting relation between PA tension and walking speed. The increase in PA tension with walking speed during early stance may represent a pre-loading protective mechanism to further support the longitudinal arch at higher impact forces.

References

1. George A: *Arangio Clin Orth and Rel Res* 1997, **339**:227–231.
2. Cheung Tak-Man Jason, et al: *J Biomech* 2005, **38**:1045–1054.
3. Erdemir Ahmet, et al: *JBS* 2004, **86**:546–552.
4. Leardini, et al: *Gait&Posture* 2007, **25**:453–462.
5. Kitaoka HB: *Foot Ankle Int* 1994, 557–60.

O43

Bearing surface modeling of the talus and calcaneus

David Chichka¹, James Stephenson¹, Antonio Paulic¹ and Frances Sheehan²

¹Mechanical and Aerospace Engineering, The George Washington University, USA

²National Institute of Health, Washington, DC, USA

E-mail: chichka@gwu.edu

Journal of Foot and Ankle Research 2008, 1(Suppl 1):O43

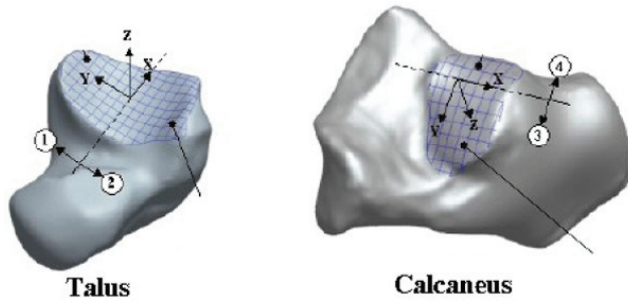
Introduction: Precise talar in vivo motion is difficult to measure due to its inaccessibility to surface based measures. Thus, most measures of talar motion have been limited to cadaver based measures, typically under static conditions. Quantitative measures of the talar bearing surfaces and their ability to mesh with the calcaneal and malleolar bearing surfaces would provide an understanding of the envelope of movements available in both in healthy and pathological joints. Such measures could exploit the availability of 3D non-invasive imaging methodologies, making it available for large-scale healthy and pathological studies. Thus, the purpose of this work is to mathematically model the bearing surfaces of the talar and calcaneal bones in order to determine the allowable motions of a healthy joint.

Methods: A three-dimensional Faro-arm scanner was used to acquire a dense cloud of points depicting the shape of skeletal bones of a single human foot. The points on the subtalar joint bearing surfaces were then fit with continuous functions. The functions were chosen from classes which provide the characteristics expected of the surfaces. The functions were relative to coordinate system defined such that the axes were parallel when the bones were assembled in a “natural” fit, with origin at the saddle point. Initial fits used bi-quadratics. The surface curve fits allowed the evaluation of several parameters. Among these, the relative curvatures of the mating surfaces was a primary measure of interest because it allows an examination of allowable motions of the surfaces relative to each other. For example, very different radii of curvature about a particular axis allows for a rocking motion, but very limited relative sliding of the surfaces.

Results: The quality of fit was good, but has not yet been compared with other possible functions. Figure 1.

The range of radii found along the y-axis (anterior-posterior) correlate well between the two bearing surfaces, allowing the surfaces to conform to one another. The overlapping radii range between the talus and calcaneus suggests that not only is the motion about the x-axis (medial-lateral) rotational, but the

Figure 1 (abstract O43)



Talus and calcaneus bearing surfaces, hashed for curve fitting. Each surface is separated into two sections, and separate fits are found for each.

curvature radii is flexible. The motion about the x-axis is not confined to a specific moment arm distance, but can change throughout the ankle's range of motion.

In contrast, the x-axis curvature values were not found to coincide, and the values for the calcaneus were larger than any of the curvature values found for the mating surface. The large radius of curvature values likely allow the calcaneus superior articulation surface to provide translation instead of rotational joint motion about the y-axis. This motion is likely constrained by other aspects of the joint.

Conclusion: At the current time this work is ongoing. After bearing surface models have been fit to 4 new scans of cadaver bones and 8 models acquired through segmenting high-resolution 3D MR images of healthy ankles, appropriate scaling factors will be investigated so that an average calcaneal and talar bearing surfaces can be created. Examination of all contact surfaces will provide further insight into allowable and expected motions of the joint.

O44
New spatial mechanisms for the kinematic analysis of the tibiotalar joint

R Franci², V Parenti-Castelli¹, C Belvedere² and A Leardini²

¹Department of Mechanical Engineering, University of Bologna, Italy

²Movement Analysis Laboratory, Istituto Ortopedici Rizzoli, Italy

E-mail: vincenzo.parenticastelli@mail.ing.unibo.it

Journal of Foot and Ankle Research 2008, 1(Suppl 1):O44

Introduction: In virtually unloaded conditions, the tibiotalar (ankle) joint behaves as a single degree-of-freedom system, and two fibres within the calcaneal-fibular and tibio-calcaneal ligaments remain nearly isometric throughout the flexion arc [1]. A relevant theoretical model also showed that three articular surfaces and two ligaments act together as a mechanism to control the passive kinematics [2]. Two equivalent spatial parallel mechanisms were formulated, with ligament fibres assumed isometric and articulating surfaces assumed rigid, either as three sphere-plane contacts, or as a single spherical pair. Predicted and measured motion in three specimens compared fairly well. Important enhancement of this previous work is here presented, with more accurate experimental data, more anatomical model surfaces, and a more robust mathematical model.

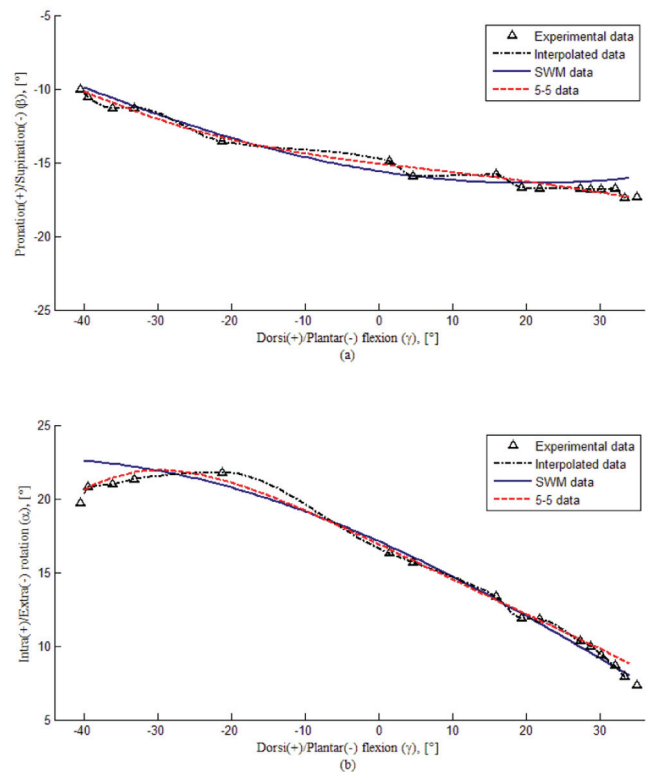
Methods: Four fresh frozen amputated legs, free of anatomical defects, were analysed under passive conditions [1]. Motion of tibia, fibula, talus and calcaneus and geometrical arrangement of the main articular surfaces and ligament attachments were obtained by a camera-based Knee Navigation System (Stryker[®], Kalamazoo, MI-USA).

A new equivalent spatial mechanism was based on three sphere-to-sphere contacts (two between the trochlea tali and tibial mortise, one between the lateral talus and the lateral malleolus) and two rigid fibres. This one degree of freedom mechanism was represented also by 5 rigid links connecting 5 points on the tibia-fibula to 5 points on the talus-calcaneus segments ('5-5' model) [3]. Because measured motion was nearly spherical, contact was also modelled as a spherical wrist ('s-w' model) [4].

For each model, a bounded optimization procedure was used to find the optimal geometric parameter set which makes it possible to obtain the best-fit between experimental and model motion. For each of the four specimens, initial tentative values for the geometrical parameters were obtained from the experiments in-vitro.

Results: Experimental motion compared very well with corresponding simulations from '5-5' model, just a little worse from 's-w' (Figure 1). The difference between initial tentative and corresponding final optimal ligament fibre attachments was found small (2-8 mm). The difference for the sphere centres was larger, accounted for the limited digitised area.

Figure 1 (abstract O44)



Experimental (black) joint rotations out-of-sagittal plane vs dorsi/platar flexion superimposed to corresponding model '5-5' (red) and 's-w' (blue) predictions.

Conclusion: The proposed models replicated well ankle passive motion, still reflecting at the same time the main anatomical structures of this joint. These models are believed to be very useful tools for ankle surgical procedures simulation and planning, as well as for ankle prosthesis design.

References

1. Leardini A, et al: *J Biom* 1999, **32**:111–118.
2. Di Gregorio R, et al: *Med Biol Eng Comput* 2007, **45**(3): 305–13.
3. Franci R, et al: *Proceedings of the ASME IDETC/CIE, Las Vegas, Nevada, USA* 2007.
4. Franci R, et al: *IAK, Lima, Peru*; 2008.

O45

A finite element foot model for simulating muscle imbalances

William R Ledoux^{1,2,3}, Evan DW Dengler¹

and Michael J Fassbind¹

¹RR&D Center of Excellence, Department of Veterans Affairs, Seattle, WA, USA

²Departments of Mechanical Engineering, University of Washington, Seattle, WA, USA

³Orthopaedic & Sports Medicine, University of Washington, Seattle, WA, USA

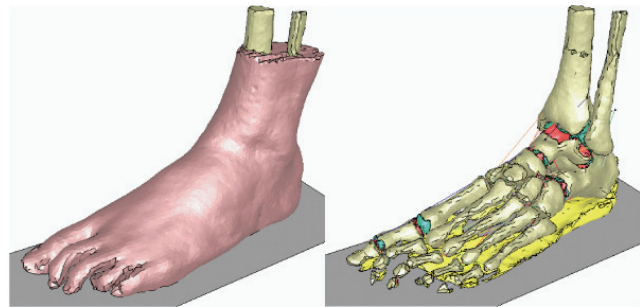
E-mail: wrledoux@u.washington.edu

Journal of Foot and Ankle Research 2008, **1**(Suppl 1):O45

Introduction: To overcome the expense and limitations of cadaveric testing, we developed a finite element (FE) foot model. Previous foot models have included hyperelastic materials, plantar fascia, and extrinsic muscle forces [1]. We also included the plantar fat pad and both distal and proximal cartilage in our model. We validated the model by comparing plantar pressures and joint angles to literature sources and cadaveric testing data.

Methods: High-resolution MRI and CT scans (0.6 mm isometric voxels) were performed on a male cadaveric foot from a 44-year-old, 823 N, non-diabetic subject. An acrylic frame held the foot in the same position between scans. ImageJ was used to segment the plantar fat, proximal and distal cartilage, and outer skin layer from MRI scans. Custom written MATLAB and IDL code was used to create STL files from the XY coordinates exported via ImageJ. Multi-Rigid was used to segment the bones from the CT scans and then register the bones to the MRI scan positions [2]. Rhinoceros was used to perform Boolean operations on the segmented cartilage. The tetrahedral automesh in ANSYS ICEM CFD v10.0.1 was used. LS-DYNA v971d was the non-linear explicit solver. The model includes: foot bones, distal and proximal cartilage of selected joints, plantar fat, with the remaining volume inside the outer skin boundary defined as a general soft tissue (Figure 1). The soft tissue and plantar fat pad were modeled using an Ogden hyper-elastic rubber formulation [3, 4], while bones were rigid bodies. Cartilage was considered a linear elastic material and included for the following joints: ankle, subtalar, talonavicular, calcaneocuboid, and metatarsophalangeal and interphalangeal joints of the 1st ray. Ligaments were modeled as 1-D non-linear springs while tendons were included using seatbelt elements and anatomically placed slipring elements. The foot was inclined at 7° to simulate midstance. For a neutral balanced standing simulation, a force of 400 N was applied down on the tibia with 200 N applied up on

Figure 1 (abstract O45)



FE foot model: with (left) and without (right) soft tissue. (pink = soft tissue, beige = bone, light blue = proximal cartilage, red = distal cartilage, yellow = plantar fat).

the calcaneus. Loads were ramped to full amplitude by 0.2 s and the simulation time was 0.4 s. Bone rotations for the calcaneus, talus, navicular, cuboid, and the 1st and 5th metatarsals were compared with cadaveric data and pressure data beneath the heel, lateral midfoot, and the 1st and 5th metatarsals to the literature [5].

Results: For the neutral balanced standing simulation, 11 of 18 bone rotation angles fall within two standard deviations of the cadaveric data and all peak plantar pressure values are within one standard deviation.

Conclusion: Our anatomically detailed FE foot model simulated correct plantar pressures, but the bone rotations are not all correct. It is possible that including cartilage at all foot joints and using wider ligament origins and insertions may address these issues. Future simulations include a clawed hallux and a flatfoot model. Future work on the model includes intrinsic muscles, wider ligaments and more cartilage.

Acknowledgements

Dept. of Veterans Affairs grant A2661C.

References

1. Cheung JT and Zhang M: *Med Eng Phys* 2008, **30**(3):269–77.
2. Hu Y, et al: *SPIE* 2006, **6141**:133–42.
3. Lemmon D, et al: *J Biomech* 1997, **30**(6):615–20.
4. Ledoux WR, et al: *J Biomech* 2007, **40**(13):2975–81.
5. Cavanagh PR, et al: *Foot & Ankle* 1987, **7**:262–76.

Foot & Ankle Biomechanics

O46

Custom foot orthoses for the treatment of foot pain: a systematic review

F Hawke¹, J Burns², J Radford³ and V du Toit³

¹Podiatry Department, University of Newcastle, Australia

²Institute for Neuromuscular Research, The Children's Hospital Westmead, Australia

³Podiatry Department, University of Western Sydney, Australia

E-mail: Fiona.Hawke@newcastle.edu.au

Journal of Foot and Ankle Research 2008, **1**(Suppl 1):O46

Introduction: Foot pain affects approximately one quarter of the population at any given time [1, 2], is disabling in nearly half of these cases [3] and can impair mood, behaviour, risk of falls, self-care ability and quality of life [4–7]. Custom-made foot orthoses

are hypothesised to alleviate foot pain by reducing the biomechanical stress applied to injured tissues [8, 9]. We aimed to systematically review the effectiveness of custom-made foot orthoses for the treatment of all types of foot pain.

Methods: The following databases were searched up to June 2007: Cochrane Central Register of Controlled Trials (The Cochrane Library Issue 2, 2007), MEDLINE (from January 1966), EMBASE (from January 1980), CINAHL (from January 1982), and the Physiotherapy Evidence Database (PEDro). Authors of included trials and known researchers in the field were contacted and the reference lists of included trials were checked recursively. No language or publication restrictions were applied. All randomised controlled trials and controlled clinical trials evaluating custom foot orthoses for any type of foot pain were included. Outcomes assessed included quantifiable level of foot pain, function, disability, health-related quality of life, participant satisfaction, adverse effects and compliance. Two reviewers independently selected trials and rated methodological quality. Data were extracted by one reviewer and independently crosschecked by two other reviewers. Study authors were contacted to provide additional information as required. Data were analysed separately for different diagnoses of foot pain and follow-up timepoints.

Results: Eleven trials involving 1,332 participants were included. Five trials evaluated custom foot orthoses for plantar fasciitis, three for foot pain in rheumatoid arthritis and one each for foot pain in pes cavus, hallux valgus and juvenile idiopathic arthritis (JIA). Comparisons to custom foot orthoses included sham orthoses; no intervention; standardised interventions given to all participants; non-custom (prefabricated) foot orthoses; combined manipulation/mobilisation/stretching; night splints; and surgery. Follow-up ranged from one week to three years. Custom foot orthoses were clearly effective for painful pes cavus (Number Needed to Treat [NNT]:5) and rearfoot pain in rheumatoid arthritis (NNT:4). Custom foot orthoses were also effective for foot pain in JIA (NNT:3) and hallux valgus (NNT:6), however, non-custom foot orthoses appeared to be just as effective for JIA, and surgery even more effective for hallux valgus. It is unclear if custom foot orthoses were effective for plantar fasciitis or metatarso-phalangeal joint pain in rheumatoid arthritis. Custom foot orthoses were a safe intervention in all studies.

Conclusion: There is limited evidence on which to base clinical decisions regarding the prescription of custom foot orthoses for the treatment of foot pain. Current evidence suggests custom foot orthoses produce clinically important improvements in foot pain and related function in some people, but not all. Further research is required to identify the precise mechanism of biomechanical effect and the characteristics accounting for the enhanced responsiveness of some people to custom foot orthoses.

References

1. Menz HB, et al: *Journal of the American Geriatric Society* 2001, **49**:1651–1656.
2. Badlissi F, et al: *Journal of the American Geriatrics Society* 2005, **53**:1029–1033.
3. Garrow AP, et al: *Pain* 2004, **110**:378–384.
4. Menz HB, et al: *Journal of the American Podiatric Medical Association* 2001, **91**:222–229.
5. Benvenuti F, et al: *Journal of the American Geriatrics Society* 1995, **43**:479–484.
6. Leveille SG, et al: *American Journal of Epidemiology* 1998, **148**:657–665.
7. Keysor JJ, et al: *Journal of Aging Health* 2005, **17**:734–752.
8. Heiderscheid B, et al: *British Journal of Sports Medicine* 2001, **35**:4–5.
9. Vicenzino B: *Manual Therapy* 2004, **9**:185–196.

O47

Intraoperative pedography – development, validation and clinical use of a novel method for intraoperative biomechanical assessment

Martinus Richter and Stefan Zech

Department for Trauma, Orthopaedic and Foot Surgery,

Coburg Medical Center, Germany

E-mail: info@foot-trauma.org

Journal of Foot and Ankle Research 2008, **1(Suppl 1)**:O47

Introduction: A new device was developed to perform intraoperative pedography (IP). The purpose of this study was to validate the introduced method with standard dynamic pedography, and to analyze the potential clinical benefit.

Methods: Development: For an intraoperative introduction of standardized forces to the footsole, a device named Kraftsimulator Intraoperative Pedographie (KIOP, manufactured by the Workshop of the Hannover Medical School, Hannover, Germany; Registered Design No. 20 2004 007 755.8 by the German Patent Office, Munich, Germany) was developed. The pedographic measurement is performed with a custom-made mat with capacitive sensors (PLIANCE™, Novel Inc., Munich, Germany).

Validation: Step 1: Comparison of standard dynamic P (three trials, walking, third step, three trials, mid stance force pattern), static P in standing position (three trials) and P with KIOP in healthy volunteers (three trials, total force 400 N). For dynamic P and P in standing position, a standard platform (EMED™, Novel Inc., Munich, Germany) was used.

Step 2: Comparison of P in standing position, P with KIOP in awake and anaesthetized patients (three trials, total force 400 N). Patients with operative procedures performed at the knee or distal to the knee were excluded. Patients with general or spinal anaesthesia were included.

The different measurements were compared (t-test, Oneway ANOVA).

Clinical use: A randomized prospective consecutive clinical study comparing treatment with and without IP has started on October 1, 2006. Patients (age 18 years and older) which sustained an arthrodesis and/or correction of the foot and ankle are included. All subjects receive preoperative clinical and radiographic assessment and standard dynamic pedography. The subjects are randomized into two groups, a) use of IP, versus b) no use of IP. One-year-follow-up including standard dynamic pedography is planned. The following scores are used: American Orthopaedic Foot and Ankle Society (AOFAS), Visual-Analogue-Scale Foot and Ankle (VAS FA), Short-Form 36 (SF36, standardized to a 100-point-maximum-scale). Intraoperative consequences after the use of IP were recorded.

Results: Validation: Step 1: 30 individuals were included (age, 26.1 ± 8.6 years; gender, male: female = 24: 6).

Step 2: 30 individuals were included (age, 55.3 ± 30.3 years; gender, male: female = 24: 6). No statistical significant differences of force distribution were found in both steps between the different methods, and between the methods of step 1 and 2 (t-test & ANOVA, p > 0.05).

Clinical use: 51 patients were included until January 31, 2008 (ankle correction arthrodesis, n = 8; subtalar joint correction arthrodesis, n = 10; arthrodesis midfoot, n = 9, correction midfoot, n = 5, correction forefoot, 18). 26 patients were randomized for the use of IP, whereas 25 had no intraoperative measurement. The mean preoperative scores were as follows: AOFAS: 52.3 ± 20.3; VAS FA: 46.1 ± 14.0; SF36: 52.3 ± 25.3. No score differences between the two groups occurred (t-test, p > 0.05). The mean interruption of operative procedure for the IP was 284 ± 37 seconds. In 12 of 26 patients (46%) changes were made after IP during the same operative procedure (correction modified, n = 6; implants modified, n = 2; correction and implants modified, n = 6). The follow-up has not been completed so far.

Conclusion: Since no statistical significant differences were found between the measurements of the introduced method for IP in anaesthetized individuals and the standard static pedography, the introduced method can be considered to be valid for intraoperative static pedography.

During the clinical use, in 46% of the cases a modification of the surgical correction were made after IP in the same surgical procedure. A follow-up of these patients has to be completed to show if these changes improve the clinical outcome.

O48

Effect of external loading on in vitro measured muscle induced calcaneal and talar motion

Ilse Jonkers^{1,2}, Koen Peeters², Joris Walraevens², Georges Van der Perre², Greta Dereymaeker^{2,3}, Jos Vander Sloten² and Pieter Spaepen²

¹FABER, K.U. Leuven, Leuven, Belgium

²Division of Biomechanics and Engineering Design (BMGO), K.U. Leuven, Leuven, Belgium

³Dep. of Orthopedics, H. Hart Ziekenhuis, Leuven, Belgium
E-mail: ilse.jonkersr@faber.kuleuven.be

Journal of Foot and Ankle Research 2008, 1(Suppl 1):O48

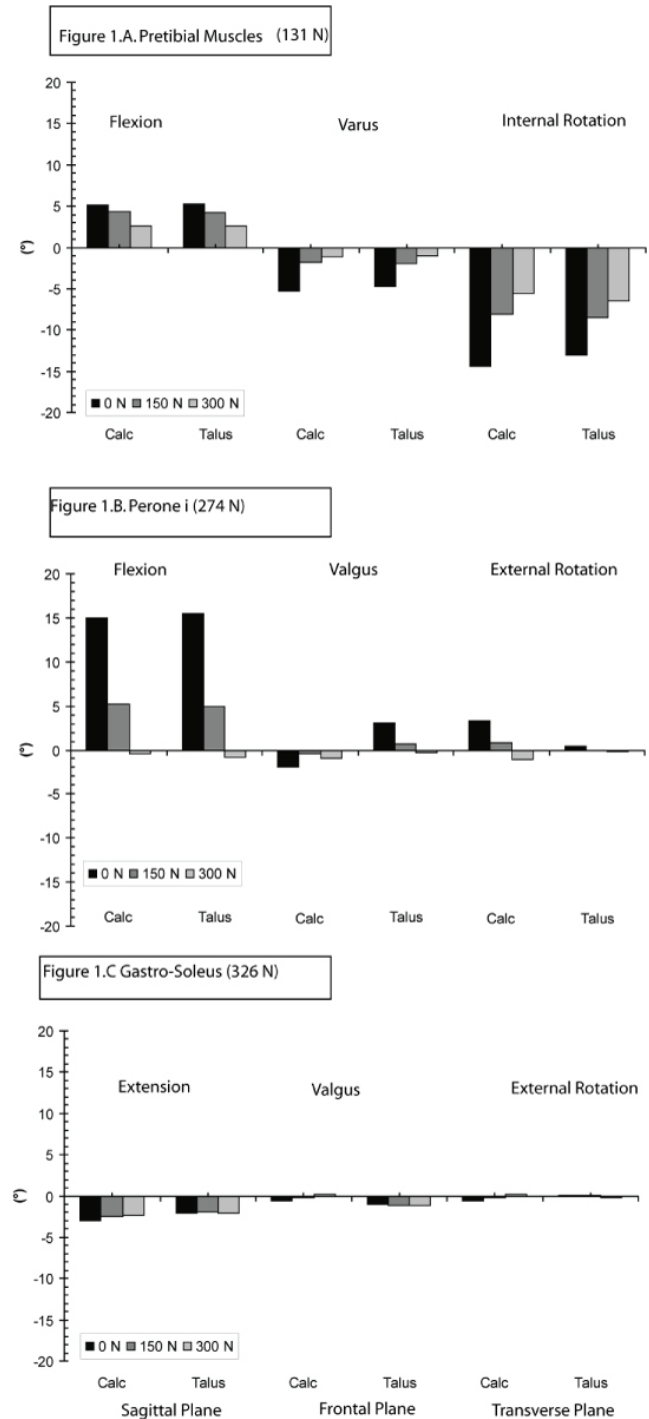
Introduction: Several foot deformities (e.g. pes planus, pes cavus) result from muscular force imbalance across the joints of the ankle and foot. The use of in vitro measurements is required to explore the causal relation between muscle forces, individual foot bone movement and resulting foot deformities. This study quantified the effect of muscle action of the pretibial muscle groups, Mm. peronei as well as the Gastro-soleus on the three dimensional rotation of calcaneus and talus using in vitro measurements with a gait simulator consisting of pneumatic actuators. Furthermore, we tested the effect of altered load bearing conditions of the foot on the observed relations.

Methods: Pneumatic actuators exerted forces with increasing magnitude onto the tendons of the pretibial muscles (M. tibialis anterior, M. extensor hallucis and M. extensor digitorum longus), the tendons of both M. peronei and the Achilles tendon of a cadaver foot, placed in an anatomical position (neutral, upright standing). The resulting motion of bone embedded LEDs was tracked using an opto-electronic system (Krypton, Metris) and the resulting three-dimensional rotation of calcaneus and talus was quantified. Changes in ground reaction forces were measured using a Kistler force platform. These tests were repeated for loading of the foot of 0 N, 150 N and 300 N.

Results: Figure 1 presents the main muscle function as derived from the three dimensional movement of the talus and calcaneus for forces applied onto the tendons of the pretibial muscles

(Figure 1A), onto the tendons of Mm. peronei (Figure 1B) and onto the Achilles tendon (Figure 1C) for the three loading conditions. A pronounced effect of the load bearing condition on the bone motion is found for the pretibial muscles and Mm. peronei. Whereas for the latter, mainly sagittal plane rotations

Figure 1 (abstract O48)



Positive values indicate flexion, valgus and external rotation.

were affected, a pronounced effect in all three planes was found for the pretibial muscles.

Conclusion: The load bearing condition of the foot needs to be accounted for when defining the causal relation between three-dimensional rotations of calcaneus and talus and forces exerted on muscle tendons through pneumatic actuators.

O49

Gradual increase of varus angle of running shoes gradually reduces pronation while maintaining cushioning properties

Torsten Brauner, Thorsten Sterzing, Nina Gras and Thomas L Milani

Department of Human Locomotion, Chemnitz University of Technology, Chemnitz, Germany

E-mail: torsten.brauner@phil.tu-chemnitz.de

Journal of Foot and Ankle Research 2008, 1(Suppl 1):O49

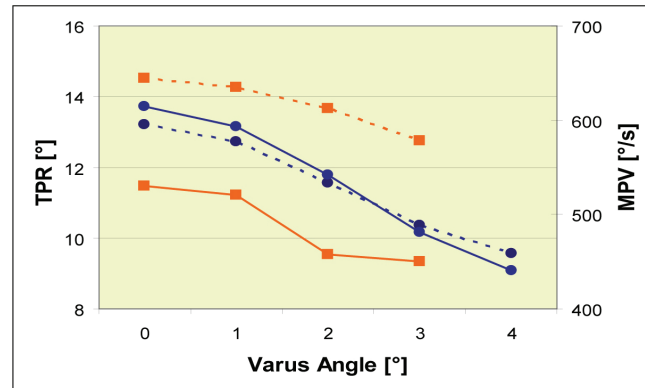
Introduction: Excessive pronation is considered to be the cause of various overuse injuries. Thus, different mechanisms to control excessive pronation have been developed (e.g. dual density and medial support shoes). Reducing effects of shoes with extreme varus angles (VA) of 8–10° on pronation (TPR) and maximum pronation velocity (MPV) have been shown [1, 2]. However, resultant GRFs, loading rate, peak acceleration, and transient rate were observed to be increased [2]. It was concluded that shoes with increased VA lead to reduced cushioning properties by reducing range of motion. The goal of this study was to analyze the effects of gradual 1°-changes in VA (0–4°) in running shoes on pronation and cushioning parameters. Furthermore, the capability of runners to perceive these VA changes should be tested.

Methods: Three studies were performed with a total of 28 recreational heel-to-toe runners (26.4 yrs (\pm 5.8), 72.0 kg (\pm 6.4 kg)). In laboratory study A and B subjects performed five repetitive running trials at a standardized running velocity of 3.5 m/s (\pm 0.1) for each VA condition. TPR and MPV were measured with an electrogoniometer [1]; cushioning parameters were obtained by vertical GRFs and tibial acceleration. In study A (n = 11) a custom-made running shoe with an experimental midsole/outsole construction consisting of easily removable structural elements that altered VA to 0°, 1°, 2°, 3°, and 4° was used. Study B (n = 10): Four regular EVA running shoe pairs were used to manifest the results of Study A. The midsoles of these shoes were abraded on the lateral side of the heel to create VA of 1°, 2°, and 3°. Study C (n = 17): Subjects performed a 40–60 mins run with in each VA condition from study B at self-selected pace. Directly after each run, perception ratings of rearfoot motion control, cushioning, and comfort properties were collected using a questionnaire. For comparison of the VA conditions one-way repeated measures ANOVA ($p < .05$) including LSD post-hoc tests, when appropriate, were run on all biomechanical parameters.

Results: Laboratory studies A and B showed highly significant reductions of TPR ($p < .001$) and MPV ($p < .001$) with increasing VA (Figure 1). Although the overall trend was highly significant, post-hoc tests of study B showed that changes of 1°-VA were insufficient to alter TPR and MPV statistically.

Between VA conditions no significant differences were found in tibial acceleration (A: $p = .79$; B: $p = .70$), peak passive vertical force (A: $p = .42$; B: $p = .13$), and peak passive vertical force rising

Figure 1 (abstract O49)



TPR (dotted) and MPV (solid) at different VA (study A squares, study B circles).

rate (A: $p = .89$; B: $p = .06$). Perception results revealed no differences between conditions for any of the questioned parameters.

Conclusion: VA between 0–4° can gradually control TPR and MPV without negative effects on cushioning properties of the shoes. Subjects do not perceive the effects of VA alteration from 0–3° in regular EVA running shoes. Long-term effects of increased VA on overuse injuries need to be studied.

Acknowledgements

This research was supported by Puma Inc., Germany.

References

1. Schnabel G, et al: *J Biomech* 1994, **27(6)**:688.
2. Perry SD, et al: *Clin Biomech* 1995, **10(5)**:253–257.

O50

Assessing talonavicular joint rotations in three dimension

Thomas M Greiner¹ and Kevin A Ball²

¹Department of Health Professions, University of Wisconsin – La Crosse, USA

²Department of Physical Therapy, University of Hartford, USA

E-mail: greiner.thom@uwlax.edu

Journal of Foot and Ankle Research 2008, 1(Suppl 1):O50

Introduction: The union of the spherical talar head with the cupped shaped navicular shows the general characteristics of a ball-and-socket joint [1]. As such, the talonavicular joint should be expected to demonstrate three rotational degrees of freedom. Yet, conventional approaches to foot motion analysis provide little opportunity to assess motion of the intrinsic foot joints. A new approach, and perspective, is adopted that permits an appreciation of the talonavicular joint that is not restricted to the confines of marker dependence or the orthogonal reference frame. Data will be presented that shows talonavicular rotation about independent axes that possess orientations that are not orthogonal to any conventional reference frame.

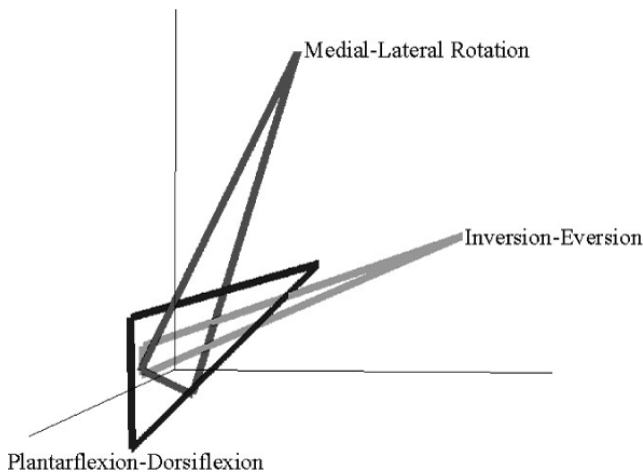
Methods: Data are derived from the legs of 23 non-pathological embalmed cadavers. Legs were prepared by removing all soft tissue, so that only ligamentous structures remained to sustain limb integrity. Each specimen was cycled through three mutually orthogonal driving actions (Plantarflexion-Dorsiflexion [PD],

Inversion-Eversion [IE], and Medial-Lateral Rotation [ML]) while monitoring the relative positions of the talus and navicular with an active-marker tracking system. The Functional Alignment method [2] was used to derive joint axis orientations and motion patterns for three rotational degrees of freedom. These results are summarized using the axis triangle technique [3].

Results: Figure 1 shows consensus (average) axis triangle representations for the three driving motions. The position of each vertex (axis point) along with its distance from the reference frame origin denotes the orientation of the rotational axis and the movement that occurs about it. The sizes and shapes of the three different triangles indicate that the talonavicular joint responds differently to each driving action. None of the vertices of these axis triangles lies on the axes of the reference frame, which indicates that every rotational axis of this joint has a highly oblique orientation.

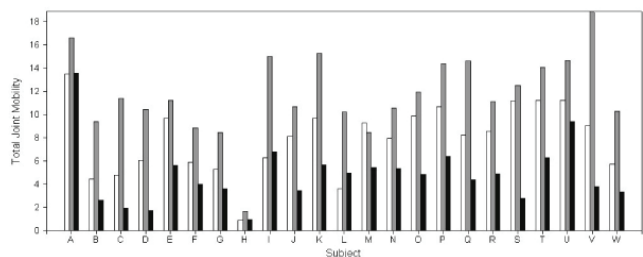
Figure 2 compares the mobility-size assessment of total joint mobility observed in the three driving motions for each subject. Although the talonavicular joint is shown to be most mobile in response to the IE driving motion, in many instances the mobility-size values associated with the other driving motions are nearly as high. This suggests that the talonavicular movement is not restricted to, or even mostly associated with, a single action of the foot.

Figure 1 (abstract O50)



The consensus axis triangles associated with the three evaluated driving actions.

Figure 2 (abstract O50)



Expressions of total joint mobility based on the three driving actions in the 23 subjects. Bars are keyed: ML White; IE Gray; PD Black.

Conclusion: The talonavicular joint is a true three degree of rotational freedom joint. It responds in unique ways to different driving inputs. To identify and understand these differences, it is necessary to adopt a perspective that is not limited to movements aligned with an orthogonal reference frame.

References

1. Kapandji IA: **The physiology of the joints.** E&S Livingstone; 1970.
2. Ball KB, et al: *Proceedings of ISB 3D 2004.* Tampa, FL 2004.
3. Greiner TM and Ball KB: *Am J Phys Anthropol Supl* 2008, **46**:107.

O51
Effects of an active prosthetic ankle during ambulation on stairs and ramps

M Alimusaj, F Braatz, O Gawron and SI Wolf
Department of Orthopaedic Surgery, University of Heidelberg, Germany
E-mail: Merkur.Alimusaj@ok.uni-heidelberg.de

Journal of Foot and Ankle Research 2008, 1(Suppl 1):O51

Introduction: Conventional prosthetic ankle foot systems are commonly not able to adapt to different conditions, e.g. stairs and ramps. Walking on inclined surfaces or stairs is therefore a particular challenge for a prosthetic user [1]. So the amputee is forced to compensate the deficits of his prosthesis by adapting the kinematics and kinetics of the proximal and the contra lateral joints [2]. The Proprio-Foot™ (Ossur) shall be able to reduce these compensating mechanisms as a result of an adaptive micro-processor controlled ankle [3].

Methods: Twenty non vascular transtibial amputees (49 ± 12 years) underwent a conventional 3D gait analysis (VICON & Kistler) [4]. Kinematics and kinetics of the lower limbs were analyzed during ambulation on an instrumented stair with five steps and an instrumented ramp with an incline of 7.5°. The condition of the adapted ankle was compared to the non-adapted ankle. For a preliminary analysis, mean values of knee kinematics and kinetics across the gait cycle was calculated (MatLab) and verified by an ANOVA for repeated measurements with SPSS 14.0 (p < 0.05) (Table 1). Ultimately, the results will be compared to those of twenty young healthy controls.

Results: Preliminary data of ten participants show significant changes in kinematics and kinetics for the knee in the involved side during ambulation with the adapted compared to the non-adapted prosthetic ankle foot system.

Particularly during ramp and stair ascend, the adaptation leads to a significantly reduced knee extension (p < 0.05) and to significantly reduced knee extensor moments in the prosthetic side (p < 0.02). Similar results could be partially found for the knee kinematics when descending the stair (p < 0.05). Although patients reported a broad benefit during ramp descend, only a small but not significant difference for the maximum knee extension could be found in the involved side (p = 0.358).

Conclusion: The preliminary findings suggest that the prosthetic ankle adaptation leads to more physiological knee kinematics and kinetics in the involved limb during walking on stairs and ramps.

For a final conclusion, complete results of twenty patients in the involved and the contra lateral sides and normal reference data have to be taken into account.

Table 1 (abstract O51) Average data (mean± std) of knee extension and knee extensor moments during ambulation on the stair and the ramp for N = 10

	Adaptation	Stair ascend	Stair descend	Ramp ascend	Ramp descend
Knee extension [deg]	ON	0.2 ± 7.9*	-10.7 ± 4.9*	-14.2 ± 5.4**	-13.0 ± 3.2*
	OFF	2.9 ± 9.7*	-7.5 ± 5.9*	-18.2 ± 4.1**	-13.7 ± 4.1*
(p-value)		(p < 0.05)	(p < 0.05)	(p < 0.002)	(p = 0.358)
Knee extending moments [Nm/kg]	ON	0.3 ± 0.2*	0.0 ± 0.2*	0.6 ± 4.2*	-0.2 ± 0.1*
	OFF	0.4 ± 0.2*	0.1 ± 0.2*	0.8 ± 2.2*	-0.2 ± 0.2*
(p-value)		(p < 0.002)	(p = 0.194)	(p < 0.02)	(p = 0.158)

Level of significance = p < 0.05; *maximum value; **mean value.

Acknowledgements

The authors would like to thank all the participants for their attendance. The financial support of Ossur Europe is gratefully acknowledged as well.

References

1. Vickers DR, et al: *Gait & Posture* 2008, **27(3)**:518–529.
2. Nolan L, et al: *Prosthet Orthot Int* 2000, **24(2)**:117–125.
3. Braatz F, et al: *Orth Tech* 2006, **8**:608–611.
4. Kadaba MP, et al: *J Orthop Res* 1989, **7(6)**:849–860.

O52

Functional evaluation of patients treated with osteochondral allograft transplantation for post-traumatic ankle arthrosis

L Berti¹, MG Benedetti¹, F Vannini², T Sforza¹, L Conti¹ and S Giannini¹

¹Movement Analysis Laboratory, Istituto Ortopedici Rizzoli, Bologna, Italy

²Department of Orthopaedic Surgery, Istituto Ortopedici Rizzoli, Bologna, Italy

E-mail: benedetti@ior.it

Journal of Foot and Ankle Research 2008, **1(Suppl 1)**:O52

Introduction: Osteochondral allograft ankle transplantation [1] seems to provide a very innovative and viable alternative for the treatment of post-traumatic ankle arthritis in selected individuals, mostly in young and active patients. The rationale behind this surgical procedure is essentially the transplantation of intact organ as hyaline articular cartilage, into a diseased or damaged area of the joint resulting in improved function [2]. The aim of our study was to evaluate functional outcome of young and active patients that underwent osteochondral allograft ankle transplantation by means of gait analysis.

Methods: Eight patients affected by grade III post-traumatic arthritis were assessed pre-operatively and at the mean follow-up of 12 months. In all cases a fresh osteochondral bipolar resurfacing of the ankle was performed. Clinical evaluations were performed according to the American Orthopaedic Foot and Ankle Society (AOFAS) score. All patients were also studied with gait analysis using the VICON (Oxford, UK) stereophotogrammetric system to evaluate kinematics data and two force platform (Kistler Instrumente AG, Switzerland) to evaluate ground reaction forces. Using electromyography (Zero Wire, Aurion) we analysed the bilateral activity of four muscles of lower limbs (rectus femoris, biceps femoris, gastrocnemius, tibialis anterior). Results were compared with those of a control group, consisting of 10 healthy subjects.

Results: Clinical AOFAS score was significantly higher at twelve months after surgery (pre-surgery 43.8 ± 14.0; post-surgery 77.1 (7.8, p < 0.0005). Gait analysis showed a wider range of motion in the sagittal plane (increased maximum dorsiflexion in stance phase, plantarflexion at toe off, maximum plantarflexion in swing phase) and improved maximum vertical force at loading response after surgery. The EMG pattern of muscle activity became more physiological in the post-operative analysis, even if most patients showed the persistence of co-contractions of gastrocnemius and tibialis anterior muscles during the first half of the stance phase.

Conclusion: Short-term functional evaluation of the osteochondral allograft ankle transplantation showed satisfactory results for these patients. The integrated gait analysis revealed only few abnormalities in kinematics, kinetics, and EMG. The persisting tibialis anterior activity during stance could be related to proprioception deficit and could be improved by time and exercise. It will be important to re-evaluate these patients also at longer follow-ups in order to confirm these positive results.

References

1. Kim CW, et al: *Foot Ankle Int* 2002, **23**:1091–1102.
2. Gross AE, et al: *Foot Ankle Int* 2001, **22**:385–391.

POSTER PRESENTATIONS

PI

Gait analysis of a novel design of ankle replacement

S Ingrosso, MG Benedetti, A Leardini, S Casanelli and S Giannini

Movement Analysis Laboratory, Istituto Ortopedici

Rizzoli of Bologna, Italy

E-mail: leardini@ior.it

Journal of Foot and Ankle Research 2008, **1(Suppl 1)**:PI

Introduction: A new three-part total ankle prosthesis was designed [1] to achieve maximal compatibility between component relative motion and ligament natural role. This results in ankle natural mobility while maintaining full conformity, achieved by a backward and forward motion of the meniscus within the flexion arc. In this study the expected early functional recovery was evaluated by a clinical scoring system and by gait analysis.

Methods: Ten patients operated with the BOX Ankle (Finsbury Orthopaedics, UK), with mean age 57.4 years (range 45–72), BMI 25.8 (range 20.4–34.1), 8 males and 2 females, 9 post traumatic osteo- and 1 psoriasis arthritis were gait analysed preoperatively

and at 6 and 12 month follow-up. The examination consisted in a clinical score (AOFAS) and in gait analysis (Vicon 612 System – Oxford UK, Kistler forceplates) adopting a recently validated protocol [2]. Results were compared with a ‘control group’ of 20 subjects, with mean age 27.9 years (range 23–36), BMI 21.9 (range 18.5–25), 11 male and 9 females. Figure 1.

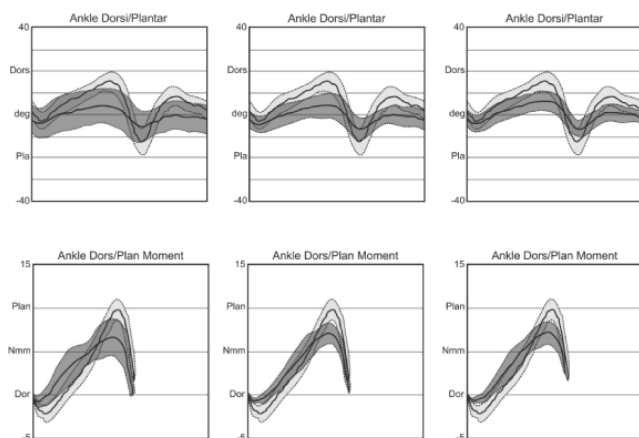
Results: AOFAS score rose from 44.3 in pre-op to 80.0 at 12 months, with an important reduction of pain (score from 17.0 to 31.0, max 40) and of ankle alignment (from 4.5 to 9.3, max 10). Spatio-temporal parameters obtained with gait analysis showed a progressive recovery to normality in the first 6 months

Figure 1 (abstract P1)



A BOX Ankle patient instrumented with the marker-set of the protocol utilised.

Figure 2 (abstract P1)



Ankle rotation (top row) and moment (bottom) in the sagittal plane (dark-grey), at pre-op (on the left), at 6 (in the centre) and 12 (on the right) months, superimposed to equivalents in the control group (light-grey).

and a successive settlement on the operated site: i.e. mean stride length normalised (%high) was 64.1 pre-op and exactly 69.7 both at 6 and 12 months; speed rose from 86.6 cm/s to 98.7 cm/s at 6 months and 100.1 cm/s at 12 months, both with statistical significance. Ankle flexion range improved in all three anatomical planes, in particular in the sagittal, where there was an increase of max dorsi-flexion in the stance phase (3.2 deg pre-op, 5.2 and 6.3 at 6 and 12 months, the latter significant), though a persistent little plantar-flexion at initial contact and a moderate reduction of plantar-flexion during swing were observed. Plantar-flexion moment showed a smoother pattern after surgery in the stance phase. Figure 2.

Conclusion: The novel ankle prosthesis seems to contribute to an early functional recovery at 6 months maintained at one year. Preliminary assessments at 24 months confirmed the improvements achieved at 12 months. With reduction of pain and recovery of joint control, gait variables of high clinical interest, such as stance balance and ability in propulsion, improve considerably.

References

1. Leardini A, et al: *Clin Orth Rel Res* 2004, **424**:39–46.
2. Leardini A, et al: *Gait & Posture* 2007, **26**(4):560–571.

P2

In vivo quantification of the Achilles tendon moment arm

Frances T Sheehan

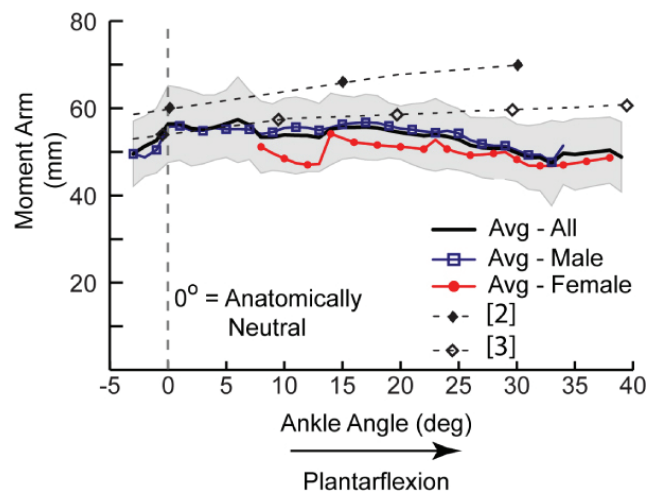
Physical Disabilities Branch, National Institutes of Health, Bethesda, MD, USA

E-mail: fsheehan@cc.nih.gov

Journal of Foot and Ankle Research 2008, 1(Suppl 1):P2

Introduction: The Achilles’ tendon moment arm (ATma) is a critical quantity in that it defines the triceps surae’s ability to generate a moment on the calcaneus, which is then transferred to the foot. In the past this measure has been primarily acquired statistically, in 2D, without muscle activation, and in small

Figure 1 (abstract P2)



Achilles’ tendon MA. Grey shading = ± 1 SD for the average of all subjects. The SD for female and male groups is similar to the SD for all subjects. Black dashed lines indicate data from past studies [2, 3].

populations. Thus, the primary purpose of this study was to establish the first *in vivo* three-dimensional measures of the ATma, measured non-invasively and *in vivo* during dynamic activity in a large normative population ($n = 19$) using a dynamic MRI technique. The ATma was defined as the shortest distance between the finite helical axis (FHA) of the calcaneal-tibial joint and the AT line of action.

Methods: Nineteen healthy subjects (25.5 ± 3.7 years, 70.1 ± 13.1 kg, 174.3 ± 7.8 cm, 6 F/14 M) participated in this IRB approved study. Subjects were placed supine in a 1.5 T MR imager (LX; GE Medical Systems, Milwaukee, WI, USA) after obtaining informed consent. An MRI-compatible device was used to apply a plantarflexion (PF) load. This device allowed natural 3D motion at both joints of the hindfoot. While subjects cyclically plantarflexed and dorsiflexed their ankle at 35 cycles/min fast-PC MR images (anatomic and x, y, and z velocity images, temporal resolution = 72 ms, imaging time = 2:48) were collected [1]. The sagittal-oblique imaging plane contained the soleus musculotendon junction, tibia, talus and calcaneus. The 3D time dependent tibial, talar and calcaneal attitudes along with the soleus displacement were derived by integrating the velocity data. From these data the FHAs and ATmas were determined. Averages are presented for PF only and for ranges represented by 3 or more subjects. The range of motion was self-selected, thus not all subjects are represented at all ankle angles.

Results: A slight decrease in the ma was seen in PF from -2° DF to 39° PF ($0^\circ =$ anatomically neutral). Women tended to have a slightly smaller ATma and stature, but a correlation between ATma and height was not found. Figure 1.

Conclusion: This study is the first to quantify the ATma non-invasively and *in vivo* during loaded PF, using a population size twice that of most past studies. The slight decrease in ATma during PF was due primarily to posterior displacement of the calcaneal-tibial FHA, but some of this change could also be attributed to the 3D change in FHA orientation. These data are similar in value to past studies, but the steady increase in value during PF was not found [2, 3]. This is likely due to the 3D nature of this experiment and that the moment arm was calculated directly from the FHA. Thus, the assumptions required for the center of rotation and tendon excursion methods did not limit the current experiment. The small number of female subjects makes comparing the two groups difficult, but the smaller ATma was expected due to the average height difference (161.3 ± 1.8 mm vs. 176.0 ± 3.4 mm). Since a correlation between height and ATma could not be established, normalization was not used.

References

1. Sheehan FT, et al: *Foot Ankle Int* 2007, **28(3)**:323–3.
2. Maganaris SN, et al: *Eur J Appl Physiol* 2004, **91**:130–9.
3. Rugg SG: *J Biomech* 1990, **23(5)**:495–501.